Division of Pharmaceutical Biosciences
Faculty of Pharmacy
University of Helsinki
Finland

Nanofibrillar cellulose for encapsulation and release of pharmaceuticals

by

Heli Paukkonen

ACADEMIC DISSERTATION

To be presented, with the permission of the Faculty of Pharmacy of the University of Helsinki, for public examination in Auditorium 2, Infocenter Korona (Viikinkaari 11, Helsinki), on the 6th July 2018, at 12 noon.

Helsinki 2018

Supervisors Associate Professor Timo Laaksonen
Laboratory of Chemistry and Bioengineering
Tampere University of Technology
Finland

Professor Marjo Yliperttula
Division of Pharmaceutical Biosciences
Faculty of Pharmacy
University of Helsinki
Finland

Reviewers Professor Jessica Rosenholm
Pharmaceutical Sciences Laboratory
Faculty of Science and Engineering
Åbo Akademi University
Finland

Professor Jukka Rantanen
Department of Pharmaceutics and Analytical Chemistry
Faculty of Health and Medical Sciences
University of Copenhagen
Denmark

Opponent Professor Anette Larsson
Department of Chemistry and Chemical Engineering
Chalmers University of Technology
Sweden

Dissertationes Scholae Doctoralis Ad Sanitatem Investigandam Universitatis Helsinkiensis

ISBN 978-951-51-4356-3 (paperback)
ISBN 978-951-51-4357-0 (PDF)
ISSN 2342-3161 (print)
ISSN 2342-317X (online)

Unigrafia Oy
Helsinki 2018

Abstract

The main role of excipients is to ensure the safety and efficacy of the whole pharmaceutical formulation throughout its shelf-life and administration. Formulation design and development as well as material testing are the key components for successful drug delivery. This is becoming increasingly complicated as new active pharmaceutical ingredients typically have poor solubility and/or bioavailability. Due to this, there is an ever increasing need to explore new excipients and material combinations as innovative formulation solutions are required. Furthermore, modified release formulations are needed to control the release rates and to adjust the desired therapeutic effects, raising even more demand for effective formulations.

The main aim of this thesis was to evaluate the performance of plant based materials nanofibrillar cellulose (NFC) and anionic carboxylated nanofibrillar cellulose (ANFC) as pharmaceutical excipients for modified release formulations and bioadhesive films. These materials are widely available from renewable sources; biocompatible with relatively low toxicity combined with high mechanical strength and large surface area available for encapsulation.

NFC and ANFC, together with HFBII protein, were used as emulsion stabilizers for encapsulation and release of poorly water-soluble drugs. The synergistic stabilization mechanism achieved with these biopolymers improved emulsions stability with extremely low concentrations. In another study, ANFC hydrogels were evaluated as matrix reservoirs for diffusion controlled drug release. Their rheological and drug release properties were shown to be preserved after freeze-drying and reconstruction. The ANFC hydrogels controlled the release kinetics of small molecular weight drugs moderately, whereas significant control was obtained in the case of large proteins. In a comparative study, three new grades of microcrystalline cellulose (MCC) hydrogels were evaluated for diffusion controlled drug release. MCC matrices efficiently controlled the release of both large and small compounds, indicating great potential for drug release applications in a similar manner to the ANFC hydrogels.

Bioadhesive NFC and ANFC based films were prepared by incorporating bioadhesive polymers mucin, pectin and chitosan into the film structure. The bioadhesive properties of the films combined with good mechanical and hydration properties, together with low toxicity makes them a feasible option for buccal drug delivery applications.

In conclusion, NFC and ANFC were shown to be versatile excipients applicable for several types of dosage forms. In the future, it is seen that these materials may be used systematically as functional excipients for modified release dosage form.

Acknowledgements

This thesis work was carried out at the Division of Pharmaceutical Biosciences, Faculty of Pharmacy, University of Helsinki during the years 2014 - 2018. I gratefully acknowledge the financial contribution of the Academy of Finland in making my Ph.D. work possible. The Doctoral Programme in Drug Research and University of Helsinki are acknowledged for supporting my conference trips financially.

I would first like to thank my supervisor Professor Timo Laaksonen for his trust in me by offering me the opportunity to do the Ph.D. in his group at the University of Helsinki. Thank you for introducing me the world of biopolymers in pharmaceutical sciences and for the positive attitude, continuous support, encouragement and discussions over the years. I would also like to thank my second supervisor, Professor Marjo Yliperttula for her enthusiasm in science and valuable discussions. She was always available when help was needed or new ideas were explored.

I am grateful to Dr. Kari Luukko from UPM for his co-operation and productive discussions regarding the properties of nanofibrillar cellulose. I extend my sincere gratitude to Professor Päivi Laaksonen for sharing her expertise and the valuable contribution for this work. I would also like to thank my co-authors for contributing to the work. Especially thanks to Patrick, Mikko, Yujiao, Tiina L., Heikki R., Tiina H., Vili, Anni and Raili. Further, I would like to thank the colleagues in our BP group for the nice scientific discussions and fun times over the years.

It is my honor to have Professor Anette Larsson from Chalmers University of Technology as my opponent, and I greatly appreciate her interest to find time from her busy schedule to attend my thesis defense. Professor Jessica Rosenholm and Professor Jukka Rantanen are sincerely thanked for reviewing this thesis and for giving valuable comments and suggestions for its improvement. Additionally, I would like to thank Associate Professor Hélder Santos and Docent Arturo García-Horsman for the participation in my doctoral thesis grading committee and attending my thesis defense.

I would like to thank all of the colleagues at the Division of Pharmaceutical Biosciences and other departments for the friendly and enjoyable working atmosphere. I want to thank especially Kristiina, Tiina L., Anna-Kaisa, Ansku, Tatu, Jaakko, Feng, Jenni, Dunja, Leena, Teemu, Mecki, Alma, Noora, Petter, Riina, Liisa, Heikki, Eva, Otto, Yan-Ru, Arto M. and Jasmi for fun moments and random discussions. Special thank is also forwarded to Timo O. for coaching me in the lab and Leena P. for taking care of everything in the day to day lab work and staying always so positive and encouraging.

I thank my family for the support and encouragement over the years. Especially I would like to thank my sister Niina for listening to my scientific ramblings. I would like to thank also all of my friends for taking my mind out of the work and for supporting me throughout the years. Finally, my warmest thanks go to Patrick for his humor, love and endless support.

Helsinki, June 2018

Heli Paukkonen

Contents

List of original publications

This thesis is based on the following publications:

I **Paukkonen, H.,** Ukkonen, A., Szilvay, G., Yliperttula, M., Laaksonen, T., Hydrophobin-nanofibrillated cellulose stabilized emulsions for encapsulation and release of BCS class II drugs, Eur J Pharm Sci, 100 (2017) 238-248.

II **Paukkonen, H.,** Kunnari, M., Laurén, P., Hakkarainen, T., Auvinen, V-V., Oksanen, T., Koivuniemi, R., Yliperttula, M., Laaksonen, T., Nanofibrillar cellulose hydrogels and reconstructed hydrogels as matrices for controlled drug release. Int J Pharm, 532 (2017) 269-280.

III Laurén, P.*, **Paukkonen, H.*,** Lipiäinen, T., Dong, Y., Oksanen, T., Räikkönen, H., Ehlers, H., Laaksonen, P., Yliperttula, M., Laaksonen, T., Pectin and Mucin Enhance the Bioadhesion of Drug Loaded Nanofibrillated Cellulose Films. Pharm Res (2018) 35: 145. *Equal contribution.

IV Dong, Y., **Paukkonen, H.**, Fang, W., Kontturi, E., Laaksonen, T., Laaksonen, P., Entangled and colloidally stable microcrystalline cellulose matrices in controlled drug release. Int J Pharm. In press.

The publications are referred to in the text by their roman numerals (I-IV). Reprinted with the permission of the publishers.

Author's contribution

Publication I

The author designed the experiments with the supervisors and co-authors. The author did most of the experiments and analyzed the results. The author wrote the paper and actively participated to complete the final paper.

Publication II

The author designed the experiments with the supervisors and co-authors. The author did most of the experiments and analyzed the results. The author was responsible for writing the first draft of the paper and actively participated to complete the final paper.

Publication III

The author designed the experiments equally with Patrick Laurén with the help of supervisors and co-authors. The author participated in all experimental parts of the work and analyzed the results together with Patrick Laurén. The author was responsible for writing the paper together with Patrick Laurén and the co-authors and actively participated to complete the final paper.

Publication IV

The author participated in the design of the experiments together with Yujiao Dong and the supervisors and co-authors. Yujiao Dong performed the experimental measurements and analyzed the results together with co-authors. The author participated in executing and optimizing preliminary experiments and in analyzing the results and writing the manuscript together with the co-authors.

Abbreviations and symbols

A	surface area
AGU	anhydroglucose unit
ANFC	anionic carboxylated nanofibrillar cellulose
API	active pharmaceutical ingredient
BSA	bovine serum albumin
c_{ini}	initial drug concentration in the matrix system
c_s	drug solubility in the wetted matrix
CMC	carboxymethylcellulose
CR	controlled-release
D	diffusion coefficient
DP	degree of polymerization
DR	delayed-release
DSC	differential scanning calorimetry
ER	extended-release
exp	excipients trehalose and polyethylene glycol
FITC-DEX	fluorescein isothiocyanate–dextran
G’	storage modulus
G’’	loss modulus
KETO	ketoprofen
L	thickness
LZ	lysozyme
M_t	cumulative amounts of drug released at time t
M_∞	cumulative amounts of drug released at time ∞
MCC	microcrystalline cellulose
MZ	metronidazole
NAD	nadolol

NFC	nanofibrillar cellulose
PDI	polydispersity index
PEG	polyethylene glycol
SR	sustained-release
TEMPO	(2,2,6,6-Tetramethylpiperidin-1-yl)oxyl
tre	trehalose
YM	Young's modulus

1 Introduction

A medicine contains essentially two parts the active pharmaceutical ingredient (API) and suitable excipients that complete the total volume/mass of a given formulation. Excipients are defined by the International Pharmaceutical Excipients Council (IPEC) as substances in the pharmaceutical formulation other than the APIs [1]. Traditionally excipients have been considered as completely inert materials necessary for the manufacturing and storage as well as administration of uniform dosage forms of the API. However, nowadays it is acknowledged that excipients have a major role in the functionality, manufacturability and storage stability of a formulation. Pharmaceutical excipients have multiple functions such as ensuring stability by protecting API during manufacturing and storage, improving the dosing accuracy of API, improving bioavailability, masking of poor organoleptic properties and improving patient compliance [2]. The major function of any excipient is to ensure the safety and efficacy of the medicine throughout the formulation shelf-life and during and after the administration.

Formulation design is becoming more complicated as new active molecules with poor solubility and high molecular weight are entering the product pipeline [3,4]. There is an ever increasing need for new pharmaceutical excipients as innovative formulation solutions are explored to facilitate the poor properties of existing and new API. Typically the oral administration route is the preferred drug delivery route for chronic therapy due to its high patient compliance and ease of administration when compared to the parenteral routes. However, the disease pathophysiology and the desired target determine the administration route in drug delivery. Other commonly used administration routes include topical, nasal and ocular routes. Formulation development and material testing are key components in successful drug delivery through the various administration routes. Furthermore, modified release formulations can be used to control the drug release rate and to adjust the desired therapeutic effect by means of formulation.

Biopolymers offer an alternative to synthetic polymers as excipients in pharmaceutical dosage forms. Usually the use of biopolymers benefits from their relatively low toxicity as well as renewable abundant sources available for production. Natural polymer cellulose can be used as a starting material for the production of nanocellulose and microcrystalline cellulose. Nanocellulose is a relatively new emerging material in the field of pharmaceutics and biomedical applications. It has been explored for these applications due to its interesting properties such as high strength and stiffness combined with low weight, biocompatibility, high surface area and renewability [5].

This thesis work focused on exploring the use of nanofibrillar cellulose (NFC) and anionic carboxylated nanofibrillar cellulose (ANFC) as pharmaceutical excipients in modified release formulations and bioadhesive films where the formulation in capable of controlling the drug release rate. So far relatively few studies have focused on exploring nanofibrillated cellulose as a pharmaceutical excipient. The main aim here was to investigate the applicability of NFC and ANFC in various modified release formulations. An additional aim of the thesis was to evaluate novel type MCC hydrogel dispersions in

controlled drug release applications. Moreover, we have used only biopolymers such as hydrophobin proteins, mucin, chitosan and pectin as additional excipients in all evaluated modified release formulations.

Firstly, NFC and ANFC were used as emulsion stabilizers together with hydrophobin class II protein HFBII. Previously a combination of NFC and hydrophobin proteins has been used to stabilize emulsions [6]. However in the thesis the purpose was to evaluate the applicability of these emulsions for the encapsulation and release of poorly water-soluble BCS II class drugs. It was hypothesized that the nanocellulose grade would affect the drug release rate.

Secondly, concentrated ANFC hydrogels were introduced as matrix reservoirs for controlled drug delivery applications of small molecules and proteins. A further aim here was to study how the freeze-drying and subsequent rehydration of ANFC hydrogel affects the rheological and drug release properties. The aggregation of NFC fibers during drying is a major manufacturing challenge in the production of dry NFC as the nanoscale dimensions are usually lost [7,8]. It was hypothesized that ANFC grade together with commonly used lyoprotectants would be a more suitable combination in terms of preserving the nanoscale dimensions in the reconstructed hydrogels after drying. Further it was hypothesized that the anionic nature and high viscosity of ANFC matrix could be used to control the drug release rates of several small and large molecular weight model compounds.

Thirdly, three types of microcrystalline cellulose (MCC) hydrogel dispersions were evaluated for controlled drug release application. Typically MCC is used as an excipient in the dry form. Here, however a novel type of manufacturing process enabled the use of MCC as highly concentrated colloidally stable hydrogel dispersions. It was hypothesized that the rheological properties as well as colloidal stability and porosity could be used to control the drug release rate in a sustained manner in comparison to commercial MCC Avicel grades.

Furthermore, mucoadhesive NFC and ANFC films were prepared. NFC and ANFC were used as film forming materials and natural mucoadhesive biopolymers mucin, pectin and chitosan were incorporated into the films to add bioadhesive functionality without further chemical modification of the NFC and ANFC structures. It was hypothesized that effective mucoadhesive properties, suitable mechanical properties in combination with low toxicity and relatively fast drug release desirable for a buccal type dosage form could be obtained.

The literature review part of this thesis will focus on the properties and pharmaceutical applications of cellulose, nanofibrillar cellulose and microcrystalline cellulose. Fundamental aspects on the topics of modified release and mucoadhesive drug delivery systems as well as freeze-drying of pharmaceuticals are covered. After the literature review, the aims of the thesis and materials and methods are introduced. Finally, the obtained results are presented and the findings are discussed.

2 Review of the literature

2.1 Cellulose

Cellulose was first discovered and isolated from green plants by a French chemist Anselme Payen in 1838 [9]. Today, cellulose is one of the most important renewable biopolymers on earth and for industrial scale manufacturing it provides a key source for the production of sustainable materials [10,11]. Wood (hardwood, softwood) and cotton are the major sources for commercial cellulose production, however other plant based materials such as seed fibers, bast fibers (hemp, jute, flax), grasses (bamboo, bagasse) as well as algae (*Valonica ventricosa*) and bacteria (*Gluconacetobacter xylinum*, *Acetobacter xylinum*) can be used as sources for production [12]. In plants cellulose is a component of the cell wall and it has a reinforcing role together with hemicelluloses, pectin and lignin [13,14].

Structurally cellulose is a linear polysaccharide homopolymer that consists of β(1→4) linked D-glucopyranose units, the so-called anhydroglucose units (AGU) (Figure 1) [15]. Every second AGU unit is rotated 180° in plane for the formation of an acetal bond between two adjacent AGU units, and the neighboring cellulose monomers form a dimer called cellobiose [16]. The length of cellulose chains, found in nature, vary greatly depending on the degree of polymerization (DP). Typically in wood cellulose the chain consists of 10000 AGU units, whereas native cotton cellulose consists of 15000 AGU units [17]. Each glucose unit has three hydroxyl groups available for hydrogen bonding and chemical modifications positioned at C-2, C-3 and C-6 atoms. Intra-and intermolecular hydrogen bonds form various types of semicrystalline structures due to the uniform distribution of hydroxyl groups [18]. Cellulose has reportedly six different polymorphs (I, II, III_I, III_{II}, IV_I, IV_{II}) with the possibility of conversion from one form to another [11]. Native cellulose from plant origin constitutes from form I cellulose with two allomorphs Iα and Iβ [19,20]. The origin of cellulose affects the ratio of Iα and Iβ (predominant in higher plants). Iα exhibits triclinic type of unit cells and is a metastable form, whereas Iβ has monoclinic type of unit cells [21].

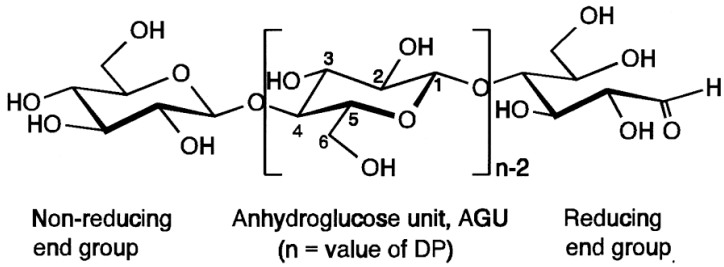

Figure 1. *Molecular structure of cellulose that is composed of repeated anhydroglucose (AGU) units [15].*

Individual cellulose chains aggregate to form long threadlike microfibrils (elementary fibrils) that are laterally stabilized by hydrogen bonds between hydroxyl groups and

oxygens of adjacent molecules [22,23]. The diameter of microfibrils ranges between 3-35 nm depending on the origin [24]. Each microfibril contains a string of crystalline regions linked by amorphous domains. Microfibrils bundle together further to form cellulose fibers, and in wood based cellulose the microfibrils are surrounded by an amorphous matrix of lignin and hemicelluloses [17]. Lignins are water insoluble amorphous polymers consisting of phenylpropane units without an ordered and regular structure [25]. In wood based cellulose, hemicelluloses crosslink cellulose fibrils in a lignin matrix. Hemicelluloses, such as xylan and glucuronoxylan, are a group of heteropolysaccharides present along with cellulose in almost all plant cell walls [14]. Due to the supramolecular structure of cellulose it is insoluble in water as well as in common organic solvents [24].

The structural properties and organization within plants affects the self-assembly and organization of cellulose based materials in manufactured products. Due to low cost, biodegrability (in nature), renewable source, good biocompatibility and low toxicity, cellulose based materials are used as excipients in pharmaceutical dosage forms [24,26]. Several chemical modifications altering the hydrophilicity of cellulose structure are possible [15]. Cellulose derivatives such as microcrystalline cellulose (MCC) and water soluble hydroxypropyl (HPC), hydroxypropylmethyl (HPMC) and carboxymethylcellulose (CMC) are all commonly used excipients in the pharmaceutical industry. Among these, MCC is the most frequently used excipient with various uses ranging from tablet binder and diluent in direct compression or wet granulation to tablet disintegrant, anti-adherent or capsule diluent [26]. On the contrary, nanofibrillar cellulose is a new emerging material in the biomedical field and extensive research has been focused in recent years on various biomedical applications. Whereas controlled drug release applications have been investigated to a lesser extent.

2.2 Nanofibrillar cellulose

The term nanocellulose refers to three types of materials: (I) nanofibrillar cellulose (NFC), also referred to as cellulose nanofibrils, microfibrillated cellulose, nanofibrillated cellulose or nanocellulose fibers, (II) cellulose nanocrystals, also referred to as cellulose nanowhiskers and nanocrystalline cellulose, and (III) bacterial cellulose [27]. In the experimental part of this thesis modified release and mucoadhesive formulations were prepared from wood based native NFC and anionic type carboxylated NFC (ANFC). Therefore, the contents of the following literature review chapters will focus on the production, properties and pharmaceutical as well as biomedical use of NFC and ANFC. Cellulose nanocrystals and bacterial cellulose are excluded from the literature review.

2.2.1 Production and morphology

During late 70s and early 80s the manufacturing of NFC via mechanical treatment was pioneered by Sandberg et al. at ITT Rayonier Inc. in USA [28,29]. The mechanical treatment is used to delaminate cellulose fibers and liberate around 2-20 nm wide microfibrils. The microfibrils have a high aspect ratio and gel-like properties in water. Major challenge for commercial NFC production with mechanical disintegration

techniques used to be the extremely high energy consumption up to 70000 kWh per ton [30]. However, technology advances and development of different mechanical, biological and chemical pretreatments prior to the principal mechanical treatment has reduced the energy consumption making the commercialization of NFC possible [31]. Several companies, such as UPM (Finland), American Process Inc. (USA), Daicel FineChem Ltd. (Japan) and Innventia (Sweden) nowadays have a commercial NFC product in their portfolio.

Never-dried and once-dried cellulose are both used as a starting material for NFC production. However the fibrillation process in less energy consuming with the never-dried material, since drying promotes irreversible hydrogen-bonding between nanofibrils, known as hornification [7,32]. Wood pulp is a commonly used starting material for NFC production. Accompanying hemicelluloses and lignin need to be removed from NFC by various cooking and bleaching methods prior to fibrillation, nevertheless some residual amounts usually remain in the final wood based NFC [33]. Hemicellulose contains carboxyl groups, and wood based NFC fibers carry an anionic charge due to the residual hemicellulose coating on the surface of the fibers [34]. NFC isolation from wood requires that the highly organized hierarchical structure is mechanically disintegrated. Non-wood plants usually contain less lignin and the fiber delignification and purification processes are therefore less demanding [35]. Also, the fibrillation process of such material is less demanding as the cellulose microfibrils are less tightly bound than in the secondary cell wall of wood [36]. Up to date the production of NFC from for example potato pulp [37],sugar beet pulp [38], soybean ponds [39], rice straw [40], pineapple leaf [41], banana [42], sisal fibers [43] and oat straw [44] has also been reported.

Figure 2 contains a schematic presentation of different possible steps used in the production and isolation of NFC including purification, pretreatments, principal mechanical treatment and post-treatment modifications [31]. Usually the NFC production process includes several different operations and the final end product properties such as morphology [45], surface chemistry [46], crystallinity [47] and DP [48] depend on the overall process. Mechanical pretreatments such as blending [40], refining [49] and grinding [50] are used to reduce the cellulose fiber diameter prior to the principal mechanical treatment where microfibrils are exposed. All of the aforementioned techniques can be used as the sole mechanical treatment for NFC production if repeated adequately. Biological and chemical pretreatments are also available to reduce the energy consumption during NFC fibrillation. Enzymatic hydrolysis can be used to reduce the degree of polymerization [48]. The surface of NFC can be activated to produce ANFC that contains carboxyl groups directly on the fiber surface for example through TEMPO [(2,2,6,6-Tetramethylpiperidin-1-yl)oxyl] oxidation [45,51]. Other common chemical pretreatments that render an anionic charge to the fiber surface include carboxymethylation [52] and sulfonation [53]. On the other hand, quaternization can be performed to cationize cellulose prior to fibrillation [54].

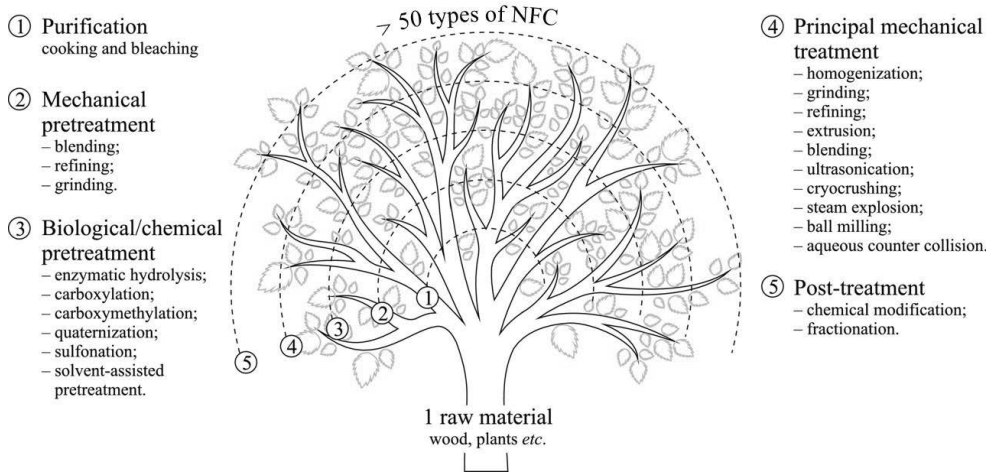

Figure 2. *Schematic presentation of NFC production process steps divided into purification, pretreatments (mechanical, biological, chemical), mechanical treatment and post-treatment modification [31].*

The principal mechanical treatments available for NFC fibrillation include homogenization [55], grinding [50], refining [49], extrusion [56], blending [40], ultrasonication [57], cryocrushing [38], steam explosion [41], ball milling [58] and aqueous counter collision [59]. After the mechanical fibrillation, further chemical modifications [60] and fiber fractioning [61] are possible. The diameter of native NFC fibers is typically 5-60 nm with a length of several micrometers [62]. The NFC fiber dimensions, hemicellulose content, surface chemistry and the quantities of crystalline and amorphous regions may vary depending on the origin of cellulose raw material as well as nanofibrillation processing [5,62]. TEMPO oxidized ANFC fibers have an anionic surface charge, 3-4 nm diameter and the length in the range of few micrometers [45,51].

2.2.2 Rheological and mechanical properties

NFC and ANFC are typically produced as aqueous hydrogel suspensions [62]. Both grades NFC and carboxylated ANFC, are highly hydrophilic materials with a high water binding capacity and high fiber surface area (due to the high aspect ratio). The abundant hydroxyl groups (-OH) on the surface of NFC favor the hydrogen bonding between adjacent NFC fibers. This results in natural self-assembly in an aqueous environment, and in the formation of a hydrogel structure due to the hydrogen bonding between fibers and the high entanglement of NFC fiber network [63]. However, the colloidal stability of NFC suspensions arises from electrostatic repulsion between fibers as the fibers have a slightly anionic surface charge caused by the residual hemicellulose coating (which contains a lot of -COOH groups) on top of NFC fibers [34]. Due to multiple reactive hydroxyl (-OH) groups on the surface of native NFC several chemical modifications are possible [12,60]. TEMPO oxidation can be used to activate NFC surface, and to produce carboxylated ANFC where anionic (–COOH) groups are directly present on the fiber surface [45].

In an aqueous environment, there is electrostatic repulsion present between adjacent ANFC fibers due to surface -COOH groups [64]. The repulsion forces improve the colloidal stability of ANFC suspensions [51]. Both grades (NFC and ANFC) have concentration dependent viscosity and exhibit the behavior of a pseudoplastic gel under increased shear rate as the shear thinning phenomenon is observed [63,65-67]. Cationic crosslinkers such as divalent Ca^{2+}, Zn^{2+}, Cu^{2+} and trivalent Al^{3+} and Fe^{3+} have been used to crosslink carboxylated ANFC and to modify the rheology of the material [68,69]. These modifications can be used to alter for example the viscosity and stiffness of the ANFC material without increasing the solid content of ANFC fibers in the hydrogel. The rheological properties of NFC and ANFC have enabled the use of these materials as stabilizers and viscosity modifiers in suspensions [70-72] and emulsions [6,73,74] in food technology, pharmaceuticals and cosmetics.

Cellulose nanofibrils (NFC and ANFC) have excellent mechanical properties combined with relatively low density and high surface area [75]. Upon drying, NFC fibers aggregate irreversibly due to a mechanism called hornification [7,8]. Here the irreversible fiber aggregation is caused by hydrogen bonds that are formed between adjacent NFC fibers when water is removed. Once dried, NFC fibers cannot be redispersed in water again. This property has been exploited for example in the production of: 1) films with Young's modulus values between 6 - 13 GPa where the film porosity and preparation affect greatly the elastic properties [76,77], 2) flexible and deformable aerogels with hierarchical porous structures (98% porosity) and low density (0.02 g/cm^3) [78] and 3) spray dried powders with low density and weight [79,80]. Interestingly, ANFC is less affected by hornification in terms of redispersability. It has been reported that ANFC can be redispersed after drying as the -COOH groups seem to act as a barrier against hornification reversing the process upon rehydration [81]. ANFC has also been used to produce films [82] as well as aerogels [83].

Cellulose nanofibrils in plants have a high elastic moduli of 140 - 150 GPa and possess high aspect ratios of over 250 [84,85]. The high stiffness is caused by the firmly bonded individual fibers present in a hierarchical alignment order. The hierarchical alignment is lost when the material is fibrillated to form NFC or ANFC. Up to date the alignment of individual nanofibrillated fibrils during drying has not been achieved for films, aerogels and powders as the alignment of the fibrils is limited by their physical dimensions [85]. Thus the mechanical strength of these dry forms is reduced significantly when compared to the potential of natural cellulose nanofibrils in plants. Nevertheless, the mechanical properties of NFC after fibrillation are still excellent as elastic modulus of 29 - 36 GPa [86] and tensile strength of 1 - 3 GPa [87,88] have been proposed for individual fibers. The elastic modulus values between 120 - 220 GPa have been reported for native cellulose crystals [89,90] and therefore NFC also possesses high toughness. Due to excellent mechanical properties NFC has been studied as a strengthener for composite materials [75]. In the composite approach the controlled alignment of the fibrils to a certain extent has been achieved resulting in the greater harnessing of the innate mechanical strength of NFC and ANFC fibrils [85].

2.2.3 Pharmaceutical and biomedical applications

Cellulose is considered to be biocompatible due to moderate, if any, foreign responses *in vivo* [91,92]. Both grades, NFC [93-95] and ANFC [94,96], have also been shown to be biocompatible and nontoxic in several *in vitro* cell models, making them appealing for pharmaceutical and biomedical applications [5,97]. NFC hydrogels have been investigated widely in biomedical field, such as in implantable drug delivery [98], cell carrier systems attached to surgical sutures [99], cell encapsulation [100] and scaffold synthesis [101]. Furthermore, NFC hydrogel is also a suitable cell culture scaffold material for HepG2 and stem cell differentiation and three dimensional cell culturing [65,102-104]. In the dry state NFC films have been used in wound healing applications to promote skin regrowth in skin graft donor sites treatment [105].

Only a few studies have focused on the use of NFC or ANFC as a pharmaceutical excipient in modified release drug delivery formulations. Valo et al. have [71,106] used NFC for stabilization of nanoparticles. They showed that nanoprecitation of itraconazole in the presence of a surface active and genetically engineered hydrophobin fusion protein HFBI coupled with two cellulose binding domains could be used to create a functional coating on the surface of itraconazole nanocrystals [71]. The protein was used to facilitate binding of the nanoparticles to NFC matrix which increased the storage stability of the suspensions both before and after freeze-drying. Furthermore, the *in vivo* performance of the itraconazole was increased due to increased dissolution rate of itraconazole resulting from the decreased particle size of itraconazole. Valo et al. [106] further showed that the drug release rate of beclomethasone dipropionate nanoparticles embedded in a NFC aerogel could be tuned depending on the NFC aerogel origin. Four different NFC aerogels with embedded nanoparticles were evaluated. Drug release was immediate from red pepper and microcrystalline cellulose aerogels, whereas sustained release profiles were obtained with bacterial cellulose, quince seed and TEMPO-oxidized birch cellulose-based aerogels. It was clearly shown, that the structure of the aerogel and the interactions between nanoparticles and cellulose determined the drug release rate.

Kolakovic et al. have explored NFC as a pharmaceutical excipient in tablets [107], spray-dried microparticles [108] and sustained release films [109]. As a tableting excipient the spray-dried NFC nanofibers were successfully used with paracetamol for direct compression and tableting after wet granulation [107]. The tablet disintegration and dissolution studies showed an immediate drug release comparable results to “golden standard” direct compression excipient microcrystalline cellulose based tablets. Opposite to this, the spray-dried NFC microparticles with an average diameter of 5 µm showed a sustained drug release profile for over 60 days for encapsulated drugs [108]. Here it was shown that NFC microparticles can sustain drug release by forming a tight fiber network that limits drug diffusion from the system. Also the NFC films, produced with a filtration method and a high drug loading capacity between 20% and 40%, had a sustained drug release profiles close to zero-order kinetics for indomethacin, itraconazole and beclomethasone up to 3 months [109]. The control for drug release was here provided by

the NFC films as the film sustains the drug release due to a tight fiber network around the incorporated drug crystals. Finally, the drug interactions with NFC films have also been explored by Kolakovic et al [110] with model drugs of different structural characteristics (size, charge, etc.). Here it was shown that the model drugs did bind to NFC films in a pH dependent manner and the main binding mechanism could be characterized as electrostatic forces.

Crosslinked ANFC nano- and microgels have been proposed by Masruchin et al. [69] for the encapsulation and sustained release of small molecule drugs. Here the internal structures of the hydrogels, namely porosities, and swelling behavior were modified with cations (H^+, Ca^{2+}, Al^{3+}), which in turn had a significant impact on drug release profiles. It was suggested that drug release could be controlled by altering the internal structure of ANFC hydrogels during preparation. Also Weishaupt et al. [111] have exploited he negatively charged carboxyl groups on the surface of ANFC fibers as binding sites for various macromolecules such as peptides and enzymes. In essence, ANFC can act as a high-density carrier which enables the immobilization of drugs and macromolecules by electrostatic interactions.

The publications highlighted above are a selected collection of research focused on NFC and ANFC use in the pharmaceutical and biomedical field. The main focus of this thesis work was to explore the potential of NFC and ANFC as excipients in pharmaceutical modified release formulations and expand the use of NFC and ANFC. The unique structural properties, high biocompatibility and low toxicity of these materials are all in favor of using them as novel pharmaceutical excipients.

2.3 Microcrystalline cellulose

MCC is used in pharmaceutical, food, polymer composite and cosmetics industries due to its renewability, economic value, non-toxicity, biodegrability, mechanical properties, high surface area and biocompatibility [112,113]. The following two chapters will give a short overview of MCC production techniques and properties as well as typical use in pharmaceutical applications.

2.3.1 Production and properties

MCC is obtained from purified and partially depolymerized α-cellulose precursor. As described in the chapter regarding cellulose structure the α-cellulose microfibrils consist of crystalline and amorphous regions at nanometer range [22-24]. The crystalline regions comprise tight bundles of microcrystals formed by cellulose chains due to hydrogen bonding and van der Waals interactions. In the preparation of MCC, the amorphous mass is removed from the microfibril structure [112]. It is possible to prepare MCC by treating α-cellulose with different processes such as acid hydrolysis [114,115], reactive extrusion [116], enzyme mediated depolymerization [117] or steam explosion [118,119]. When microfibrils are subjected to acid hydrolysis the amorphous regions are readily hydrolyzed

resulting in the production of shorter and crystalline fragments of MCC [114,115]. Typically MCC surface has a slight negative charge due to hydroxyl residues. By means of processing, the DP of the cellulose chain can be reduced with negligible weight loss. For MCC, the DP is typically less than 350 glucose units and the material has a high degree of crystallinity between 55 % - 80 % range [120].

After the removal of amorphous regions and filtration the neutralized MCC slurry is typically spray-dried to a pure fine particle size MCC powder or alternatively co-processed with a water-soluble polymer to obtain a colloidal suspensions form [112]. MCC suspensions are thixotropic and shear-thinning the extent however differs depending on raw material and MCC preparation method [121]. Avicel® was the first commercialized MCC grade in 1962 [122]. Nowadays, several commercial MCC grades are readily available with for example different particle sizes, densities, porosities, hydration swelling capacities, compressibility, moisture sorption capacity and mechanical properties.

Recently, a new MCC grade named AaltoCell™ has been produced from never dried cellulose pulp under scalable conditions [123]. As the cellulose material remains undried during the processing, the resulting MCC material is more porous (due to lack of hornification) [124] and the cellulose matrix remains water-swollen. Furthermore, the production process of this new MCC grade has been deemed as environmentally sustainable and the processing conditions enable the adjustment of solid cellulose content in the dispersions [123].

2.3.2 Pharmaceutical applications

MCC is the most frequently used cellulose based pharmaceutical excipient and it can be used in the manufacturing of several dosage forms. Generally MCC is considered to be the diluent with the best binding properties and it is one of the preferred binders in direct compression of tablets [125]. MCC also has self-disintegrating properties which can be utilized together with superdisintegrants to promote fast disintegration of tablets [126]. In wet granulation process MCC is useful as a binder [127].

MCC is also applicable for the stabilization of emulsions, suspensions, and foams [113]. In emulsions and suspensions the stabilization is achieved through thickening and viscosity enhancement or steric hindrance. The amphiphilic nature useful for emulsion stabilization arises from the presence of the free hydroxyl groups on the MCC surface that acts as hydrophilic points, whereas the crystalline portion functions as the hydrophobic domain [128,129]. MCC can also be used in combination with other cellulose derivatives to provide suspension stabilization. For example, Dan et. al [130] have used MCC mixed with CMC sodium (MCCS) as a dispersant for the spray-drying of drug suspension. The study showed that MCCS prevented the aggregation of drug nanoparticles in the suspension state, agglomeration during spray-drying process and furthermore enabled fast redispersability of the suspension.

Up to date MCC has been used extensively as an excipient in various pharmaceutical formulations. However, MCC is mostly used as the dried powdered form for tablet production or used in combination with other excipients in emulsion or suspension stabilization. So far, the use of the new MCC grade AaltoCell™ as a pharmaceutical excipient has not been reported. This thesis has aimed at exploring the use of concentrated MCC hydrogel dispersions (AaltoCell™) as platforms for controlled drug release applications. The hydrogel-like properties of these dispersions in addition to the enhanced colloidal stability of the new MCC material may be of use as a drug release rate controlling matrix in the hydrated state as currently the majority of commercial Avicel grades are better suited as excipients for pharmaceutical formulations in the dry state.

2.4 Modified release systems

In the literature, the term modified-release drug product is used to describe products that can alter the timing and/or the release rate of a drug compound [131]. Several types of drug products with different drug release characteristics can be defined under the term modified-release (Table 1). Based on the drug release characteristics of the products multiple different terms can be used to define and describe the various types of modified release products. Extended-release, delayed-release, targeted-release and orally disintegrating tablets can all be defined as modified-release drug products. The physicochemical, pharmacokinetic and pharmacodynamic properties of a drug compound as well as the properties of other materials used to formulate the dosage form define the basis for the design of modified-release formulations for different drug administration routes.

Table 1. *Drug release characteristics of modified release drug products [131].*

Modified release drug products	Mode of action	Drug release characteristics
Extended-release (ER)	At least a twofold reduction in dosage frequency compared to conventional dosage form	Controlled-release (CR) Sustained-release (SR) Long-acting drug products
Delayed-release (DR)	A time delay in the drug release after administration, after which the dose is released	Delayed-release of the dose due to e.g. enteric-coating
Targeted-release	Drug release at or near the physiological target	Either immediate- or extended-release
Orally disintegrating tablets	Rapid disintegration in the saliva present at oral cavity	Immediate release

By definition, controlled-release formulations belong as a subgroup to the wider group of modified-release formulations. Controlled release drug delivery systems provide temporal and/or spatial control of drug release in the human body [132]. Additionally these systems may protect the drug from undergoing degradation or elimination under physiological

conditions. Figure 3 shows the effect of drug release profiles of conventional, sustained and zero-order controlled release on drug plasma concentration [133]. The therapeutic window of drug therapy lies between minimum effective concentration and minimum toxic concentration. Conventional single dosing of a tablet or intravenous injection may results initially for an elevated plasma concentration followed by a fast decrease in drug concentration below the therapeutic range. On the contrary, extended release systems can be utilized to adjust the plasma drug concentration within the therapeutic window with less fluctuation for a prolonged duration of time. Extended release (ER) formulations include sustained release (SR) and controlled release (CR) dosage forms. The difference between these two lies in the control of drug release rate. For a SR formulation the drug release is maintained over a sustained period, whereas from a CR formulation the drug release rate is kept constant over a sustained period. Overall, the goal with these formulations is to improve patient compliance and efficacy of drug therapy with reduced side-effects.

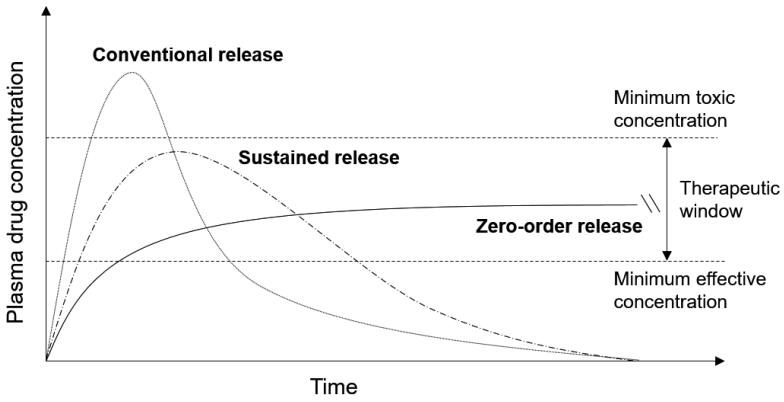

Figure 3. *Simplified schematic of different drug release profiles [133]. Figure modified from reference.*

A significant effort has been focused on developing different controlled and modified release technologies over the past 40 years [133]. Polymeric material is often the component that controls drug delivery and is usually the key ingredient in controlled release formulations [134,135]. Controlled release drug delivery systems have been classically divided in to the following four types based on the technique that regulates the drug release profile: a) pre-programmed rate, b) activation modulated, c) feedback regulated and d) site targeted [136].

Delivery systems with a pre-programmed release profile have a predefined specific release rate for the cargo. The drug release rate may be defined with several parallel mechanisms such as wetting of the system, porosity of the system, water diffusion into the system, drug dissolution followed by diffusion, osmotic effects, polymer swelling and/or degradation and drug-excipient interactions [137,138]. Generally the mechanisms that are controlling the drug release from pre-programmed release systems include diffusion, swelling (water

penetration) or chemical control (erosion of polymer matrix), and the slowest process defines the overall drug release from the device [132,134].

Activation modulated systems require an internal or external stimuli for drug release to occur. Extensive research has been focused on triggers such as pH changes [139], light exposure [140], magnetic field [141], temperature changes [142] and exposure to enzymes [143]. Feedback-regulated systems are capable of self-regulating and adjusting the release according to the cues from physiological environment. Up to date e.g. carbon dioxide responsive [144] and glucose sensitive systems [145,146] have been explored. Site targeted systems are ideally capable of precise spatial control into the desired physiological target site. The development of these systems has been explored especially in cancer therapy where the efficacy of the treatment with minimal side-effects to healthy tissues is of utmost importance [147,148].

In the experimental part of this thesis, the potential of NFC and ANFC as drug release rate controlling polymers was explored in several modified release formulation types such as emulsions, hydrogels and mucoadhesive films. In the emulsions, the fibers in the continuous aqueous phase were used to encapsulate the oil phase droplets that contained the poorly water-soluble drugs. The ability of different cellulose fiber grades to control the drug release rate was evaluated. Potentially these emulsions could be used to solubilize effectively poorly-water soluble drugs and to provide tunable drug release characteristics in the gastrointestinal tract. In the hydrogel formulations, ANFC as well as MCC were evaluated as matrices for diffusion controlled drug release applications. ANFC hydrogels consist of a fiber network, whereas MCC hydrogel dispersions consist of a network of individual MCC particles. The hydrogel structure itself can be thought of as matrix type release rate controlling barrier. The mucoadhesive NFC/ANFC films were designed to be used in location-specific applications, where the drug release will occur at the oral mucosal membrane. Here the NFC/ANFC films were used for drug encapsulation and as platforms for the bioadhesive functionality imparted by mucoadhesive biopolymers. Diffusion was the main release mechanism in all the explored formulations throughout this thesis. The following chapter will describe the fundamentals of diffusion controlled drug delivery systems in more detail.

2.4.1 Diffusion controlled drug delivery systems

Diffusion is a mass transport process, where the net movement of molecules, ions or atoms occurs from a high concentration region to low concentration region against a concentration gradient. Diffusion has a significant role for drug release in most controlled drug delivery systems [137]. For diffusion controlled systems, other mass transport systems do not affect the drug release rate or the impact of other mechanisms can be considered negligible. The systems can be classified based on the physical structure as well as the ratio of initial drug loading to drug solubility. Figure 4 demonstrates diffusion controlled drug delivery systems that can be divided as reservoir devices and matrix systems. Based on the geometry of the device, mathematical equations for each type of

system can be used as tools for quantitative prediction of drug release mechanism, effect of formulation and processing [149,150]. The desired drug release profile can be achieved with the understanding of optimal formulation, device composition and manufacturing process.

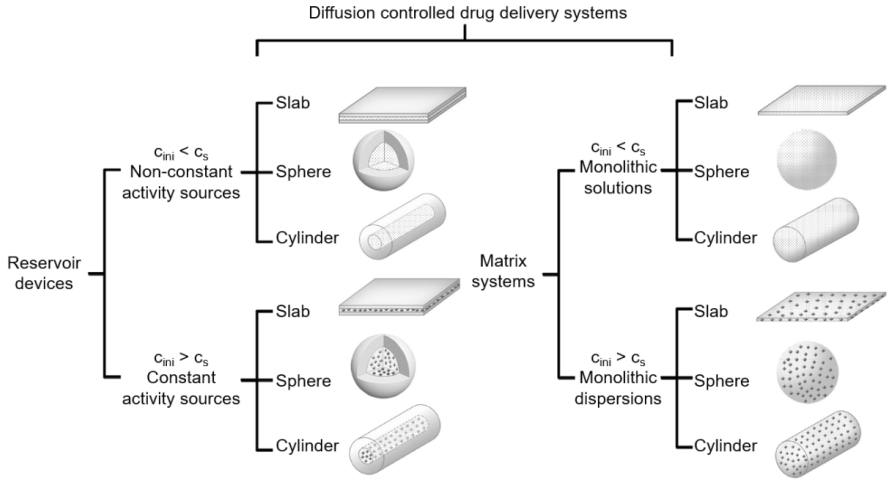

Figure 4. *Schematic presentation of diffusion controlled reservoir and matrix type drug delivery systems [151]. The dots indicate completely dissolved drug molecules whereas the circles non-dissolved drug particles. Abbreviations:* c_{ini} *= initial drug concentration,* c_s *= drug solubility.*

2.4.1.1 Reservoir devices

For reservoir devices, the molecularly dispersed drug within the core and the release rate controlling barrier material in the shell are completely physically separated [151]. For non-constant activity source devices the initial concentration of drug (c_{ini}) in the core does not exceed drug solubility (c_s) and there is no excess drug present in the core. The released molecules are not replaced over time and first order release kinetics is obtained for all geometries (slab, sphere and cylinder) with an exponentially decreasing release rate. For constant activity source devices the initial concentration of drug in the core does exceed drug solubility and there is an excess amount of drug present in the core. The released molecules are replaced as there is a saturated drug solution present in the core. Due to this, the drug concentration at the inner membranes surface remains constant and zero-order release kinetics is obtained as the cumulative amount of released drug increases linearly over time.

2.4.1.2 Matrix systems

In matrix systems, the drug and the release rate controlling material are distributed evenly throughout the device [151]. Based on initial drug loading to drug solubility ratio these systems can be divided as monolithic solutions and monolithic dispersions.

Monolithic solutions

In monolithic solutions ($c_{ini} < c_s$) the drug is rapidly completely dissolved upon water penetration as the initial drug concentration is below solubility. Fick's second law of diffusion can be solved for each geometry (slab, sphere and cylinder), which can be useful if it is necessary to calculate the cumulative drug release over time [151,152]. Also, if a parameter such as diffusion coefficient in a specific polymer matrix is unknown the equations can be fitted to experimental data. For thin films with negligible diffusional mass transport through the edges (slab geometry) of the film compared to diffusion through the main surface of the film Equation 1 can be used [153]:

Monolithic solutions with slab geometry (Eq. 1):

$$\frac{M_t}{M_\infty} = 1 - \frac{8}{\pi^2} \sum_{n=0}^{\infty} \frac{exp[-D(2n+1)^2\pi^2 t/L^2]}{(2n+1)^2} \quad (1)$$

where M_t and M_∞ signify the cumulative amounts of drug released at time t and infinite time ∞, D is the diffusion coefficient of the drug within the matrix system and L represents the thickness of the film. Alternatively early times ($M_t/M_\infty \leq 0.6$) and late times ($M_t/M_\infty \geq 0.4$) approximations depicted by Equation 2 and 3 may be used [151]:

Early times:

$$\frac{M_t}{M_\infty} = 4\left(\frac{Dt}{\pi L^2}\right)^{\frac{1}{2}} \quad , \frac{M_t}{M_\infty} \leq 0.6 \quad (2)$$

Late times:

$$\frac{M_t}{M_\infty} = 1 - \frac{8}{\pi^2} exp\left(-\frac{\pi^2 Dt}{L^2}\right) \quad , \frac{M_t}{M_\infty} \geq 0.4 \quad (3)$$

Monolithic dispersions

In monolithic dispersions ($c_{ini} > c_s$) an excess amount of drug is present in relation to solubility. As water penetrates into the system the drug is only partially dissolved and therefore dissolved and non-dissolved drug is present in the matrix during drug release. The classical Higuchi equation (Eq. 4) can be used to quantify drug release from monolithic dispersions with slab geometry [154,155]:

$$M_t = A\sqrt{D c_s (2c_{ini} - c_s)t} \quad (4)$$

where M_t signifies the cumulative amount of drug released at time t, A is the total surface area of the film exposed to the release medium, D is the diffusion coefficient of the drug within the matrix system, c_s drug solubility in the wetted matrix and c_{ini} the initial drug concentration in the matrix system. However, there are several conditions that have to be taken into account when the Higuchi equation is used to approximate drug release [151,156]:

- Water penetration into the slab as well as drug transport in release medium are fast, however the drug transport within the slab is rate limiting.
- Dissolution of unsolved drug particles inside the slab is fast in comparison to the diffusion of dissolved molecules within the system.
- Sink conditions are maintained in the receiving bulk solution throughout the release experiment.
- The size of drug particles is smaller than the slab thickness and the drug is homogenously distributed in the matrix.
- The diffusion coefficient remains constant.
- The slab does not exhibit swelling or dissolve, and the surface area of the slab is high compared to the thickness.

2.5 Oral mucoadhesive drug delivery systems

The oral route is the most popular drug administration route with the highest patient compliance. An alternative administration route with ease of administration and high patient compliance is by diffusion into and through oral mucosae located in the oral cavity. Sublingual and buccal mucosae have been studied most extensively and there are currently several formulation types, such as buccal tablets, films, and sublingual tablets, on the market that utilize mucoadhesion for local drug administration into the oral cavity or through the sublingual mucosa [157]. Buccal formulations have been developed for example for the prevention of migraine [158] and for the local antibiotic treatment of periodontal diseases [159]. Advantages of mucoadhesive drug delivery include [160,161]: (a) extending the residence time of drug compounds and localizing the effect at the target site, (b) high absorption rate induced by blood supply and good blood flow rates (sink conditions for absorption), (c) higher bioavailability through avoidance of first-pass metabolism, (d) less drug degradation as acidic conditions in gastrointestinal tract are avoided and (e) rapid onset of action.

The oral mucosa is covered with a visco-elastic layer of mucus which constitutes mainly of mucins that are high molecular weight glycoproteins with a negative net charge close to neutral pH of oral cavity [162-164]. Absorption of mucins results in well hydrated mucus layers on top of epithelial cells. The role of mucin on mucosal membranes varies from lubricants to defensive components in the mucus layer protecting against pathogens [165]. Furthermore, mucin also functions as a biochemical filter that can bind nutrients as well as a wide variety of different compounds [166]. These high binding capabilities of mucins have been exploited in the design of bioadhesive applications in pharmaceutical and biomedical sciences. Mucoadhesion is defined as the attachment of formulation to the biological membrane; however several different mechanisms occur at the formulation-mucus interface [167]. The mucoadhesion process involves two steps where first a close contact with the bioadhesive and mucus membrane is achieved and the bioadhesive material is wetted or swells due to the contact. Secondly, the bioadhesive material penetrates into the surface of the mucus membrane. Processes involved in mucoadhesion, in addition to wetting and surface penetration, include electronic interlocking between negatively charged mucus membrane and positively charged polymers [168], diffusion of

mucoadhesive polymer chains into the glycoprotein network of the mucus layer [169] and adsorption due to hydrogen bonding and van der Waals forces [170].

Polymers, both natural and synthetic, are typically used as mucoadhesive materials in buccal films and tablets for the encapsulation and incorporation of drugs into the mucosal membrane. The most important characteristics required from mucoadhesive formulations include sufficient swelling and wetting capabilities, hydrogen-bonding functional groups and flexibility to accommodate polymer network entanglement [162]. Other important factors are low irritation to mucosa tissue, non-toxicity, biocompatibility and biodegrability [171]. Typical natural polymers used are chitosan [172,173], pectin [174] and mucin [163,175]. They all offer high mucoadhesive properties with low toxicity. An example of a synthetic class polymers, poly(acrylic acid), cellulose ester derivatives, and polymethacrylate derivatives are the most commonly used [162].

Key aspects that are studied *in vitro* in the development of mucoadhesive film formulations include tensile strength, thickness, swelling, dissolution rate, and mucoadhesion strength [161]. Generally, buccal films should be small and flexible in order to be non-irritant and acceptable to patients. The swelling should be moderate to facilitate drug dissolution and absorption while keeping the formulation attached. The toxicity and irritability of the formulation should also be assessed with suitable *in vitro* models prior to *in vivo* testing. TR146 cell-line has been utilized as a model of the human buccal epithelium in predicting permeability through the human buccal mucosa and toxicity [176,177].

The mucoadhesiveness strength of a formulation is a key parameter for ensuring the prolonged contact time of a formulation at the target site, which is essential for the success of drug therapy. Texture analysis techniques have been widely used in the evaluation of mucoadhesive properties *in vitro*, such as mucoadhesiveness strength [178,179]. Various formulations such as hydrogels, tablets and films have been investigated with mucin disks and porcine buccal mucosa tissue as binding substrates. Texture analysis methods measure the adhesiveness between the binding substrate and the formulation. Typical outputs for these measurements are peak force adhesiveness and work of adhesion. Further *in vivo* evaluation contains usually a buccal absorption test, perfusion study, residence time and pharmacokinetic study [161]. The *in vitro* tools offer a feasible option for formulation development and optimization prior to *in vivo* testing.

In the experimental part of this thesis, bioadhesive NFC/ANFC films were prepared by incorporating natural origin biopolymers into the films. The potential of these films as mucoadhesive drug delivery systems for the local delivery of drugs into the oral mucosal tissue was evaluated *in vitro*.

2.6 Freeze-drying of pharmaceuticals

Freeze-drying (or lyophilization) is a commonly used method for drying of heat sensitive materials such as protein pharmaceuticals and biological samples [180-182]. The freeze-drying process consists of three subsequent process steps of freezing, primary drying and

secondary drying. The low temperatures during the process protect the active materials. Freeze-dryers consist of chamber, condenser, vacuum pump and cooling components [183]. Various parameters that have an impact on the freeze-drying include the product (formulation, solid content), type of container (geometry, fill volume, heat transfer), equipment (freeze-dryer model, probes) and process (shelf/chamber temperature, chamber pressure, time) [182,184,185]. The following chapter will give an overview of the freeze-drying process parameters as well as formulation aspects. Only the freeze-drying of aqueous solutions is considered, although it is possible to use other solvents as well for materials that do not dissolve in water.

The first step in the freeze-drying process is to freeze the material in suitable vials. As the formulation contains essentially solutes in an aqueous solvent the resulting solution has a lower freezing point than the pure solvent or solute [186]. The term freezing-point depression is used to describe this phenomenon. The freezing rate of the material affects the nucleation of ice and the formation of ice crystals [187,188]. At high cooling rates (above 5°C/min) a large amount of small ice crystals is quickly formed, but the ice sublimation time is long [189,190]. Slow cooling rates (1-5°C/min) result in slower formation of fewer large ice crystals resulting in shorter ice sublimation time. The ice growth affects the texture and porosity of the final product [191]. Fast cooling rate can be obtained with liquid-nitrogen dipping and it has been shown to be a more suitable freezing method e.g. for the preservation of nanoparticle structures during freeze-drying as opposed to slow freezing rate [192]. Depending on the freeze dryer model, the freezing step may be performed prior to moving the material inside the freeze-dryer chamber, but in shelve temperature controlled models the freezing rate is adjusted by adjusting the temperature of the shelves.

After freezing, the pressure inside the freeze-drying chamber is reduced below the conditions at the triple point of water (where water exists as solid, liquid and gas simultaneously) [193]. Lowered temperature and pressure allows the vacuum sublimation of solid frozen ice crystals directly from solid phase to gas phase. The vapor pressure of ice provides the driving force for water removal in lowered temperature and pressure [194]. The sublimation of ice crystals is called the primary drying cycle. Approximately 95% of water is removed during primary drying [195]. The sublimation process usually moves as a “sublimation front” from the outermost exposed parts into the deeper layers of a sample, therefore the water vapor needs to move through the freeze-dried sample [196]. Vial fill volume (height of liquid statue) and dimensions as well as the solid content in the formulation create resistance to sublimation and affect the duration of primary drying.

After primary drying the secondary drying is performed to remove any unfrozen water ionically-bound or adsorbed to the freeze concentrated material [197,198]. The temperature is typically raised higher than during primary drying to break the bonds between the material and remaining water molecules. The freeze-drying cycle is complete after the secondary drying. Normal atmospheric pressure can be restored with an inert gas and the vials stoppered inside the drying chamber under sterile conditions. Freeze dried materials have porous structure with typically low residual moisture content of 1-5 % [189].

The stability of the active material during freeze-drying and storage as well as the total duration of the process are the main concerns for optimization of the freeze-drying process. From a formulation perspective the critical properties include eutectic melting temperature (T_e), amorphous collapse temperature (T_c), glass transition temperature of maximally freeze-concentrated solution (Tg'), properties of the excipients and the stability of the drug itself [180]. An optimized freeze-drying process operates near the maximum allowable product temperature. During primary drying, the temperature should be kept below T_e for a crystalline eutectic system and below T_c as well as Tg' for an amorphous system [199]. For mixed systems that contain both crystalline and amorphous material lower than critical temperatures should be used (i.e. below T_e, T_c, Tg'). Otherwise, the eutectic crystalline solid melts down or the viscosity of the amorphous solute phase decreases resulting in the loss of macroscopic structure, collapse of the structure and high residual moisture content [199,200]. T_c is typically from ca. 2°C to several degrees higher than Tg' depending on the ice sublimation rate [201]. The critical temperatures of any formulation can be analyzed with freeze-drying microscopy or thermal analysis prior to freeze-drying to avoid quality issues [202,203]. The final product should have a porous structure with good dehydration properties and acceptable appearance.

The main reason for freeze-drying of drugs and protein pharmaceuticals is to improve their storage stability [204]. Drugs, peptides, proteins and other complex molecules may undergo chemical reactions such as hydrolysis, crosslinking, oxidation, aggregation and disulfide rearrangements in aqueous solutions that affect the product stability and efficacy [205-207]. In the dry state these reactions can be substantially retarded thus improving stability during storage [208,209]. Typically excipients are added to create physical stability as the active material is present at low concentration in the formulation and may require support against dehydration stress [185,204,210]. Several, cryo- and lyoprotectants can be selected to increase the physical stability of proteins during-freeze-drying [211,212]. Generally cryoprotectants protect against protein denaturation in the freezing step and lyoprotectants prevent protein inactivation due to dehydration stress during drying [213]. Polyols such as mannitol [214,215] and disaccharides such as trehalose [216,217] and sucrose [218-220] and polyhydric alcohols such as polyethylene glycols (PEGs) [221-223] are among the most commonly used protectants. Table 2 summarizes some of the most widely used cryo- and lyoprotectants used as stabilizing excipients in the freeze-drying of proteins.

Table 2. *Cryo- and lyoprotectants used in the freeze-drying of proteins.*

Group	Compound	References
Polyols	Mannitol, sorbitol, glycerol	[224,225]
Disaccharides	Sucrose, trehalose, lactose, melibiose, glucose	[216,218,219,226,227]
Polymers	Bovine serum albumin, dextran, PVA, PEGs, HPMC	[219,226,228-231]
Non-aqueous solvents	Dimethylsulphoxide, PEGs, glycerol	[221-223,232,233]
Surfactants	Tween 80, Brij 35	[231,234]
Amino acids	Glycine, proline	[222,235]

Freeze-drying process has been utilized for the production of highly porous NFC and ANFC aerogel structures [78,83]. These aerogel matrices can be used as templates for encapsulation and controlled release of pharmaceuticals [106]. However, rehydration of the aerogels back into hydrogel form has not been extensively studied due to the tendency of NFC/ANFC fibers to aggregate during drying. However, the carboxyl groups present on the ANFC fiber surface improve the rehydration of the material after drying and reverse the hornification to some extent [81]. In principle, cryo- and lyoprotectants could be used as stabilizing excipients to preserve the nano-scale structures of NFC and ANFC fibers during freeze-drying as there is already abundant evidence in the literature showing that cryo- and lyoprotectants have been used to preserve the structure and activity of therapeutic proteins during freeze-drying (Table 2). The structural loss of NFC and ANFC fiber dimensions during drying is caused by the hornification process where adjacent fibers aggregate together when hydrogen bonds with water molecules are lost [7]. As shown with proteins, cryo- and lyoprotectants can be used to replace the lost hydrogen bonds with water [236,237]. The fiber hornification somewhat limits the use of NFC/ANFC aerogels solely into the dry form as upon reconstruction back into the hydrogel form the rheological properties may be lost especially for NFC [79,238].

Consequently, there is a need to explore new materials and material combinations suitable for providing protection to the NFC and ANFC nano-scale structures during freeze-drying. As a part of this thesis, the freeze-drying and consequent rehydration of ANFC hydrogels in the presence of commonly used cryo- and lyoprotectants (trehalose and PEG 6000) was explored. More specifically, the rheological and drug release properties were evaluated after reconstruction of ANFC aerogels back into hydrogels. As such, the freeze-drying could provide opportunities for the long term storage of therapeutics encapsulated in cellulose fiber aerogels. Furthermore, successful rehydration could expand the use of these cellulose based aerogels into hydrogel dosage form that can be stored in the dry aerogel state and administered upon need as rehydrated hydrogels.

3 Aims of the study

The aim of this thesis project was to evaluate natural cellulose based polymers for the encapsulation of active materials in several pharmaceutical formulation types. Nanofibrillated cellulose (NFC), anionic type nanofibrillated cellulose (ANFC) and novel microcrystalline cellulose (MCC) grades were used in the preparation of emulsions, hydrogels, aerogels, films and dispersions.

The specific aims of the present study were:

1. To test the suitability of NFC, ANFC and MCC for the encapsulation and controlled release of active materials **(I, II, IV).** For this purpose emulsions, hydrogels, aerogels and dispersions were prepared and the performance with regard to drug release properties was evaluated.

2. To utilize the functionality of cellulose based materials (NFC, ANFC and MCC) without further chemical modification. Properties of cellulose-based materials were exploited for drug release applications, e.g. as release rate controlling matrices and to prolong the contact time at drug absorption target site (**III, IV**).

3. To promote the use of NFC and ANFC in various drug release and therapeutic applications. As a stabilization agent, mucoadhesive film forming material and as a hydrogel and aerogel matrix for modified drug release applications **(I-III).**

4 Experimental

Complete details of all the materials, methods and equipment used in this thesis work can be found in the respective original publications (**I-IV**).

4.1 Materials

4.1.1 Nanofibrillar cellulose (I-III)

1.73% NFC (GrowDex®) and 0.56 % oxidized ANFC (-COOH 1.02 mmol/g pulp) nanofibrillated cellulose hydrogels were kindly provided by UPM-Kymmene Corporation, Finland (**I**). Due to birch-based raw material, the NFC contained some soluble hemicelluloses. NFC hydrogel was diluted with ultrapure water to form 5 mg/ml stock solution and ANFC at 5.6 mg/ml was used as received (**I**). 3.2 % and 6.8 % ANFC (-COOH 1,06 mmol/g pulp) hydrogels (FibDex™) were kindly provided by UPM-Kymmene Corporation, Finland (**II**). The diameter of most of the fibrils was in the range of 4–10 nm with length of 500 – 10 000 nm (**II**). 1.5% NFC (GrowDex®) and 2.7 % ANFC (-COOH 1.03 mmol/g of fibers) hydrogels were purchased from UPM-Kymmene Corporation, Finland and used as film forming polymers (**III**).

4.1.2 Microcrystalline cellulose (IV)

Three un-dried microcrystalline cellulose grades (AaltoCell™) termed as non-dispersed MCC, mechanically dispersed MCC-D and lignin containing mechanically dispersed MCC-L were prepared according to an earlier protocol by Vanhatalo et al. [123]. These were used as 2.4 %, 5 %, 10 % and 12 % (wt) gels (**IV**).

4.1.3 Biopolymers: HFBII, pectin, mucin, chitosan (I, III)

Hydrophobin class II protein HFBII from *Trichoderma reesei* was provided as lyophilized powder by VTT Technical Research Centre of Finland, Finland and used as a 5 mg/ml stock solution for the preparation of emulsions (**I**). Mucin from bovine submaxillary gland (EMD Millipore, USA), chitosan oligosaccharide lactate (Sigma-Aldrich, USA) and pectin from apple (Sigma-Aldrich, China) were used as mucoadhesive polymers in NFC and ANFC films (**III**).

Microcrystalline cellulose (MCC, Avicel PH200, FMC BioPolymer, Ireland) and mucin from porcine stomach (Type-II) (Sigma-Adrich, USA) were used to prepare 600 mg mucin tablets (4:1 mass ratio) used as binding substrates in the evaluation of mucoadhesive strength (**III**). Tablets were wetted with 1 % solution of mucin from bovine submaxillary glands (Type-I) (Sigma-Aldrich, USA) prior to adhesion testing.

4.1.4 Model compounds and reagents (I-IV)

Naproxen (NAP, Sigma-Aldrich, USA) and ibuprofen (IBU, Sigma-Aldrich China) were prepared as 1 mg/ml stock solutions in soybean oil (Sigma-Aldrich, USA) (**I**). The solubility of NAP and IBU in soybean oil and ethyl oleate was experimentally determined after equilibrating excess amounts of drugs for 72 h at 25 °C. 4 kDa FITC-dextran (FITC-DEX, Sigma-Aldrich, Sweden, **II**), metronidazole (MZ, Sigma-Aldrich, China, **II, III, IV**), nadolol (NAD, Sigma-Aldrich, Finland, **II**), ketoprofen (KETO, Orion Pharma, Finland, **II**), lysozyme from hen egg (LZ, Roche, Germany, **II, IV**) were obtained from various suppliers. The most important physicochemical properties of model compounds are given in Table 3.

Table 3. *Physicochemical properties of model compounds.*

Compound	MW (g/mol)	Solubility (mg/ml)	pKa/pI	Charge at pH 7.0	Ref.
NAP	230.3	0.0159 (MQ) 2.8 - 3.6 (pH 7.4)	4.15	-	[239,240]
IBU	206.3	0.021 (MQ) 6 (pH 7.4)	4.85	-	[241-243]
KETO	254	0.107 (25 °C), ~ 40.7 (pH 7)	4.06	-	[244-247]
NAD	309	8.3 (25 °C), 8.3 (pH 7)	9.28	+	[246,248]
MZ	171	10.5 (25 °C), 10.5 (pH 7)	2.38	ø	[246,249, 250]
BSA	6.65×10^4	40	4.6 - 4.8	-	[251,252]
LZ	1.47×10^4	>10	11.1	+	[253,254]
FITC-DEX	4000	50		ø	[252]

Soybean oil (Sigma-Aldrich, USA) and ethyl oleate (Sigma-Aldrich, UK) were used as oil phases in emulsions (**I**). Polyethylene glycol 6000 (Fluka, Switzerland) D-(+)-trehalose dihydrate (tre, Sigma-Aldrich, USA) were used as freeze-drying excipients (**II**). Sodium phosphate salts (Sigma-Aldrich, Germany) were used in the preparation of 0.1 M pH 7.4 phosphate buffer (**I**) and 50 mM pH 6.8 phosphate buffer (**III**). Dulbecco's Phosphate Buffered Saline (10X) concentrate without calcium and magnesium (Gibco, UK) was used as pH 7.4 drug release buffer (**II, IV**). Bio-Rad Protein Assay reagent (Bio-Rad, USA) was used for LZ assay (**II**). Acetonitrile (ACN) was of analytical grade (Sigma-Aldrich, Germany) (**I-III**). All model compounds and reagents were of analytical grade. All other chemical were at least of analytical grade. Ultrapure water was used to prepare all the solutions.

4.2 Production techniques

4.2.1 Emulsification (I)

Oil-in-water (o/w) emulsions with a 1 ml final volume and 10% oil phase were prepared from combinations of ultrapure water, soybean oil, ethyl oleate, HFBII, NFC and ANFC stock solutions. For IBU and NAP emulsions, the stock solutions of drugs in soybean oil were used in combination with the other formulation components. All formulations were premixed by repeated pipetting in Eppendorf tubes prior to ultrasound- sonication with a high intensity ultrasound processor (Sonics, USA) equipped with a 2 mm stepped microprobe (power 750 W, frequency 20 kHz and amplitude 30%). The samples were kept in an ice bath during 4 x 30 s of sonication and afterwards the samples were homogenized further in an ultrasonic bath for 1 h.

4.2.2 ANFC hydrogel formulations (II)

3 % and 6.5 % ANFC hydrogel formulations with 2 % MZ, 1.7 % NAD, 3.4 % KETO, 1 % FITC-DEX, 1 % BSA and 0.5 % LZ were prepared in 10 ml syringes (**II**). The hydrogels were homogenized with the model compounds by mixing inside two attached syringes (200 times through the syringe nozzle). For MZ, NAD and KETO an excess amount of the drug in relation to solubility (at pH 7) was mixed with the ANFC hydrogels resulting in monolithic dispersions. For FITC-DEX, BSA and LZ the solubility limit (at pH 7) was not exceeded thus resulting in monolithic solutions in ANFC hydrogels. The 3 % and 6.5 % ANFC hydrogel formulations with MZ, NAD, KETO and BSA were also prepared with 1 % of PEG6000 and 0.3 % of trehalose.

4.2.3 Freeze-drying (II)

Pure ANFC hydrogels, ANFC hydrogels with 1% of PEG6000 and 0.3 % of trehalose and ANFC hydrogels with MZ, NAD, KETO, BSA with 1 % of PEG6000 and 0.3 % of trehalose were used for the production of aerogels with a freeze-drying process (**II**). 2.5 ml of each hydrogel type was placed inside a 10 ml syringe, followed by fast liquid nitrogen freezing for 1 min. The frozen samples were immediately transferred to a freeze dryer (FreeZone 2.5, LabConco, USA) and freeze-dried in a vacuum (70 mTorr) at a sublimating temperature of -52 °C for 29 h. The freeze-dried aerogels were rehydrated gravimetrically with ultrapure water into their original concentrations. Homogenization inside two syringes was used to redisperse the aerogels back into their hydrogel forms.

4.2.4 Film production by liquid molding (III)

NFC or ANFC hydrogels were thoroughly mixed with the powders of mucoadhesive polymers pectin, mucin or chitosan in 10:1, 2:1 and 1:1 (NFC/ANFC: polymer) mass ratios relative to the dry NFC/ANFC fiber contents in 20 ml glass vials. For mucoadhesive strength measurements without MZ, 4 g of the hydrogel formulations (all mass ratios with each polymer) in plastic petri dishes (4 cm diameter) were dried for 18 h at 45 °C in an

oven. Films for swelling, tensile strength, solid state characterization, drug release and toxicity studies were prepared from 9.0 g of the hydrogel formulations placed in a 3D printed (Ultimaker 2+ 3D printer, Netherlands) round PLA mold (4 cm diameter) attached with Teflon bottom and oven dried for 18 h at 45 °C. For these measurements only films with 2:1 mass ratio of NFC/ANFC to either pectin or mucin were evaluated. MZ amount was set to 10% of cellulose and polymer dry mass in drug containing films. Films were prepared without MZ for tensile strength measurements, whereas for swelling, drug release studies, SEM imaging, solid state characterization and toxicity studies, MZ containing films were also used. NFC/ANFC-mucin films retained the diameter of 4 cm during drying, whereas for pectin films the diameter was reduced to 3.5 cm after drying. The films were stored inside a silica desiccator at 25 °C until used.

4.2.5 MCC matrices (IV)

MCC (AaltoCell™) was prepared from undried pulp according to a previously described method [123]. The preparation of the MCC formulations with 1% of model compounds, MZ and LZ, was carried out by mixing the compounds as powders to the 12% MCC, MCC-D and MCC-L dispersions. A manual mixing procedure was carried out by pressing the sample several times through the nozzle of two attached syringes. For MZ and LZ the solubility limit was not exceeded thus resulting in monolithic solutions in MCC, MCC-D and MCC-L dispersions.

4.3 Characterization of formulations

4.3.1 Emulsion characterization (I)

The zeta-potential values of emulsion droplets were measured by a ZetaSizer Nano-ZS (Malvern Ltd., UK) in water at 25°C in a folded capillary cell (Malvern Ltd., UK). Hydrodynamic diameter and size distribution of emulsion droplets were measured by dynamic light scattering (DLS) measurements by a ZetaSizer Nano-ZS (Malvern Ltd., UK) in water at 25°C in disposable polystyrene cuvettes (Sarstedt, Germany). DLS measurements were performed at day 1 and at day 28 after the emulsion preparation, whereas zeta-potential measurements were performed only at day 1. The stability of the emulsions during 1 month storage in glass vials at 4°C was evaluated by following the phase separation with qualitative emulsion stability index (ESI) values. Digital camera images were taken to follow the phase separation of emulsions, namely the separation of the clear aqueous phase from the volume fraction of opaque emulsion phase. The digital camera images were analyzed with ImageJ software (National Institutes of Health, Bethesda, USA). ESI values were calculated from the volume of separated water and total volume as follows (5):

$$ESI = 1 - \frac{V_{w,separated}}{V_{total}} \quad (5)$$

where ESI value 1 corresponds to completely unseparated emulsion whereas 0 is a value for completely separated system. Optical microscopy images of emulsions were taken as a quality control with an optical microscope (Leica DMLB, Germany) and a microscope coupled digital camera. The morphologies of emulsions were further imaged and characterized with 200 kV Tecnai F20 Cryo-TEM microscope (FEI Company, Holland).

4.3.2 Rheology (I-II, IV)

Dilute NFC and ANFC solutions (I):

The shear viscosities of ultrapure water, 0.1 % and 0.15 % NFC and ANFC solutions were measured at 4°C with HAAKE Viscotester iQ Rheometer (Thermo Fisher Scientific, Karlsruhe, Germany) equipped with a Peltier system for temperature control. Cup and double-gap cylinder geometry was used with a 4.0 mm gap and 2.64 ml sample volume. Before each measurement (n=3), the samples were allowed to rest for 2 min at 4°C after which the measurements were performed by increasing the shear rate from 100 to 1900 1/s.

ANFC hydrogels (II):

The rheological measurements were performed a with HAAKE Viscotester iQ Rheometer (Thermo Fisher Scientific, Germany) at 37°C equipped with a Peltier system for temperature control. Parallel 35 mm diameter steel plate-and-plate geometry was used with a 1 mm gap in all measurements. The samples were allowed to rest for 5 min at 37°C prior to measurements. Shear viscosity was measured by increasing the shear rate from 0.1 to 1000 1/s. The linear viscoelastic region was determined with controlled stress amplitude sweeps with constant angular frequency ω = 1 Hz and oscillatory stress between $1x10^{-4}$ – 500 Pa. In the measurements for storage (G') and loss modulus (*G*") the chosen oscillatory stresses for frequency sweeps were τ = 50 Pa (3% ANFC) and τ = 100 Pa (6.5% ANFC) and the angular frequency range was 0.6 - 125.7 $rads^{-1}$.

MCC matrices (IV):

The rheological properties (n=3) of the different MCC grades were studied at 22 ˚C by oscillatory shear rheometer (AR-G2 Magnetic Bearing Rheometer, TA Instruments) with a parallel 20 mm diameter steel plate geometry and 1000 µm gap. The rheological properties of the different MCC grades were investigated by oscillatory stress sweep and viscosity test. In the oscillatory stress sweep, the storage (G') and loss (G'') modulus were measured at a constant angular frequency of 1 Hz and oscillatory stress between 0.01 – 100 Pa. Shear viscosities were measured as a function of the shear rate ranging from 0.01 to 1000 s^{-1}. Commercial Avicel® PH-101 (Merck, Germany), was used as a reference material in the rheology experiments.

4.3.3 Tensile strength (III)

Film sample sizes were 20 x 2 mm, length and width respectively, and the films were equilibrated at 50 % relative humidity and stored at 20 ˚C overnight before the tensile test. The film samples were displaced on a measuring table with a support for displacement sensor (215−514 comparator stand, Mitutoyo, Japan) and film thicknesses (n=3) were measured by the displacement sensor (LGF-0110L-B, Mitutoyo, Japan) with a digital reader (EH-10P, Mitutoyo, Japan). After which, tensile test (n=3) were performed with the tensile tester (100 N load cell, Kammrath & Weiss GmbH, Germany) in Tensile/Compression Module 5 kN in a humidity controlled chamber. Average of strain-stress curves were obtained by dividing the tensile load curve with the cross-sectional area of the respective sample and were used to calculate the Young's modulus (YM), tensile strength, elongation and toughness.

4.3.4 Film swelling (III)

Film samples (n=3) of NFC/ANFC in combination with pectin or mucin (in 2:1 mass ratio) with approximately 1 cm^2 surface area were immersed into 50 mM pH 6.8 phosphate buffer for 15 s or 5 h at 25 °C. The film weight was measured prior to and after the hydration period in the buffer and also after re-drying for 20 h at 45 °C. The weight increase as hydration percentage (n=3) was calculated with the following equation:

$$\textbf{\textit{Hydration \%}} = (X_t - X_0) / X_0 \times 100 \quad (6)$$

where X_t is the weight of the swollen sample and X_0 is the original weight of the sample. The mass of the original sample was compared to the corresponding weight after the swelling test and re-drying to obtain mass loss percentage (n=3) as follows:

$$\textbf{\textit{Mass loss \%}} = (X_0 - X_d)/X_0 \times 100 \quad (7)$$

where X_d is the weight of the re-dried sample. The effect of swelling on surface area after 30 min exposure to the release buffer was evaluated only for selected formulations used in the drug release studies. The original dry film thickness was obtained from SEM images (n = 10), whereas surface area in dry and wetted state, as well as thickness in the wetted state were obtained from digital camera images with ImageJ software (National Institutes of Health, Bethesda, USA).

4.3.5 Mucoadhesive strength (III)

Mucoadhesive strength of the NFC/ANFC films combined with pectin/mucin/chitosan was evaluated with a texture analyzer TA.XT plus (5 kg load cell, Stable Microsystems Ltd, UK) in texture profile analysis (TPA) mode. 13 mm diameter mucin-MCC tablets were direct compressed (force 3000 kg, 30 s) in a Carver press and the tablets were attached horizontally into the lower end of a 10 mm diameter TA.XT plus probe and the whole tablet surface was wetted with 1 % mucin solution. Each film type (n=3) was placed under the analytical probe in flat Petri dishes and the probe was lowered until the mucin disc was in close contact with the surface of the sample. Parameters used in the

measurements included: 0.50 mm/s pre-test speed, 0.30 mm/s test speed, 0.3 mm/s post-test speed, 100 g applied force, 4 mm return distance, 15 s contact time and 3 g trigger force. Exponent software (Stable Microsystems Ltd., UK) was used is results analysis and peak adhesion force (N) required to detach the mucin tablet from the surface of the film was used as the measure of mucoadhesive strength.

4.3.6 Solid state analysis (II-III)

ANFC aerogels (II):

The morphology of the freeze-dried aerogels was evaluated from cross-section and surface structure micrographs obtained with a scanning electron microscope Quanta FEG250 (SEM, FEI Company, USA). Aerogel samples fixed onto a two-sided carbon tape were sputtered with platinum for 25s with an Agar sputter device (Agar Scientific Ltd., UK) prior to imaging. The residual moisture content of the aerogels was determined by heating the samples from 25 to 240°C at a heating rate of 10°C/min in nitrogen (40 ml/min) atmosphere using a TGA (TGA 850, Mettler-Toledo, Switzerland). Mass loss (%) of evaporated water was used to quantify the residual moisture content of the aerogels. Thermal analyses of ANFC aerogels were carried out using a differential scanning calorimeter Mettler Toledo DSC 823e (Mettler Toledo, Giessen, Germany). The samples were placed in sealed aluminum pans with closed lids and heated at a scanning rate of 10 °C/min between 25 and 200 °C in nitrogen atmosphere.

Bioadhesive NFC and ANFC films (III):

The morphology of the films was evaluated from cross-section and surface structure micrographs obtained with a scanning electron microscope (SEM, FEI Company, USA). Prior to imaging, the samples fixed onto a two-sided carbon tape were sputtered with platinum for 25s with an Agar sputter device (Agar Scientific Ltd., UK). Thermal analysis of selected films was carried out by heating the samples at a scanning rate of 10 °C/min between 25 and 220 °C in nitrogen atmosphere using a differential scanning calorimeter Mettler Toledo DSC 823e (Mettler Toledo, Giessen, Germany). ATR-FTIR spectroscopy was carried out to characterize the films, using a Vertex 70 FTIR spectrometer (Bruker Optik GmbH, Germany) with a MIRacle^{TM} single reflection ATR crystal (Pike Technologies, Inc., USA). The analytical range in the measurements was 650 to 4000 cm^{-1} with a spectral resolution of 4 cm^{-1}. Principle component analysis (PCA) was used to evaluate the data, and it was performed with standard normal variate (SNV) transformed and mean-centered spectra using SIMCA software (Sartorius Stedim Biotech, Sweden). Raman spectroscopy analysis was performed for the films with a Raman RXN1 spectrometer, equipped with a PhAt probe head and a 20-mW laser source operating at 785 nm (Kaiser Optical systems, Inc., USA). The spectra were analyzed after removal of elevated baselines using a rubberband correction method (Opus software, Bruker Optik GmbH, Germany). The spectra were normalized by SNV transformation and mean centering before analysis by PCA (SIMCA software, Sartorius Stedim Biotech, Sweden).

4.3.7 Dissolution studies (I-IV)

Emulsions (I):

In order to determine the drug release characteristics of NAP and IBU from emulsions the side-by-side-diffusion cells (Laborexin, Finland) were used. Nuclepore Track-Etch polycarbonate membrane filters (0.4 µm pore size, surface area of 0.785 cm^2) were clamped between two identical halves of diffusion cells. 0.8 ml of drug containing emulsion (0.1 mg/ml of drug) was transferred into the donor compartment (n=3). Donor and acceptor compartments were filled to 3.5 ml final volume with buffer solution (0.1 M phosphate pH 7.4). The diffusion cells were kept at 37°C by a surrounding water socket to mimic physiological conditions. The control samples in the donor compartment contained free drug solutions of NAP and IBU at 0.08 mg drug / 3.5 ml volume corresponding to 100 % of drug in the emulsions. Samples were collected from the acceptor compartment up to 8 h and replaced with fresh buffer.

ANFC hydrogels (II) and MCC matrices (IV):

1.07 g of ANFC hydrogel formulations were used to fill disc molds with a constant flat surface area of 1.33 cm^2 exposed to the release buffer (**II**). The discs were placed inside 150 ml amber glass vials, which were then filled to a final volume of 70 ml with pH 7.4 phosphate buffered saline and kept at 37°C under constant magnetic stirring (400 rpm) on top of a multi-position magnetic stirrer IKA RT10 (IKA-Werke GmbH & Co KG, Germany). Samples were withdrawn up to 144 h and replaced with fresh buffer (n=3). The diffusion coefficients for NAD, KETO and MZ (**II**) inside hydrogels (initial drug concentration > drug solubility) with slab geometry were calculated with Higuchi equation (5) which was reduced to (6) as in the system $C_{ini} > C_s$ [154-156,255]:

$$Q = \sqrt{D(2C_{ini} - C_s)C_s t} \tag{8}$$

$$D = \frac{Q^2}{2C_{ini}C_s t} \tag{9}$$

where Q is the amount of drug released in time t per unit area, D is the diffusion coefficient of the drug within the matrix system, C_{ini} represents the initial drug concentration in the matrix system, C_s is the drug solubility in the matrix media. Diffusion coefficients for FITC-DEX, BSA and LZ (**II**) inside ANFC hydrogels (initial drug concentration < drug solubility) with slab geometry were calculated with the unsteady-state form of Fick's second law of diffusion (2) with early values of time when $0 < M_t/M_\infty < 0.6$ [151]:

$$\frac{M_t}{M_\infty} = 4\left(\frac{Dt}{\pi L^2}\right)^{\frac{1}{2}} \quad , \frac{M_t}{M_\infty} \leq 0.6 \tag{2}$$

where M_t and M_∞ denote the cumulative amounts of drug released at time t and infinite time ∞; D is the diffusion coefficient of the drug within the matrix system; L represents

the thickness (1 cm) of the hydrogel. D was obtained from fitting the data of M_t/M_∞ at selected time points.

For MCC matrices, the setup for the drug release studies of MZ and LZ (**IV**) was similar to that of ANFC hydrogels, however here 1.11 g of MCC formulations were used to fill the disc molds and for both compounds: initial drug concentration < drug solubility. The diffusion coefficients inside MCC matrices were calculated with the unsteady-state form of Fick's second law of diffusion (2) with early values of time when $0 < M_t/M_\infty < 0.6$. D was obtained from fitting the data of M_t/M_∞ at selected time points.

NFC and ANFC mucoadhesive films (III):

Films were cut into squares with an area of 1 cm^2 and placed inside 20 ml glass vials, which were filled with 10 ml of 50 mM pH 6.8 phosphate buffer. The drug release studies (n=3) were performed inside an incubator shaker Titramax 1000/Incubator 1000 (Heidolph, Germany) at 37 °C (200 rpm) and samples were collected up to 30 min and replaced with fresh buffer.

4.3.8 Analysis of the model compounds (I-IV)

NAP (**I**), IBU (**I**), KETO (**II**), NAD (**II**) and MZ (**III**) concentrations from the drug release samples (**I**) were analyzed with Ultra performance liquid chromatography (UPLC) instrument Acquity UPLC (Waters, USA). UPLC parameters are summarized in Table 4.

Table 4. *UPLC parameters for quantification of the drugs.*

Drug	Column	Mobile phase	λ (nm)
NAP	BEH Shield 1.7 µm (Waters, USA)	ACN:15 mM phosphate buffer pH 2 30:70 ratio	231
IBU	HSS-C18 1.8 µm (Waters, USA)	ACN:15 mM phosphate buffer pH 2 60:40 ratio	219
KETO	HSS-C18 1.8 µm (Waters, USA)	ACN:15 mM phosphate buffer pH 2 25:75 ratio	255
NAD	HSS-T3 1.8 µm (Waters, USA)	ACN:15 mM phosphate buffer pH 2 10:90 ratio	215
MZ	Primesep 100 5 µm (Waters, USA)	ACN:15 mM phosphate buffer pH 2 20:80 ratio	317

FITC-DEX quantification (**II**), at excitation wavelength of 490 nm and emission wavelength of 520 nm, was performed by fluorescence intensity measurements with Varioskan Flash (Thermo Fisher Scientific, Finland). MZ (**II, IV**) and LZ (**II, IV**) quantification at wavelengths of 320 nm and 280 nm respectively was performed by spectrophotometric analysis with Cary 100 UV-Vis (**II**) or Cary 50 UV-Vis (**IV**) spectrophotometer (Varian Inc., USA). BSA quantification (**II**) was performed by linearized colorimetric Bio-Rad protein assay, which is based on Bradford dye-binding

method [256,257], by measuring absorbance at 470 nm and 595 nm with Varioskan Flash (Thermo Fisher Scientific, Finland).

4.3.9 Toxicity studies with TR146 human buccal epithelium model (III)

Human squamous cell carcinoma, TR146 (passage #9, Sigma-Aldrich, UK) cells were cultured in Dulbecco's Modified Eagle Medium: Nutrient Mixture F-12 (DMEM/F-12, Gibco™, Thermo Fisher, USA) supplemented with 10 % Fetal Bovine Serum (FBS, Thermo Fisher, USA) and 2mM L-glutamine (GlutaMAX™, Thermo Fisher, USA). Cells were sub-cultured and incubated at 37°C, 5 % CO_2, and seeded into a standard cell culture 96-well plate for cytotoxicity studies ($2x10^4$ cells/well). Round pieces (Ø = 5 mm, n = 4) of bioadhesive films were cut and inserted into the wells with and without cells and incubated for 24 hours. After the incubation the films were removed and the cell proliferation reagent resazurin (alamarBlue®, Thermo Fisher, USA) was introduced into the wells followed by incubation and well plate measurement with Varioskan LUX multimode microplate reader (Thermo Fisher, USA) at excitation 565 nm and emission 585 nm wavelengths.

5 Results and discussion

5.1 NFC and ANFC as emulsion stabilizers (I)

It has been shown in our previous study that hydrophobin fusion proteins and NFC can be effectively used to stabilize o/w emulsions prepared from hexadecane and water solutions [6]. In the follow-up study presented here, the emulsions were further evaluated for: a) the ability of HFBII and NFC to stabilize the emulsions with pharmaceutically acceptable oils, b) the ability to control the drug release rate of poorly water-soluble BCS class II drugs naproxen (NAP) and ibuprofen (IBU) and c) the effect of the two different fiber grades, NFC and ANFC, on the stability and drug release.

5.1.1 Emulsion stability optimization

All emulsions were prepared with ultrasound sonication. The composition of the emulsions was 10% soybean oil/ethyl oleate and 90% water, which included the stabilizers. Reportedly HFBII is applicable for emulsion stabilization even at low concentrations due to the tendency of HFBII to adsorb on hydrophobic interfaces, converting them into hydrophilic and vice versa [258]. A series of HFBII stabilized emulsions were prepared to estimate the minimum amount of the protein required to gain stable emulsion droplets with the sonication method. Droplet diameters and zeta potential values as a function of protein concentration were measured. Higher HFBII concentrations above 0.5 mg/ml improved the stability, as the emulsion droplet sizes were effectively reduced, while the zeta potential values increased. After storage for 28 days a significant increase in droplet size and PDI values were observed for emulsions with low HFBII

content indicating insufficient stabilization. On the contrary, emulsions with HFBII content above 1 mg/ml had a decrease in the droplet sizes and PDI values at day 28. As HFBII has a tendency to self-associate and form tetramers in an aqueous solution at 0.5 - 10 mg/ml concentration range [259] it is likely that the changes were caused by the loss of excess protein at the o/w interface. The diameter of HS-3 emulsion droplets (~300 nm) was least susceptible to changes during storage, and therefore the 1 mg/ml (0.1 %) HFBII concentration was selected for further emulsion stabilization studies with NFC and ANFC. The ultrasound sonication process produced polydisperse size distribution for emulsion droplets; therefore other production techniques such as microfluidization [260] could offer more feasible options for the process scale-up and production of monodisperse droplets.

The emulsion stability index (ESI) was used as a qualitative measure for phase separation in further emulsion stability studies. NFC or HFBII at a predetermined concentration range of 0.1 - 1.5 mg/ml [6] were tested as sole emulsion stabilizers (Figure 5A and 5B). The stability was increased in direct proportion to the stabilizer amount.

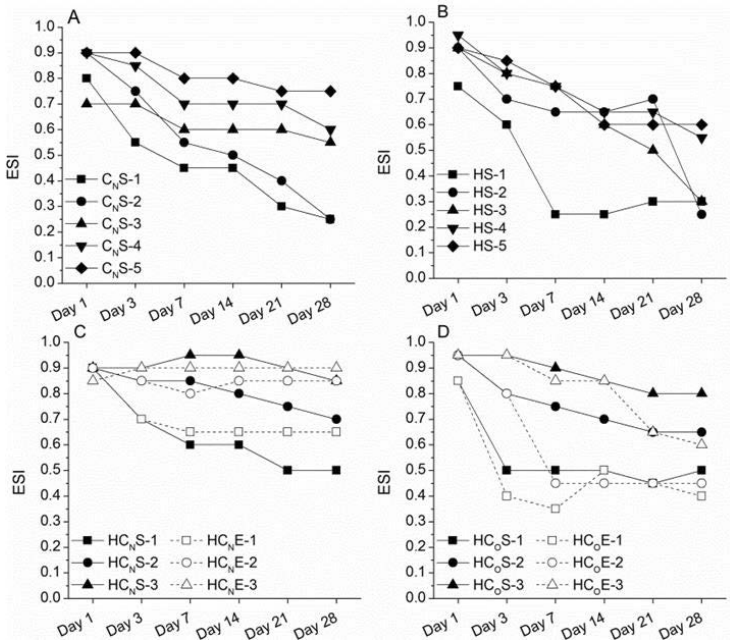

Figure 5. *Emulsion stability study up to 28 days. Emulsion stability index (ESI) values describe the phase separation of emulsions (ESI = 1 unseparated, ESI = 0 completely separated). The different emulsion formulations were: A) NFC-N/S (0.1-1.5mg/ml), B) HFBII/S (0.1-1.5mg/ml), C) HFBII-NFC-N (1/0.5-1.5 mg/ml)/S or E, D) HFBII-NFC-O (1/0.5-1.5 mg/ml)/ S or E. Abbreviations: H = HFBII, C_N = NFC-N (NFC), C_O = NFC-O (ANFC), S = soybean oil and E=ethyl oleate.*

In the previous study [6] it was shown that a continuous NFC matrix is formed in the aqueous phase of o/w emulsions at approximately 1 mg/ml NFC concentration and further stabilization was achieved by combining NFC with hydrophobin proteins (HFBs). Similar results were obtained in our study as the emulsion stability was further increased when

adequate amount of NFC or ANFC (1 - 1.5 mg/ml) was combined with HFBII (Figure 5C and 5D). Based on ESI values the soybean oil emulsions were more stable in comparison to ethyl oleate ones when adequate amounts of stabilizers were used.

The stabilizing effect of NFC/ANFC was hypothesized to be attributed to the concentration dependent viscosity modification of the continuous aqueous phase with NFC/ANFC. This reportedly creates a polymer network that limits drop collision, thus reducing the coalescence phenomena [72,73,261,262]. Shear viscosities of NFC and ANFC were measured in order to distinguish between the differences in the ability to modify the viscosity of the continuous aqueous phase (Figure 6). The viscosity profile of NFC up to 0.15 % was similar to pure water, whereas ANFC had a moderate shear thinning behavior and approximately ten times higher viscosity values than NFC. Clearly, ANFC even at these fairly low concentrations ANFC was more effective rheology modifier than NFC. The stabilizing effect of NFC at low concentrations was likely attributed to the reduced emulsion droplet movement rather that the increased viscosity of the continuous phase.

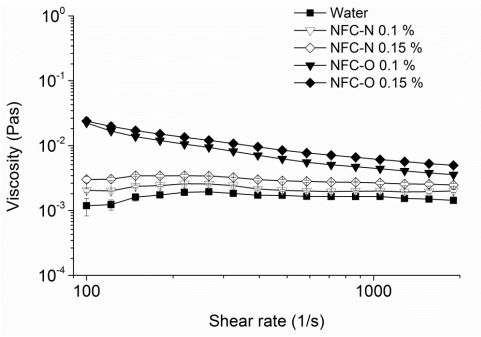

Figure 6. *Shear rate viscosities of water, 0.1 % and 0.15 % of NFC-N (NFC) and NFC-O (ANFC) at 4 °C (mean ± S.D., n=3).*

In order to select the preferable oil phase for the emulsions, the solubilizing capacity of soybean oil and ethyl oleate was determined for model compounds NAP and IBU (Table 5). Ethyl oleate had a higher solubilizing capacity for both drugs than soybean oil. The structural differences of the vegetable origin soybean oil and the fatty acid ester ethyl oleate attribute to the different drug solubilizing capacities of these oils [263-265]. Nevertheless, the solubility of both drugs in the oils was significantly (at least 100-fold) higher than the corresponding aqueous solubility in unbuffered water (MQ) ensuring effective solubilization in the emulsion formulations.

Table 5. Physicochemical properties of NAP and IBU. Solubility in soybean oil and ethyl oleate was verified experimentally.

Compound	Molar mass (g/mol)	pKa	logP	Solubility in aqueous media	Solubility in soybean oil	Solubility in ethyl oleate
NAP	230.3	4.15	3.18	15.9 mg/L, MQ[a] 2.8 - 3.6 g/L, pH=7.4[b]	2.8 g/L	5.1 g/L
IBU	206.3	4.85	3.97	21 mg/L, MQ[c] 6 g/L, pH=7.4[d,e]	46.2 g/L	98.7 g/L

[a] [240], [b] [239], [c] [241], [d] [242], [e] [243]

As in the preliminary experiments, soybean oil based emulsions were more stable than ethyl oleate formulations; soybean oil was selected for drug containing formulations. The formulations contained 0.1 % (1 mg/ml) of HFBII alone or in a combination with either NFC or ANFC in 1:1 or 1:1.5 mass ratios to HFBII. Based on solubility screening, the drug amount in the emulsions could be improved simply by increasing the drug concentration in the oil phase or alternatively by increasing the volume of the oil phase. However, further studies would be required to optimize the stabilizer amounts for emulsions with a higher oil phase volume.

5.1.2 Morphology and drug release

Light microscopy and cryo-TEM was used to confirm the expected stabilization mechanism for emulsions selected for drug release studies: a combination of HFBII stabilized oil droplets within NFC/ANFC fiber network. Spherical morphology and polydisperse droplet size, with diameters ranging from below 100 nm to few micrometers, was observed (Figure 7). HFBII coated droplets were encapsulated within the NFC and ANFC fiber networks. Interestingly, ANFC emulsions were more stable upon dilution as a more uniform droplet distribution and even distribution in the fiber network was observed. Furthermore, the shorter ANFC fibers effectively surrounded the droplets that had a tendency to form clusters. Conversely, upon dilution uneven NFC network was observed with less uniform distribution of the emulsion droplets within the NFC matrix.

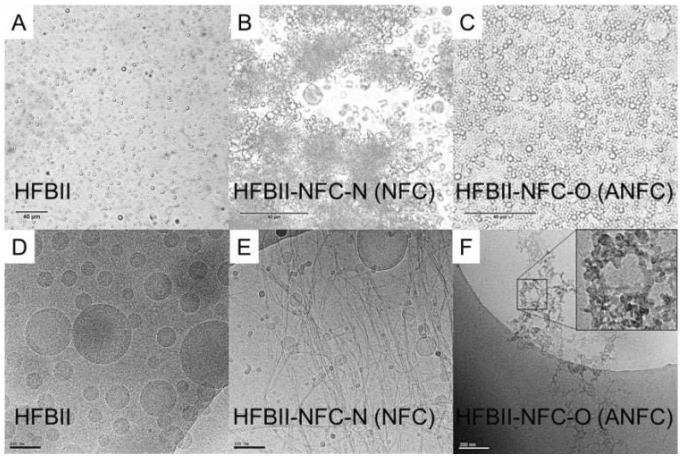

Figure 7. *Light microscopy images at 1:10 dilution (A-C) and cryo-TEM images (D-F) of HFBII, HFBII-NFC-N (NFC) and HFBII-NFC-O (ANFC) emulsions (1:1 mass ratio). Scale bar is 40 µm for A-C, 100 nm for D-E and 200 nm for F images.*

The drug release profiles of both model compounds, NAP and IBU, are presented in Figure 8. Major differences were observed based on the NFC and ANFC fiber grade. The drug release from NFC formulations reached 64 - 70 % for NAP and 67 % for IBU during 8h and resembled immediate release profiles of free drug solutions. Sustained release profiles were obtained with ANFC emulsions as only 18 – 27 % of NAP and 20 - 23 % of

IBU was released during 8h. Surprisingly, for solely HFBII stabilized emulsions an immediate release profile was obtained for IBU whereas a more sustained release for NAP was observed. Physical interactions such as stability, viscosity and the diffusion barrier of the emulsion droplets were most likely the critical traits in determining the drug release rates. ANFC and NFC are both negatively charged at pH 7.4. However, the carboxylated ANFC fibers have a greater negative net charge [45,111]. It is likely that the sustained release profiles from ANFC formulations were attributed to a greater surface barrier on the emulsion droplets created at the o/w-interphase through electrostatic attraction between negatively charged ANFC and positively charged HFBII. For NFC the effect was not as pronounced, resulting in immediate drug release profiles.

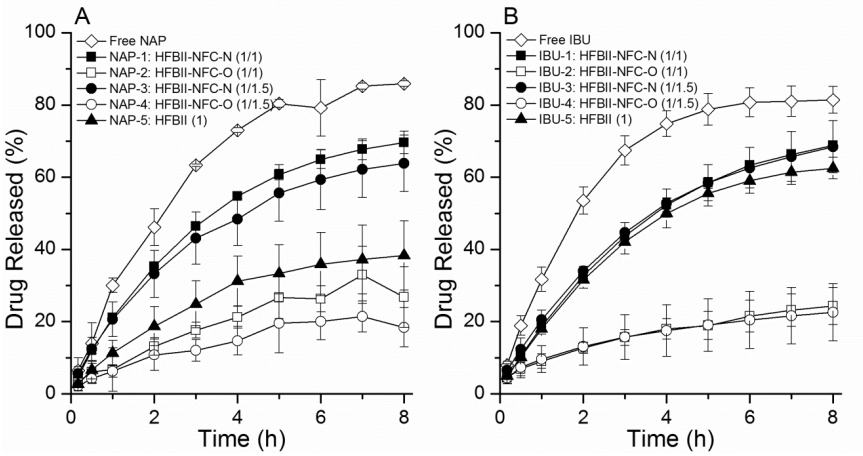

Figure 8. *Drug release studies with NAP and IBU: A) cumulative release (%) of NAP (mean ± S.D., n=3-5) and B) cumulative release of IBU (mean ± S.D., n=4-5) from different formulations. Mass ratios of HFBII to NFC-N (NFC) or NFC-O (ANFC) are in brackets. Free drug solutions of NAP and IBU were used as controls for immediate release.*

For solely HBFII stabilized emulsions, the solubility differences of model compounds at pH 7.4 were reflected in the release rates as it has been reported that the solubility of the diffusing species can have a greater effect on drug release rate than the interfacial film properties of the emulsion droplets [266]. HFBII controlled the drug release to some extent, but it was beneficial to add NFC / ANFC into the formulations to gain well defined release profiles. Chemical interactions with the drug molecules, such as aromatic π stacking, hydrogen bonding and electrostatic interactions were possible reasons for this effect [106,110,267]. Nevertheless, physical interactions were most likely more significant in determining the drug release rates.

In summary, the study showed that natural biopolymers HFBII, NFC and ANFC are applicable for stabilization of pharmaceutical emulsions. The stabilization was achieved with extremely low concentrations, providing an alternative to synthetic polymers. Furthermore, the drug release profiles could be tuned by the choice of fiber grade. HFBII-ANFC emulsions were effective in controlling the drug release rate, indicating the

suitability of these materials for controlled drug release applications. HFBII-NFC emulsions on the contrary, were more suitable for immediate drug release applications. Further studies are needed to determine the long term storage stability as well as stability in the gastrointestinal tract. Proteases (enzymes that perform proteolysis) present in the gastrointestinal tract could greatly affect the drug release properties from protein stabilized emulsions.

5.2 ANFC hydrogels and reconstructed hydrogels (II)

The potential of concentrated 3 % and 6.5 % ANFC hydrogels as controlled drug release matrices for several types of small (< 500 M) and large (> 1 kDa) molecular weight compounds was evaluated. The storage stability of pharmaceutical formulations is typically improved in the dry form, and therefore the hydrogels were freeze-dried and rehydrated back into the hydrogel form in order to evaluate the effect of the freeze-drying process on the performance of the hydrogels as controlled release matrices. The rheological and drug release properties were evaluated prior to and after freeze-drying and consequent rehydration to distinguish quality differences. Since cellulose-based ANFC fibers have a tendency to aggregate during drying, a combination of trehalose and PEG 6000 was evaluated as a cryo- and lyoprotectant against the hornification of ANFC fibers in order to preserve the nano-scale structure of ANFC fibers.

5.2.1 Aerogel characterization

The produced ANFC aerogels did not shrink considerably during freeze-drying and had a clear porous structure (Figure 9). High porosity and similar morphology was observed for all aerogels and the addition of model compounds did not alter the morphology significantly. As rapid liquid nitrogen freezing produces a large number of small ice crystals [180], the selected fast freezing method promoted the formation of porous ANFC aerogel structure during freeze-drying. Furthermore, the high protonation of ANFC carboxyl groups aids in the formation of porous ultrathin lamellar aerogel structures and high water uptake upon rehydration [268]. Regardless of the rather similar morphology of 3 % and 6.5 % ANFC aerogels, differences were observed in the rheological properties before and after the freeze-drying and rehydration process. The wettability and re-gelling of the aerogels was improved by the use of PEG 6000, which is recognized as a hygroscopic polymer that improves water uptake [269].

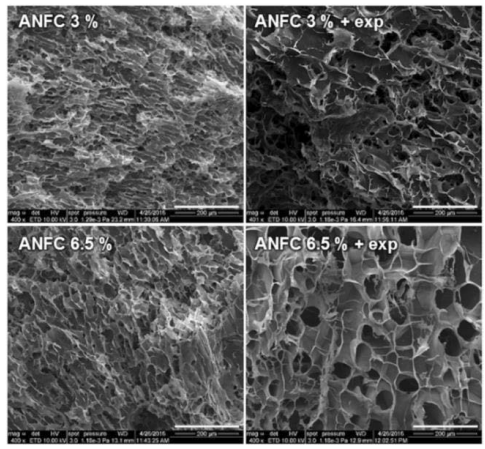

Figure 9. *SEM micrographs of highly porous 3 % and 6.5 % ANFC aerogels, 200 µm scale bar. Aerogels were freeze-dried without (left) and with the excipients (right, abbreviation: exp = 0.3 % trehalose/1 % PEG 6000).*

The residual moisture content was low in all aerogels indicating effective water sublimation during freeze-drying (Table 6). The small differences in residual moisture contents between 3 % and 6.5 % ANFC aerogels were likely attributed to the higher fiber content present in the 6.5 % starting material as the tightly bound surface water amount remained higher. The ability of trehalose to perform as a cryo-/lyoprotectant is attributed to its ability to replace water molecules hydrogen bonded to polar groups on the surface of materials during freeze-drying [236,237]. The amount of surface bound water on ANFC fibers was reduced due to this mechanism and lower residual moisture contents were observed when trehalose and PEG were used in the formulations. The hydrophilicity of model compounds was reflected on residual moisture contents of aerogels.

Table 6. *TGA and DSC analysis of ANFC aerogel formulations after freeze-drying (n=1). All formulations expect plain ANFC aerogels contained excipients. Abbreviation: exp = 0.3 % of trehalose / 1 % of PEG 6000.*

Formulation	Water content (%)	Tm (^{0}C) for drug or ANFC
ANFC 3 %	6.77	171.5
ANFC 3 % + exp	4.11	170 (ANFC/trehalose)
ANFC 6.5 %	7.48	174.0
ANFC 6.5 % + exp	5.81	187 (ANFC/trehalose)
BSA 1 % / ANFC 3 %	4.79	nd
BSA 1 % / ANFC 6.5 %	6.05	nd
MZ 100 % reference	nd	159.4
MZ 2 % / ANFC 3 %	2.42	148.7
MZ 2 % / ANFC 6.5 %	4.98	143.5
NAD 100 % reference	nd	128.8
NAD 1.7 % / ANFC 3 %	2.90	127.3
NAD 1.7 % / ANFC 6.5 %	4.79	128.3
KETO 100 % reference	nd	94.6
KETO 3.4 % / ANFC 3 %	1.96	81
KETO 3.4 % / ANFC 6.5 %	3.84	84

Thermal analysis with DSC showed a reduction in the onset melting points of model compounds with regard to pure references indicating interactions between the ANFC fibers and model compounds (Table 6). However, further binding studies would be required to confirm the binding mechanism of the drugs with the cellulose fibers.

5.2.2 Rheological properties

The aerogels were rehydrated and reconstructed with enhanced mechanical mixing. The rheological properties after reconstruction were compared to the original hydrogels. Shear viscosities of plain 3 % and 6.5 % ANFC hydrogels were significantly higher (ca. 150%) than the corresponding viscosity values of reconstructed hydrogels (Figure 10). This indicates the formation of aggregates in the hydrogels, since free individual fibers are responsible for the high viscosity of ANFC and NFC. A striking difference was seen when the excipients were included in the hydrogels: the viscosity values before and after-freeze drying were nearly overlapping. The addition of model compounds into hydrogels with excipients did not significantly alter the viscosity profiles (before and after freeze-drying) regardless of the high (i.e. undissolved) amount of small molecules (MZ, KETO and NAD). The shear-thinning behavior of a pseudoplastic material typical for ANFC hydrogels [63,65-67] was observed for all samples.

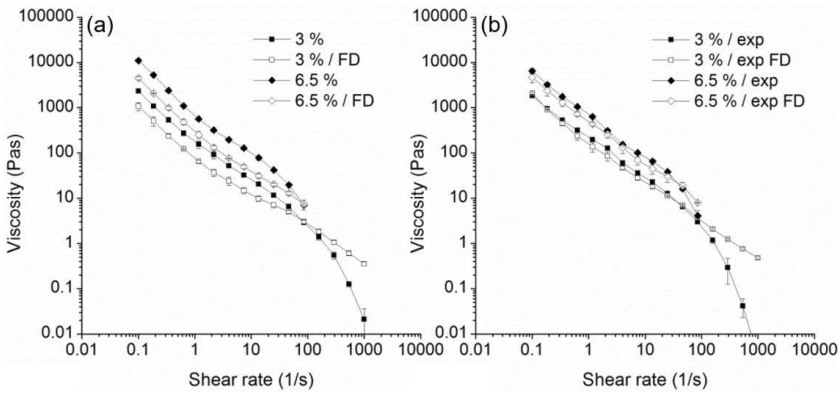

Figure 10. *Shear viscosity of plain 3 % and 6.5 % ANFC hydrogels before and after freeze-drying and redispersion without (a) and with (b) excipients (mean ± S.D., n=3). Abbreviations: FD = freeze-drying, exp = 0.3 % trehalose / 1 % PEG 6000.*

The viscoelastic properties of ANFC hydrogels prior to and after freeze-drying (with and without excipients) were also studied (Figure 11). The storage modulus (G') decreased after freeze-drying for all samples. Nevertheless, the G' values could be recovered significantly better with the use of excipients. The G' values of reconstructed ANFC hydrogels containing excipients resembled the values of original plain ANFC hydrogels without excipients prior to freeze-drying on both concentrations (3 % and 6.5 %).

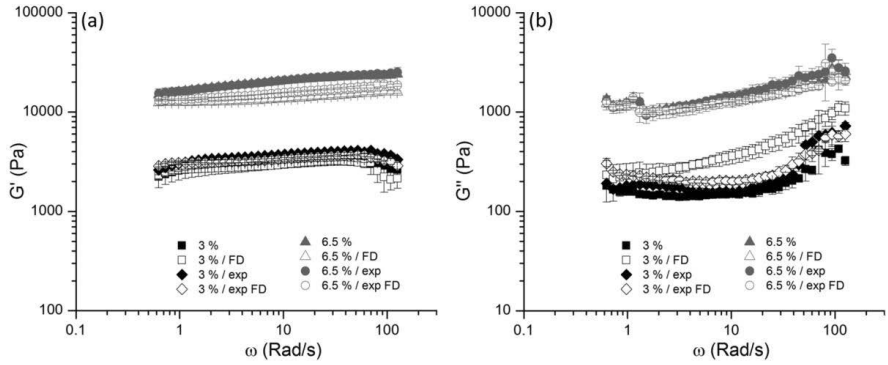

Figure 11. *Storage (G') and loss modulus (G'') of ANFC hydrogels before and after freeze-drying and redispersion (mean ± S.D., n=3). Abbreviations: FD= freeze-drying, exp= 0.3 % trehalose / 1 % PEG 6000.*

All samples, including hydrogels with model compounds, had higher G' than G'' values indicating an elastic behavior in ANFC hydrogels [63]. The presence of excipients reduced the effects of freeze-drying as at higher frequencies both G' and G'' reminded those of the original samples, indicating higher preservation of the elastic properties when compared to samples freeze-dried without excipients. Without excipients, the ratio of G' and G'' decreased and the viscous characteristics became more apparent over the elastic properties [270]. Based on the rheological measurements, the excipients preserved the structural integrity and limited the formation of aggregates. Therefore, it was apparent that excipients aided in the preservation of the rheological properties of ANFC hydrogels during freeze-drying.

5.2.3 Drug release and diffusivity

Based on previous publications, pH dependent electrostatic forces were expected to be the main binding mechanism of cationic drugs into ANFC fibers, whereas π stacking and hydrogen bonding may take place for neutral and anionic drugs in addition to electrostatic interactions [110]. The measured release profiles are presented in Figure 12. The diffusion coefficients of model compounds were calculated for the evaluation of diffusion rates without the impact of solubility inside ANFC hydrogels (Table 7).

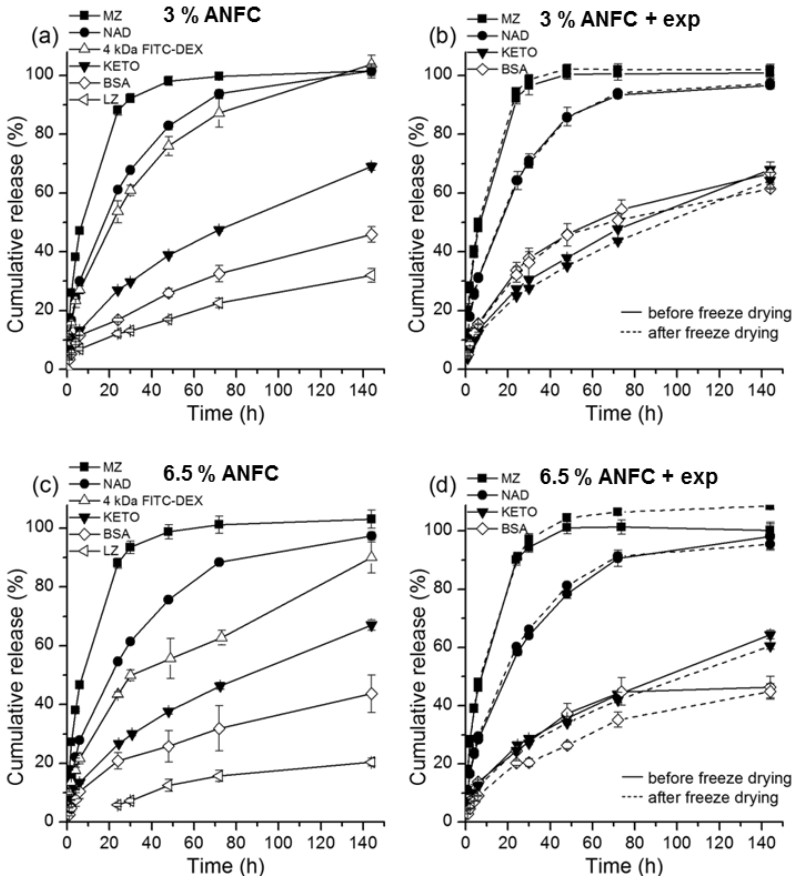

Figure 12. *Cumulative release profiles of MZ, NAD, KETO, BSA, LZ and 4 kDa FITC-DEX from ANFC hydrogels (mean ± S.D., n=3): (a) plain 3 % ANFC, (b) 3 % ANFC with excipients before and after freeze-drying, (c) plain 6.5 % ANFC and (d) 6.5 % ANFC with excipients before and after freeze-drying. Release buffer was PBS (pH 7.4) at 37°C.*

Table 7. *Diffusion coefficients in different ANFC hydrogel matrices. Freeze-dried formulations were reconstructed prior to diffusion studies. The net charge of model compounds at pH 7 in parenthesis. Abbreviation: exp= 0.3 % trehalose / 1 % PEG 6000.*

Compound	Diffusion coefficients in different ANFC hydrogels (10^{-8} cm^2/s)					
	3% ANFC	3% ANFC/exp	FD 3% ANFC/exp	6.5% ANFC	6.5 % ANFC/exp	FD 6.5% ANFC/exp
Ketoprofen (-)	62.9	60.9	54.5	58.0	52.8	47.4
NAD (+)	365.6	393.4	383.4	301.1	322.3	349.7
Metronidazole (ø)	745.7	823.0	841.5	733.3	761.8	779.6
BSA (-)	7.7	23.4	22.0	7.4	15.2	9.5
Lysozyme (+)	4.0	*nd*	*nd*	2.3	*nd*	*nd*
4 kDa FITC-dextran (ø)	58.9	*nd*	*nd*	35.6	*nd*	*nd*

The obtained release profiles were rather similar from corresponding plain and excipient containing hydrogels for both ANFC concentrations. Typically, small molecules have diffusion coefficients between 600 - 900 x 10^{-8} cm^2/s in water [271], whereas diffusivity values of 104 x 10^{-8} x cm^2/s and 60 x 10^{-8} cm^2/s for LZ and BSA have been reported [272,273]. In this regard, apart from MZ, ANFC hydrogels provided significant control for diffusion-mediated release of both small and large compounds.

The charge of small molecules had a weak to moderate impact on the cumulative release profiles from anionic ANFC matrices. Freeze-drying and rehydration had only minimal impact, whereas 6.5 % fiber concentration hindered the diffusion of small molecules more than the 3 % concentration. For the larger model compounds, net charge at pH 7, molecular size and ANFC fiber content all had a significant impact on the cumulative release profiles. Fastest release occurred in the order of 4 kDa FITC-DEX (ø) > 66.5 kDa BSA (-) > 14.7 kDa LZ (+). Therefore, the charge of the molecule could be more significant than the hydrodynamic diameter for large molecules (> 14 kDa), in terms of impact on the diffusivity in the ANFC matrices.

In summary, this study demonstrated that ANFC hydrogels can be freeze-dried and redispersed without affecting rheological and drug release properties. The cryoprotectants aided in preserving the structure of ANFC fibers during the freeze-drying process as rheological properties remained unaltered upon rehydration. As such the aerogel form of ANFC can be easily hydrated and administered upon need thus benefitting from higher storage stability in the dry form. Furthermore, ANFC hydrogel matrices are applicable for controlled drug release applications of several types of molecules.

5.3 MCC dispersions (IV)

Novel type MCC hydrogel dispersions (AaltoCell™), manufactured from never-dried pulp, were evaluated for their rheological properties and further for their applicability in controlled drug release applications. The evaluated matrices consisted of non-dispersed MCC, mechanically dispersed MCC-D and mechanically dispersed lignin containing MCC-L. Due to their colloidal stability, similarity in their rheological properties and feasible manufacturing processes, the new MCC hydrogels were evaluated as potential matrices for similar applications as NFC/ANFC hydrogels in the field of controlled drug release.

5.3.1 Morphology and rheology

The morphology of MCC (non-dispersed) prior to mechanical homogenization (Figure 13) reminded the form of cellulose fibers used as the starting material in the process, and rather large particles were visible in addition to finer fibers and their pieces. In the close up images of the mechanically treated grades, MCC-D and MCC-L, the material appeared to consist mostly of small fiber fragments and fine fibers with opened fibrillar structure. Therefore, the mechanical treatment effectively reduced the particle size of MCC and the majority of the needle-like fibrillary surface cellulose crystals had dimensions below 10

µm (MCC-D, MCC-L). Furthermore, the porosity of AaltoCell™ MCC grades is reportedly high, with pores in a 27 - 216 nm diameter range [124].

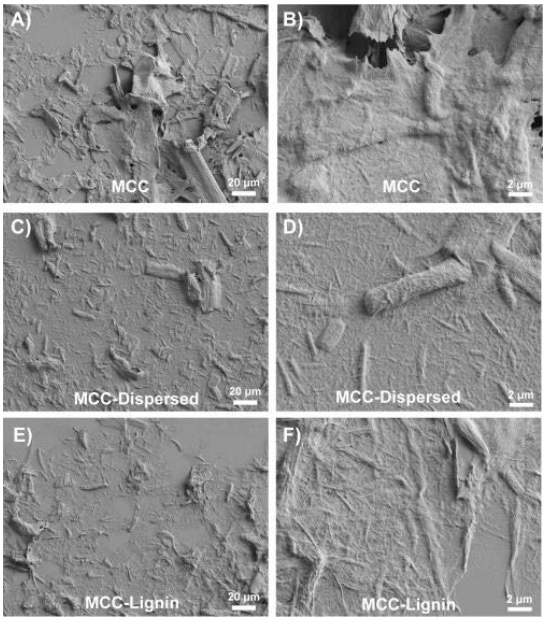

Figure 13. *SEM images of MCC (non-dispersed, A - B), MCC-D (mechanically dispersed, C - D) and MCC-L (lignin containing, E - F). Scale bar 20 µm (A, C, E) or 2µm (B, D, F).*

The rheological measurements (Figure 14, Figure 15) confirmed the gel-forming ability of MCC, MCC-D and MCC-L matrices. The mechanically dispersed MCC-L had the highest elastic modulus (~ 100kPa), followed by MCC-D (~ 10 kPa) and the non-dispersed MCC (~ 1 kPa). The Avicel suspension (used as a reference) had the lowest values at the Pa range. For MCC-D, the concentration dependent elastic moduli were confirmed between 2.4 – 12 wt-%. In the viscosity measurements, a shear thinning behaviour with linear dependence between viscosity and shear rate was observed. Similarly to elastic moduli values, MCC-L had the highest viscosity followed by MCC-D, MCC and Avicel. The mechanical treatment of MCC-D and MCC-L resulted in higher viscosity as well as higher elasticity, thus the ability to form a gel was greater than for the non-dispersed MCC or commercial Avicel. Structurally the hydrogels consist of individual MCC particles in a network, and for MCC-D and MCC-L colloidal stability was obtained via mechanical treatment.

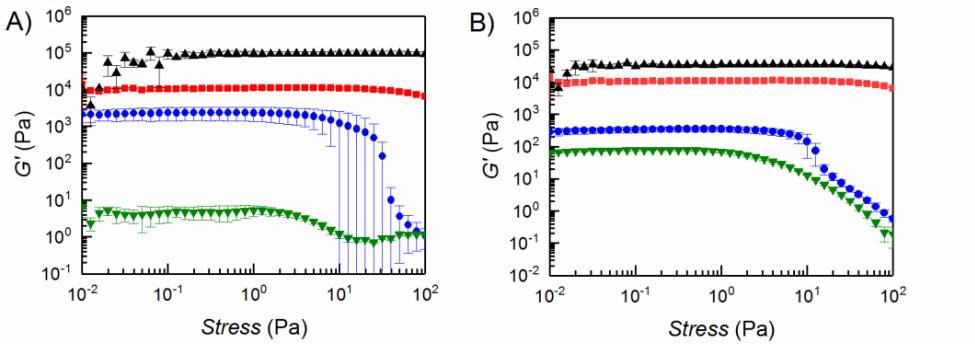

Figure 14. *A) Storage modulus as a function of the oscillatory stress at 10 wt-% for MCC-L (black up-pointing triangles), MCC-D (red squares), MCC (blue dots) and Avicel (green down-pointing triangles). B) Storage modulus as a function of the oscillatory stress for MCC-D at 12 wt-% (black up-pointing triangles), 10 wt-% (red squares), 5 wt-% (blue dots) and 2.4 wt-% (green down-pointing triangles). Results presented as mean ± S.D., n=3.*

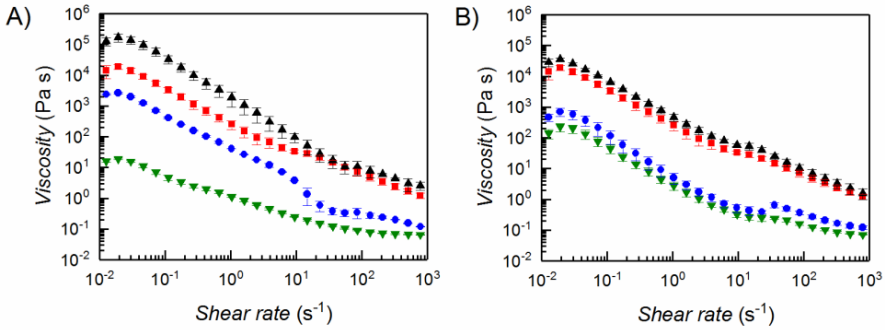

Figure 15. *A) Shear viscosity for 10 wt-% MCC-L (black up-pointing triangles), MCC-D (red squares), MCC (blue dots) and Avicel (green down-pointing triangles). B) Shear viscosity for MCC-D at 12 wt-% (black up-pointing triangles), 10 wt-% (red squares), 5 wt-% (blue dots) and 2.4 wt-% (green down-pointing triangles). Results presented as mean ± S.D., n=3.*

5.3.2 Drug release and diffusivity

The porosity and viscosity of the matrices were the most significant factors that controlled the diffusivity and release rate of encapsulated model compounds MZ and LZ, as no swelling was observed under test conditions. The experimental and simulated release profiles of MZ and LZ from different MCC matrices are presented in Figure 16. The experimental results up to 60 % release fitted well to theoretical predictions by an early times Fickian model. The release of neutral small molecule MZ was significantly faster from all tested matrices when compared to sustained release profiles obtained for a cationic and larger protein compound LZ (14.7 kDa). However, for both compounds the release rates from different MCC matrices were in the order MCC-D > MCC > MCC-L. The variances between different matrices were negligible for MZ and 92 – 100 % release

was reached at 48 h, depending on matrix, indicating full release. For LZ the release % was lower from all matrices and only 51 – 80 % was reached at 144 h.

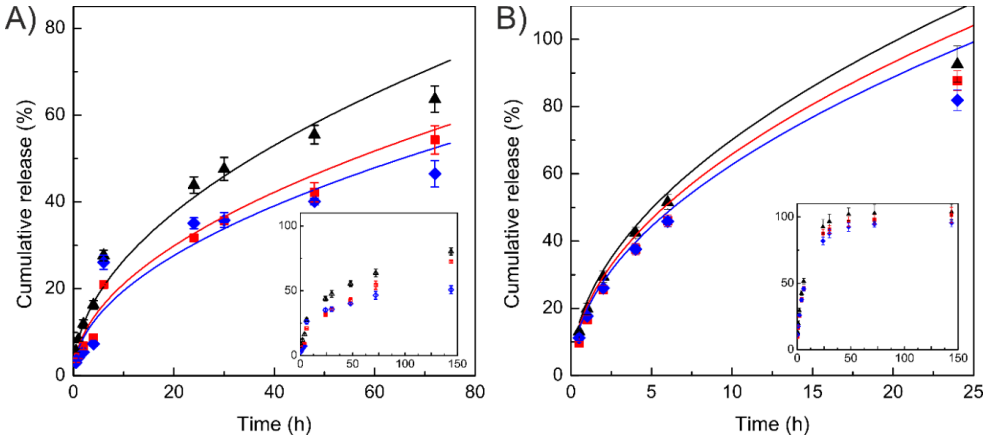

Figure 16. *Experimental (mean ± S.D., n=3) and simulated cumulative release profiles of MZ (A) and LZ (B) from different matrices.* Experimental results are presented as symbols *MCC-D (black triangles), MCC (red squares) and MCC-L (blue diamond). Theoretical predictions of the unsteady-state form of Fick's second law of diffusion, with early values of time when 0 < Mt/M∞ < 0.6, are marked as fits with solid lines.*

The diffusion coefficients were calculated in order to compare the diffusivities of model compounds inside MCC matrices (Table 8). Diffusion coefficients in mechanically dispersed MCC-D matrices for both compounds were higher than from non-dispersed MCC matrices. This may be due to a more homogenous MCC-D matrix where interconnected water capillaries are more evenly distributed, creating pathways for diffusion. MCC-L matrix most significantly prolonged the release rates of both compounds, which is reflected as the lowest diffusion coefficient values. It has been reported that the amorphous and relatively hydrophobic structure of lignin can be utilized for drug encapsulation [274]. Additionally, the MCC-L hydrogel had the highest viscosity. Both effects are expected to contribute to the slower release rate from the MCC-L matrices.

Table 8. *Diffusion coefficients for model compounds MZ and LZ in different MCC-based matrices.*

Matrix	D_{MZ} (×10^{-8} cm^2 s^{-1})	D_{LZ} (×10^{-8} cm^2 s^{-1})
MCC	237	24
MCC–D	269	38
MCC–L	215	21

In the previous study (**II**) with ANFC hydrogels, higher diffusion coefficients were obtained for MZ than for the MCC matrices. Therefore, the release rate control for MZ was even higher in case of MCC, at least with these cellulose contents. Conversely, the ANFC hydrogels provided, via electrostatic attractive forces, a greater control for LZ diffusion. Based on these results, MCC-based matrices may function similarly as ANFC in controlled release applications but certain variation is to be expected.

In summary, this study showed the applicability of novel MCC matrices for controlled drug release applications. Benefits of MCC (AaltoCell™ grades) are dispersability and colloidal stability for MCC-D and MCC-L. The mechanical treatment of MCC-D and MCC-L was highly beneficial for enhancing the gel-forming ability. Furthermore, the bulk material processing allows adjustments of different solid MCC and lignin contents.

5.4 Bioadhesive NFC and ANFC films (III)

Bioadhesive properties of buccal films enable the targeted-release of drugs directly into the mucosal membrane in the oral cavity. This drug delivery approach benefits from prolonged residence time of drug compounds at the target site and enables the localized treatment of oral diseases. Bioadhesive drug releasing NFC and ANFC films, potentially suitable for oral local drug delivery, were prepared by incorporating mucoadhesive biopolymers mucin, pectin and chitosan into the film structure. Films were prepared by simple liquid molding method that does not require chemical modifications, thus reducing processing steps and avoiding potentially toxic residues resulting from any chemical treatment. The suitability of the films, as mucoadhesive drug delivery platforms, was confirmed with several *in vitro* methods.

5.4.1 Mucoadhesive film characterization

NFC and ANFC were used as film forming materials whereas natural biopolymers pectin, mucin and chitosan were added to introduce mucoahesive properties. The mucoadhesive properties of films with NFC/ANFC in 10:1, 2:1, 1:1 mass ratios (wt/wt) to pectin, mucin and chitosan were evaluated with texture analysis measurements. The adhesiveness peak force (N) that describes the maximum force required to detach the analytical probe from the formulation was used as a measure of mucoadhesiveness. Highest mucoadhesive properties were obtained for NFC/ANFC films prepared with either pectin or mucin in 2:1 mass ratio (Figure 17). These films were selected for futher mechanical strength and hydration capacity evaluations.

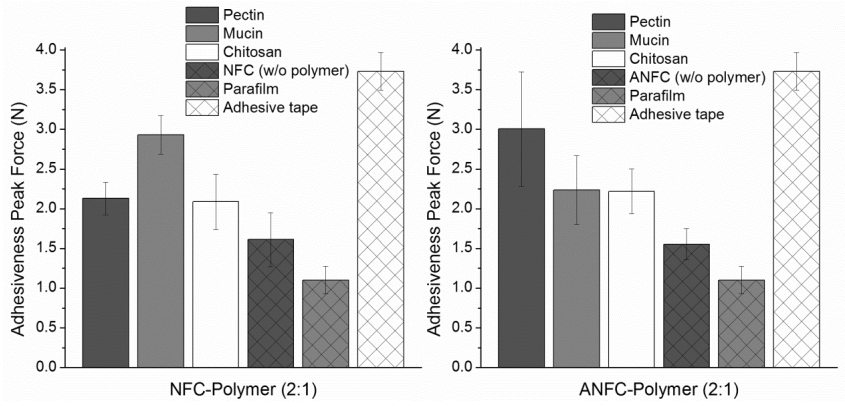

Figure 17. *Adhesiveness peak force for NFC and ANFC films combined with pectin, mucin and chitosan in 2:1 mass ratio (mean ± S.D., n=3).*

The mechanical properties of different films (Table 9) were evaluated in terms of thickness (µm), tensile strength (MPa), elongation (%), Young's modulus (GPa) and toughness (MJ/m^3). The addition of mucoadhesive polymers increased the film thickness for both NFC and ANFC based films and altered the mechanical properties of films, resulting in higher mechanical strength for NFC-based films. For ANFC, the mechanical strength was reduced. Typical Young's modulus and tensile strength values reported in the literature are 6 - 13 GPa and 129 - 214 MPa for NFC films and papers [76,77] and 10 GPa and 191 MPa for ANFC films [82]. However, the preparation method and film porosity have an effect on these values. The mechanical strength of the studied film compositions was not as strong as in previously published works in terms of tensile strength and Young's modulus, but still suitable for handling of oral patches.

Table 9. *Mechanical strength evaluation of bioadhesive films (mean ± S.D., n=5). Mass ratio of NFC/ANFC to mucin/pectin was 2:1. Abbreviation: YM = Young's Modulus.*

Formulation	Film Thickness (µm)	Tensile strength (MPa)	Elongation (%)	YM (GPa)	Toughness (MJ/m^3)
NFC	95.0 ± 11.4	83.0 ± 29.0	10.3 ± 3.0	3.6 ± 1.6	6.0 ± 4.0
ANFC	68.0 ± 5.6	65.8 ± 28.2	3.9 ± 2.0	5.8 ± 1.3	2.2 ± 1.4
NFC-Mucin	128.9 ± 29.5	82.7 ± 10.2	4.1 ± 2.1	5.9 ± 0.8	2.3 ± 1.3
ANFC-Mucin	129.2 ± 16.5	30.0 ± 3.8	4.1 ± 1.1	2.9 ± 0.1	0.9 ± 0.4
NFC-Pectin	161.4 ± 30.9	75.7 ± 11.7	3.9 ± 0.3	5.6 ± 1.0	2.0 ± 0.4
ANFC-Pectin	231.0 ± 47.7	27.0 ± 4.0	2.2 ± 1.1	2.8 ± 0.7	0.4 ± 0.3

The hydration properties and sufficient swelling are important properties for mucoadhesive formulations in addition to hydrogen bonding capacity [162]. Film pieces were immersed into pH 6.8 phosphate buffer, simulating the pH of oral cavity, for 15 s or 5 h to evaluate the effect of fast or prolonged hydration (Table 10). Mass loss was used to evaluate the integrity of the films and indicated the amount of polymers eroded from the films. ANFC-based films had higher hydration capacity overall in fast and prolonged exposure. The carboxyl groups directly on ANFC fibers increase the hydrophilicity of the material in comparison to NFC, which explains the higher hydration capacity of ANFC films [275]. For mucin and pectin containing films, the hydration was lower at 15 s but more extensive at 5 h. Both polymers are very hydrophilic and capable of retaining large amounts of water, which likely caused the relatively high hydration % after long exposure to water [276]. The pectin containing films had higher hydration % and also mass loss % at 5 h when compared to mucin films. Therefore, erosion of the lamellar film structure occurred due to loss of pectin, but regardless of this the remaining film structure had high hydration. Based on the results, all bioadhesive polymer containing films had high hydration capacity required from mucoadhesive films.

Table 10. *Hydration and mass loss of films after exposure to pH 6.8 phosphate buffer (mean ± S.D., n=3). Mass ratio of NFC/ANFC to mucin/pectin was 2:1.*

Swelling studies in pH 6.8 phosphate buffer for 15 s or 5 h						
Formulation	**mg water/ mg film, 15 s**	**Hydration (%), 15 s**	**Mass loss (%)**	**mg water/ mg film, 5 h**	**Hydration (%), 5 h**	**Mass loss (%)**
NFC	0.9 ± 0.1	89.9 ± 7.1	3.1 ± 0.8	1.8 ± 0.0	176.1 ± 4.3	0.6 ± 0.9
ANFC	1.7 ± 0.4	144 ± 12.1	4.6 ± 0.2	4.4 ± 0.1	436.8 ± 0.2	4.6 ± 0.2
NFC-Mucin	0.7 ± 0.3	52.3 ± 17.7	2.3 ± 0.3	4.3 ± 0.0	430.5 ± 3.8	12.2 ± 0.2
ANFC-Mucin	1.2 ± 0.1	123.5 ± 11.4	3.3 ± 1.2	5.2 ± 0.0	516.0 ± 3.4	12.5 ± 0.3
NFC-Pectin	0.7 ± 0.3	48.2 ± 9.8	4.3 ± 2.3	4.8 ± 0.0	467.8 ± 19.4	32.0 ± 1.3
ANFC-Pectin	0.5 ± 0.0	48.5 ± 0.6	4.6 ± 2.1	6.8 ± 0.0	682.7 ± 4.1	21.3 ± 0.5

5.4.2 Morphology and solid state characterization

Metronidazole (MZ) containing films imaged with SEM revealed lamellar structures for the films (Figure 18). ANFC-based films were more densely packed with thicknesses of 97.6 µm for ANFC-Mucin-MZ and 107.6 µm for ANFC-Pectin-MZ. Whereas, loosely packed lamellar layers were observed for NFC based films with total thicknesses of 238.8 µm for NFC-Mucin-MZ and 228.2 µm for NFC-Pectin-MZ.

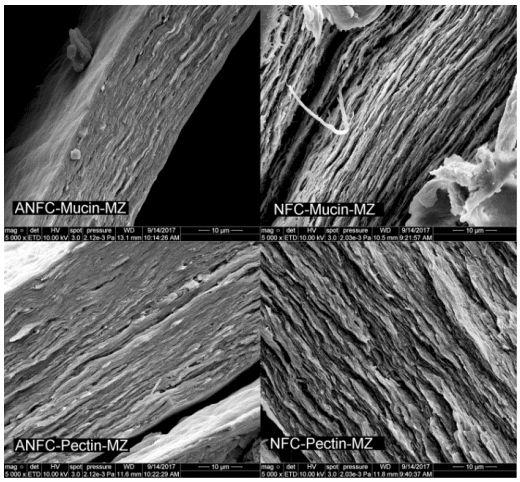

Figure 18. *SEM micrographs of ANFC/NFC films containing mucin/pectin, and metronidazole. Scale bar is 10 µm.*

Similar thermal behavior was observed in DSC for all films with reduced melting points for MZ (Figure 19A). The reduced melting point of MZ may indicate interactions between the NFC/ANFC fibers and MZ. However, only for NFC-Pectin-MZ (151.8 °C) the melting point was significantly reduced. In the other films, the melting points were close to the 161.9 ^{0}C of pure MZ reference.

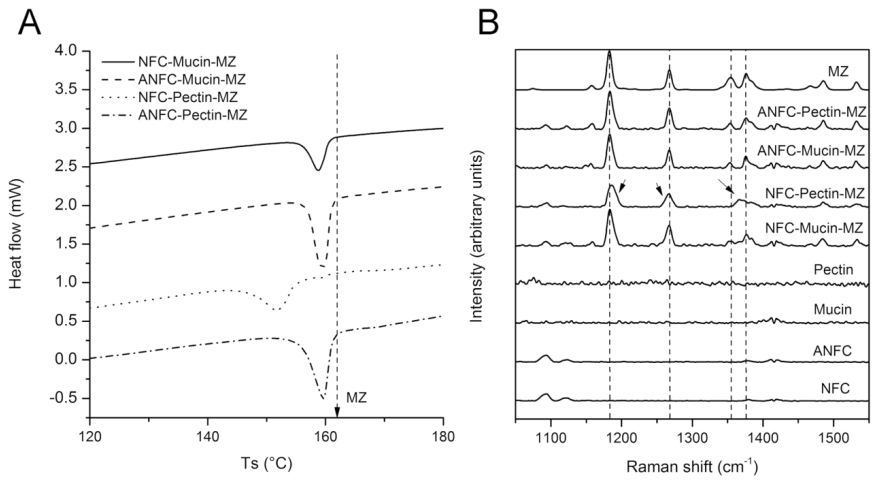

Figure 19. *Solid state characterization of films with DSC (A) and Raman spectroscopy (B). Dashed line marks the melting point of pure MZ at 161.9 ^{0}C (A). Characteristic Raman peaks of MZ are marked with dashed lines and arrows depict the broadening and shifting of MZ in the NFC-Pectin-MZ film (B).*

The characteristic Raman peaks for MZ at 1183 cm^{-1}, 1267 cm^{-1}, 1354 cm^{-1} and 1376 cm^{-1} were observed in all films (Figure 19B). However, the broadening and shifting of the MZ peaks was only observed in the NFC-Pectin-MZ film. The differences between NFC-Pectin-MZ films in relation to the other films may have been caused by binding interactions between pectin side chains and NFC, which consequently may alter the interactions of these polymers with MZ [277,278]. Intermolecular hydrogen bonding between pectin, NFC and MZ may have caused the peak widening at 1183 cm^{-1} and peak shifting of 1267 cm^{-1} to a lower wavenumber [279-283]. Also, at 1354 cm^{-1} and 1376 cm^{-1} the widening of MZ may indicate the formation of hydrogen bonds [279]. It has been reported that pectin-cellulose interactions may result in intermediate binding affinity of pectin into cellulose via neutral pectin side chains which reduces cellulose-cellulose interactions [14,284,285]. Also, hemicelluloses (e.g. xyloglycan) have binding affinity to pectin as well as cellulose microfibrils [278]. These factors may explain why NFC-Pectin-MZ films had different solid state characteristics from the other films as NFC and pectin polymers may have favorable interactions for MZ encapsulation. ANFC fibers are coated with carboxyl groups which may reduce the binding interaction with pectin as there are fewer neutral binding sites in ANFC fiber structure and a lack of hemicellulose content.

5.4.3 Drug release and toxicity

The drug release properties of different films were evaluated at pH 6.8 in order to evaluate the effect of formulation on MZ release (Figure 20A). A relatively high burst release of 20 - 40 % occurred for all formulations during the first 5 min. This phenomenon was likely attributed to the release of MZ on the surface of films. The mucin containing thinner films had overall a higher MZ release as opposed to the thicker pectin containing films. Overall, the highest drug release extent of 84.7 % was observed for NFC–Mucin-MZ, while the

smallest drug release of 59. 6 % was obtained with ANFC–Pectin-MZ. The drug release was slightly lower from ANFC films than NFC films with both mucoadhesive polymers. This could be explained with the apparent porosity observed in SEM images, where ANFC structure was denser than NFC. Furthermore, ANFC-based films had higher hydration capability and greater swelling in the vertical direction creating a larger barrier for diffusion. This was especially apparent for ANFC–Pectin-MZ films, which had the slowest drug release and where the swollen matrix was expected to create the longest diffusion path.

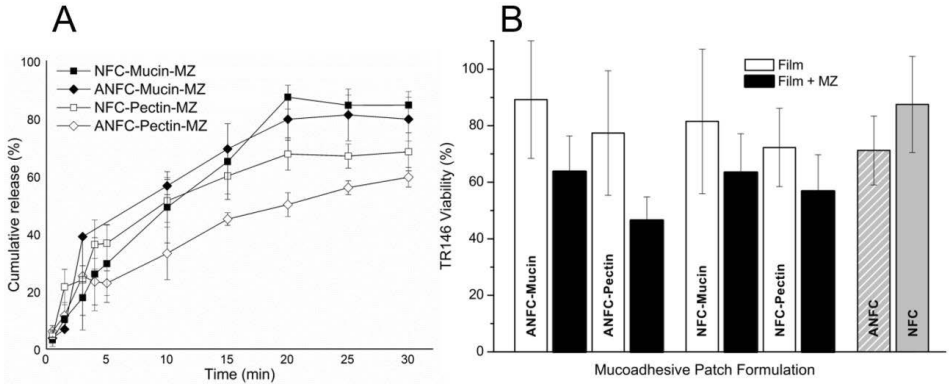

Figure 20. *Drug release profiles (mean ± S.D., n=3) of MZ from different mucoadhesive formulations (A). TR146 cytotoxicity assays (mean ± S.D., n=4) on different mucoadhesive films with and without MZ after 24 h incubation.*

All films had rather suitable drug release profiles for MZ. Especially in buccal drug delivery applications, fast drug release from the film into the mucosal membrane would be advantageous. Mucoadhesion combined with fast drug release properties could be used to promote site-specific drug delivery of MZ for e.g. treatment of periodontal diseases in the oral cavity. Human TR146 cell line was used in cytotoxicity studies of film patches (Figure 20B). The cell line has been previously used as a tool to model human buccal epithelium effectively [176,177]. Patches without MZ had no significant cytotoxic effects on the cells. MZ containing patches showed slight cytotoxic effect, which is probably due to the high local concentration of MZ during the experiment. It has been previously shown that above 5 mM concentration, MZ may induce cytotoxic effects [286]. Therefore, the film forming polymers and incorporated mucoadhesive polymers were shown to be nontoxic on TR146 cells.

In summary, this study demonstrated that NFC and ANFC can be used as film forming materials for mucoadhesive pharmaceutical patches. Furthermore, the patches consisting of all natural polymers had high mucoadhesive properties in combination with good mechanical, water retention and drug release properties as well as low toxicity.

6 Conclusions and future outlook

In this thesis, the applicability of nanofibrillar cellulose (NFC and ANFC) as novel pharmaceutical excipient was evaluated in a variety of formulations ranging from emulsions and hydrogels/reconstructed hydrogels to mucoadhesive films. The innate structural properties such as high mechanical strength, water retention capability, pseudoplastic properties and high surface area were utilized for the encapsulation of active materials.

Emulsification with a relatively simple sonication method was used to produce HFBII-NFC and HFBII-ANFC emulsions for immediate and sustained release applications respectively. It was demonstrated that tunable drug release properties were achieved with the choice of NFC/ANFC fiber grade. ANFC fibers created a higher diffusion barrier for drug release together with the HFBII coating on the oil droplets, whereas longer NFC fibers did not control the drug release as significantly, most likely due to negligible interactions with HFBII. However, both nanofibrillar cellulose grades, NFC and ANFC, could be used to increase the storage stability of emulsions when combined with HFBII. The concentrations of HFBII/NFC/ANFC required for stabilization were extremely low at 0.1 - 0.15 %. As synthetic polymers are traditionally used for the stabilization of pharmaceutical emulsions, these new biopolymers with low toxicity and good biocompatibility could provide a viable option for formulation development in the future. Also, micro-dosing of potent drugs with this type of emulsions through the oral route could be further explored. Furthermore, enhancing the solubility of other poorly soluble drugs with these emulsions at a higher oil phase volume could be explored for controlled release applications of poorly soluble BCS class II drugs. In the future, however the stability of the formulations in the aqueous environment of gastrointestinal tract should be defined as for example proteases may affect the stability of protein stabilized formulations and consequent bioavailability.

The ANFC hydrogels proved to be suitable for the freeze-drying and consequent rehydration without significant loss on rheological properties or drug release properties. The manufacturing of dry forms of ANFC and NFC has been a challenge with regard to preserving the nano-scale structure as usually the fibers tend to aggregate during drying due to hornification. Here the structure of ANFC was effectively preserved in the presence of commonly used cryo- lyoprotectants trehalose and PEG6000. This is a highly desirable feature for manufacturing of pharmaceutical dosage forms as the shelf-life of hydrolysis sensitive compounds can be increased by the dry state of an aerogel. The high fiber content of 3 % and 6.5 % ANFC hydrogels was effective in controlling the release of large molecular weight compounds, whereas a moderate control was obtained for small molecules. The results indicate the suitability of ANFC hydrogels for controlled delivery of several types of molecules. In the future, the hydrogels could be used as such directly on topical administration of therapeutic molecules for example in wound healing applications, where the high water content of the hydrogel combined with antibiotics, corticosteroids or growth factors could enhance the healing rate. The ANFC hydrogel as well as aerogel matrices would likely perform well also in matrix systems as structurally

the hydrogel and aerogel matrices themselves provide direct control for the drug release. Furthermore, the applicability of ANFC hydrogels could be explored in reservoir type drug delivery systems such as osmotic pump capsules where the water absorption capability of ANFC could be utilized in combination with a rate controlling membrane.

The comparable study with new MCC hydrogel dispersions showed that the non-dispersed, dispersed and lignin containing MCC grades proved to be effective in controlling the drug release of small and large molecules. These new MCC grades showed high potential in terms of usability in controlled drug release applications as hydrogel platforms in similar manner to ANFC hydrogels. However, as the material is relatively new, a considerable effort should be focused on exploring the full potential of these new MCC grades in drug release applications in the future. Especially, the colloidally stable MCC-D and MCC-L should be explored as stabilizers for dispersions and emulsions as well as for spray-dried and freeze-dried dosage forms as structurally these grades provide high encapsulation potential for therapeutic compounds. The dispersability and higher colloidal stability of these new grades, when compared to conventional Avicel grades, could be utilized in multiple different pharmaceutical dosage forms in the future.

The bioadhesive NFC and ANFC films prepared with natural adhesive polymers mucin, pectin and chitosan had high hydration capability, good mucoadhesion strength and adequate mechanical properties. Furthermore, the fast drug release properties obtained for encapsulated antibiotic metronidazole combined with the bioadhesive properties and low toxicity showed high potential for buccal drug delivery applications. These films were prepared with a simple liquid molding method without any requirement for further chemical modification. The quality of the films could be enhanced even further in the future with other processing techniques such as filtration or hot pressing, ensuring higher manufacturability. Furthermore, these films could provide a platform for local delivery of therapeutic compounds into other mucosal tissues besides the oral cavity.

As a summary, this thesis clearly demonstrated the applicability of new nano- and microcellulose-based products, namely NFC, ANFC and a new grade of MCC, as pharmaceutical excipients for many types of dosage forms. The structural properties of these natural biopolymers enable their versatile use, and future studies in the field of formulation development will certainly advance their utilization as components in conventional and novel drug delivery systems.

References

[1] A. Abdellah, M.I. Noordin, W.A. Wan Ismail, Importance and globalization status of good manufacturing practice (GMP) requirements for pharmaceutical excipients, Saudi Pharm. J. 23 (2015) 9-13.

[2] C.G. Abrantes, D. Duarte, C.P. Reis, An Overview of Pharmaceutical Excipients: Safe or Not Safe?, Journal of Pharmaceutical Sciences. 105 (2016) 2019-2026.

[3] S. Stegemann, F. Leveiller, D. Franchi, H. de Jong, H. Lindén, When poor solubility becomes an issue: From early stage to proof of concept, European Journal of Pharmaceutical Sciences. 31 (2007) 249-261.

[4] P. Zarmpi, T. Flanagan, E. Meehan, J. Mann, N. Fotaki, Biopharmaceutical aspects and implications of excipient variability in drug product performance, European Journal of Pharmaceutics and Biopharmaceutics. 111 (2017) 1-15.

[5] N. Lin, A. Dufresne, Nanocellulose in biomedicine: Current status and future prospect, European Polymer Journal. 59 (2014) 302-325.

[6] S. Varjonen, P. Laaksonen, A. Paananen, H. Valo, H. Hähl, T. Laaksonen, M.B. Linder, Self-assembly of cellulose nanofibrils by genetically engineered fusion proteins, Soft Matter. 7 (2011) 2402-2411.

[7] J.F. Diniz, M. Gil, J. Castro, Hornification—its origin and interpretation in wood pulps, Wood Science and Technology. 37 (2004) 489-494.

[8] J. Wan, Y. Wang, Q. Xiao, Effects of hemicellulose removal on cellulose fiber structure and recycling characteristics of eucalyptus pulp, Bioresource Technology. 101 (2010) 4577-4583.

[9] D.N. Hon, Cellulose: a random walk along its historical path, Cellulose. 1 (1994) 1-25.

[10] R.D. Preston, X-ray analysis and the structure of the components of plant cell walls, Physics Reports. 21 (1975) 183-226.

[11] A.C. O'Sullivan, Cellulose: the structure slowly unravels, Cellulose. 4 (1997) 173-207.

[12] V. Varshney, S. Naithani, Chemical functionalization of cellulose derived from nonconventional sources, in: S. Kalia, B. Kaith, I. Kaur (Eds.), Cellulose Fibers: Bio-and Nano-Polymer Composites, Springer, Berlin, Heidelberg, 2011, pp. 43-60.

[13] A. Dufresne, Nanocellulose: a new ageless bionanomaterial, Materials Today. 16 (2013) 220-227.

[14] J. Gu, J.M. Catchmark, The impact of cellulose structure on binding interactions with hemicellulose and pectin, Cellulose. 20 (2013) 1613-1627.

[15] T. Heinze, T. Liebert, Unconventional methods in cellulose functionalization, Progress in Polymer Science. 26 (2001) 1689-1762.

[16] D. Klemm, B. Philipp, T. Heinze, U. Heinze, W. Wagenknecht, General Considerations on Structure and Reactivity of Cellulose: Section 2.1–2.1.4, in Comprehensive Cellulose Chemistry: Fundamentals and Analytical Methods, Volume 1, Wiley-VCH Verlag GmbH & Co. KGaA, Weinheim, 1998.

[17] E. Sjöström, Wood Chemistry: Fundamentals and Applications, 2nd ed., Academic Press, San Diego, 1993.

[18] S. Salmon, S.M. Hudson, Crystal morphology, biosynthesis, and physical assembly of cellulose, chitin, and chitosan, Journal of Macromolecular Science, Part C. 37 (1997) 199-276.

[19] D.L. VanderHart, R. Atalla, Studies of microstructure in native celluloses using solid-state carbon-13 NMR, Macromolecules. 17 (1984) 1465-1472.

[20] R.H. Atalla, D.L. VanderHart, Native cellulose: a composite of two distinct crystalline forms, Science. 223 (1984) 283-286.

[21] H. Kono, S. Yunoki, T. Shikano, M. Fujiwara, T. Erata, M. Takai, CP/MAS 13C NMR study of cellulose and cellulose derivatives. 1. Complete assignment of the CP/MAS 13C NMR spectrum of the native cellulose, J. Am. Chem. Soc. 124 (2002) 7506-7511.

[22] M.A. Azizi Samir, F. Alloin, A. Dufresne, Review of recent research into cellulosic whiskers, their properties and their application in nanocomposite field, Biomacromolecules. 6 (2005) 612-626.

[23] L. Fan, M.M. Gharpuray, Y. Lee, Nature of cellulosic material, in: Cellulose Hydrolysis, Biotechnology Monographs, Vol 3, Springer, Berlin, Heidelberg, 1987, pp. 5-20.

[24] D. Klemm, B. Heublein, H. Fink, A. Bohn, Cellulose: fascinating biopolymer and sustainable raw material, Angewandte Chemie International Edition. 44 (2005) 3358-3393.

[25] H. Hatakeyama, T. Hatakeyama, Lignin structure, properties, and applications, in: A. Abe, K. Dusek, S. Kobayashi (Eds.), Biopolymers, Advances in Polymer Science, Springer, Berlin, Heidelberg, 2009, pp. 1-63.

[26] R.C. Rowe, P.J. Sheskey, P.J. Weller, Handbook of Pharmaceutical Excipients, Pharmaceutical press, London, 2003.

[27] T. Abitbol, A. Rivkin, Y. Cao, Y. Nevo, E. Abraham, T. Ben-Shalom, S. Lapidot, O. Shoseyov, Nanocellulose, a tiny fiber with huge applications, Current Opinion in Biotechnology. 39 (2016) 76-88.

[28] A.F. Turbak, F.W. Snyder, K.R. Sandberg, Microfibrillated cellulose, a new cellulose product: properties, uses, and commercial potential, J. Appl. Polym. Sci.: Appl. Polym. Symp. 37 (1983) 815-827.

[29] F.W. Herrick, R.L. Casebier, J.K. Hamilton, K.R. Sandberg, Microfibrillated cellulose: morphology and accessibility, J. Appl. Polym. Sci.: Appl. Polym. Symp. 37 (1983) 797-813.

[30] O. Eriksen, K. Syverud, O. Gregersen, The use of microfibrillated cellulose produced from kraft pulp as strength enhancer in TMP paper, Nordic Pulp & Paper Research Journal. 23 (2008) 299-304.

[31] O. Nechyporchuk, M.N. Belgacem, J. Bras, Production of cellulose nanofibrils: A review of recent advances, Industrial Crops and Products. 93 (2016) 2-25.

[32] M. Spinu, N. Dos Santos, N. Le Moigne, P. Navard, How does the never-dried state influence the swelling and dissolution of cellulose fibres in aqueous solvent? Cellulose. 18 (2011) 247-256.

[33] A. Ferrer, E. Quintana, I. Filpponen, I. Solala, T. Vidal, A. Rodríguez, J. Laine, O.J. Rojas, Effect of residual lignin and heteropolysaccharides in nanofibrillar cellulose and nanopaper from wood fibers, Cellulose. 19 (2012) 2179-2193.

[34] A.B. Fall, S.B. Lindström, O. Sundman, L. Ödberg, L. Wågberg, Colloidal stability of aqueous nanofibrillated cellulose dispersions, Langmuir. 27 (2011) 11332-11338.

[35] I. Siró, D. Plackett, Microfibrillated cellulose and new nanocomposite materials: a review, Cellulose. 17 (2010) 459-494.

[36] E. Dinand, H. Chanzy, M. Vignon, Parenchymal cell cellulose from sugar beet pulp: preparation and properties, Cellulose. 3 (1996) 183-188.

[37] A. Dufresne, D. Dupeyre, M.R. Vignon, Cellulose microfibrils from potato tuber cells: processing and characterization of starch–cellulose microfibril composites, J Appl Polym Sci. 76 (2000) 2080-2092.

[38] A. Dufresne, J. Cavaillé, M.R. Vignon, Mechanical behavior of sheets prepared from sugar beet cellulose microfibrils, J Appl Polym Sci. 64 (1997) 1185-1194.

[39] B. Wang, M. Sain, Isolation of nanofibers from soybean source and their reinforcing capability on synthetic polymers, Composites Science and Technology. 67 (2007) 2521-2527.

[40] F. Jiang, Y. Hsieh, Chemically and mechanically isolated nanocellulose and their self-assembled structures, Carbohydr. Polym. 95 (2013) 32-40.

[41] B.M. Cherian, A.L. Leão, S.F. de Souza, S. Thomas, L.A. Pothan, M. Kottaisamy, Isolation of nanocellulose from pineapple leaf fibres by steam explosion, Carbohydrate Polymers. 81 (2010) 720-725.

[42] B. Deepa, E. Abraham, B.M. Cherian, A. Bismarck, J.J. Blaker, L.A. Pothan, A.L. Leao, S.F. de Souza, M. Kottaisamy, Structure, morphology and thermal characteristics of banana nano fibers obtained by steam explosion, Bioresource Technology. 102 (2011) 1988-1997.

[43] G. Siqueira, S. Tapin-Lingua, J. Bras, D. da Silva Perez, A. Dufresne, Morphological investigation of nanoparticles obtained from combined mechanical shearing, and enzymatic and acid hydrolysis of sisal fibers, Cellulose. 17 (2010) 1147-1158.

[44] T. Ho, T. Zimmermann, R. Hauert, W. Caseri, Preparation and characterization of cationic nanofibrillated cellulose from etherification and high-shear disintegration processes, Cellulose. 18 (2011) 1391-1406.

[45] T. Saito, S. Kimura, Y. Nishiyama, A. Isogai, Cellulose nanofibers prepared by TEMPO-mediated oxidation of native cellulose, Biomacromolecules. 8 (2007) 2485-2491.

[46] K. Missoum, M.N. Belgacem, J. Bras, Nanofibrillated cellulose surface modification: a review, Materials. 6 (2013) 1745-1766.

[47] I. Besbes, M.R. Vilar, S. Boufi, Nanofibrillated cellulose from Alfa, Eucalyptus and Pine fibres: Preparation, characteristics and reinforcing potential, Carbohydrate Polymers. 86 (2011) 1198-1206.

[48] J.Y. Zhu, R. Sabo, X. Luo, Integrated production of nano-fibrillated cellulose and cellulosic biofuel (ethanol) by enzymatic fractionation of wood fibers, Green Chem. 13 (2011) 1339-1344.

[49] F. Carrasco, P. Mutje, M. Pelach, Refining of bleached cellulosic pulps: characterization by application of the colloidal titration technique, Wood Sci. Technol. 30 (1996) 227-236.

[50] T. Taniguchi, K. Okamura, New films produced from microfibrillated natural fibres, Polym. Int. 47 (1998) 291-294.

[51] T. Saito, Y. Nishiyama, J. Putaux, M. Vignon, A. Isogai, Homogeneous suspensions of individualized microfibrils from TEMPO-catalyzed oxidation of native cellulose, Biomacromolecules. 7 (2006) 1687-1691.

[52] L. Wågberg, G. Decher, M. Norgren, T. Lindström, M. Ankerfors, K. Axnäs, The build-up of polyelectrolyte multilayers of microfibrillated cellulose and cationic polyelectrolytes, Langmuir. 24 (2008) 784-795.

[53] H. Liimatainen, M. Visanko, J. Sirviö, O. Hormi, J. Niinimäki, Sulfonated cellulose nanofibrils obtained from wood pulp through regioselective oxidative bisulfite pre-treatment, Cellulose. 20 (2013) 741-749.

[54] C. Aulin, E. Johansson, L. Wågberg, T. Lindström, Self-organized films from cellulose I nanofibrils using the layer-by-layer technique, Biomacromolecules. 11 (2010) 872-882.

[55] S. Iwamoto, A.N. Nakagaito, H. Yano, M. Nogi, Optically transparent composites reinforced with plant fiber-based nanofibers, Appl. Phys. A. 81 (2005) 1109-1112.

[56] T. Ho, K. Abe, T. Zimmermann, H. Yano, Nanofibrillation of pulp fibers by twin-screw extrusion, Cellulose. 22 (2015) 421-433.

[57] S. Xiao, R. Gao, L. Gao, J. Li, Poly(vinyl alcohol) films reinforced with nanofibrillated cellulose (NFC) isolated from corn husk by high intensity ultrasonication, Carbohydrate Polymers. 136 (2016) 1027-1034.

[58] L. Zhang, T. Tsuzuki, X. Wang, Preparation of cellulose nanofiber from softwood pulp by ball milling, Cellulose. 22 (2015) 1729-1741.

[59] T. Kondo, R. Kose, H. Naito, W. Kasai, Aqueous counter collision using paired water jets as a novel means of preparing bio-nanofibers, Carbohydrate Polymers. 112 (2014) 284-290.

[60] S. Kalia, S. Boufi, A. Celli, S. Kango, Nanofibrillated cellulose: surface modification and potential applications, Colloid Polym. Sci. 292 (2014) 5-31.

[61] A. Tanaka, V. Seppänen, J. Houni, A. Sneck, P. Pirkonen, Nanocellulose characterization with mechanical fractionation, Nordic Pulp and Paper Research Journal. 27 (2012) 689-694.

[62] D. Klemm, F. Kramer, S. Moritz, T. Lindström, M. Ankerfors, D. Gray, A. Dorris, Nanocelluloses: A new family of nature-based materials, Angewandte Chemie International Edition. 50 (2011) 5438-5466.

[63] M. Pääkkö, M. Ankerfors, H. Kosonen, A. Nykänen, S. Ahola, M. Österberg, J. Ruokolainen, J. Laine, P.T. Larsson, O. Ikkala, T. Lindström, Enzymatic hydrolysis combined with mechanical shearing and high-pressure homogenization for nanoscale cellulose fibrils and strong gels, Biomacromolecules. 8 (2007) 1934-1941.

[64] A. Isogai, T. Saito, H. Fukuzumi, TEMPO-oxidized cellulose nanofibers, Nanoscale. 3 (2011) 71-85.

[65] M. Bhattacharya, M.M. Malinen, P. Lauren, Y. Lou, S.W. Kuisma, L. Kanninen, M. Lille, A. Corlu, C. GuGuen-Guillouzo, O. Ikkala, A. Laukkanen, A. Urtti, M. Yliperttula, Nanofibrillar cellulose hydrogel promotes three-dimensional liver cell culture, J. Controlled Release. 164 (2012) 291-298.

[66] K. Benhamou, A. Dufresne, A. Magnin, G. Mortha, H. Kaddami, Control of size and viscoelastic properties of nanofibrillated cellulose from palm tree by varying the TEMPO-mediated oxidation time, Carbohydr. Polym. 99 (2014) 74-83.

[67] O. Nechyporchuk, M.N. Belgacem, F. Pignon, Rheological properties of micro-/nanofibrillated cellulose suspensions: Wall-slip and shear banding phenomena, Carbohydr. Polym. 112 (2014) 432-439.

[68] H. Dong, J.F. Snyder, K.S. Williams, J.W. Andzelm, Cation-induced hydrogels of cellulose nanofibrils with tunable moduli, Biomacromolecules. 14 (2013) 3338-3345.

[69] N. Masruchin, B. Park, V. Causin, I.C. Um, Characteristics of TEMPO-oxidized cellulose fibril-based hydrogels induced by cationic ions and their properties, Cellulose. 22 (2015) 1993-2010.

[70] S. Napso, D.M. Rein, R. Khalfin, O. Kleinerman, Y. Cohen, Cellulose gel dispersion: From pure hydrogel suspensions to encapsulated oil-in-water emulsions, Colloids and Surfaces B: Biointerfaces. 137 (2016) 70-76.

[71] H. Valo, M. Kovalainen, P. Laaksonen, M. Häkkinen, S. Auriola, L. Peltonen, M. Linder, K. Järvinen, J. Hirvonen, T. Laaksonen, Immobilization of protein-coated drug nanoparticles in nanofibrillar cellulose matrices—Enhanced stability and release, J. Controlled Release. 156 (2011) 390-397.

[72] K. Dimic-Misic, P. Gane, J. Paltakari, Micro-and nanofibrillated cellulose as a rheology modifier additive in CMC-containing pigment-coating formulations, Ind Eng Chem Res. 52 (2013) 16066-16083.

[73] C.A. Carrillo, T.E. Nypelö, O.J. Rojas, Cellulose nanofibrils for one-step stabilization of multiple emulsions (W/O/W) based on soybean oil, J. Colloid Interface Sci. 445 (2015) 166-173.

[74] T. Winuprasith, M. Suphantharika, Properties and stability of oil-in-water emulsions stabilized by microfibrillated cellulose from mangosteen rind, Food Hydrocoll. 43 (2015) 690-699.

[75] C. Salas, T. Nypelö, C. Rodriguez-Abreu, C. Carrillo, O.J. Rojas, Nanocellulose properties and applications in colloids and interfaces, Current Opinion in Colloid & Interface Science. 19 (2014) 383-396.

[76] E.D. Cranston, M. Eita, E. Johansson, J. Netrval, M. Salajková, H. Arwin, L. Wågberg, Determination of Young's modulus for nanofibrillated cellulose multilayer thin films using buckling mechanics, Biomacromolecules. 12 (2011) 961-969.

[77] M. Henriksson, L.A. Berglund, P. Isaksson, T. Lindstrom, T. Nishino, Cellulose nanopaper structures of high toughness, Biomacromolecules. 9 (2008) 1579-1585.

[78] M. Pääkkö, J. Vapaavuori, R. Silvennoinen, H. Kosonen, M. Ankerfors, T. Lindström, L.A. Berglund, O. Ikkala, Long and entangled native cellulose I nanofibers allow flexible aerogels and hierarchically porous templates for functionalities, Soft Matter. 4 (2008) 2492-2499.

[79] Y. Peng, D.J. Gardner, Y. Han, Drying cellulose nanofibrils: in search of a suitable method, Cellulose. 19 (2012) 91-102.

[80] Y. Peng, Y. Han, D.J. Gardner, Spray-drying cellulose nanofibrils: effect of drying process parameters on particle morphology and size distribution, Wood Fiber Sci. 44 (2012) 448-461.

[81] K. Kekäläinen, H. Liimatainen, M. Illikainen, T.C. Maloney, J. Niinimäki, The role of hornification in the disintegration behaviour of TEMPO-oxidized bleached hardwood fibres in a high-shear homogenizer, Cellulose. 21 (2014) 1163-1174.

[82] S. Fujisawa, Y. Okita, H. Fukuzumi, T. Saito, A. Isogai, Preparation and characterization of TEMPO-oxidized cellulose nanofibril films with free carboxyl groups, Carbohydr. Polym. 84 (2011) 579-583.

[83] F. Jiang, Y. Hsieh, Super water absorbing and shape memory nanocellulose aerogels from TEMPO-oxidized cellulose nanofibrils via cyclic freezing–thawing, Journal of Materials Chemistry A. 2 (2013) 350-359.

[84] S. Iwamoto, W. Kai, A. Isogai, T. Iwata, Elastic modulus of single cellulose microfibrils from tunicate measured by atomic force microscopy, Biomacromolecules. 10 (2009) 2571-2576.

[85] T. Saito, T. Uematsu, S. Kimura, T. Enomae, A. Isogai, Self-aligned integration of native cellulose nanofibrils towards producing diverse bulk materials, Soft Matter. 7 (2011) 8804-8809.

[86] S. Tanpichai, F. Quero, M. Nogi, H. Yano, R.J. Young, T. Lindström, W.W. Sampson, S.J. Eichhorn, Effective Young's modulus of bacterial and microfibrillated cellulose fibrils in fibrous networks, Biomacromolecules. 13 (2012) 1340-1349.

[87] T. Saito, R. Kuramae, J. Wohlert, L.A. Berglund, A. Isogai, An ultrastrong nanofibrillar biomaterial: the strength of single cellulose nanofibrils revealed via sonication-induced fragmentation, Biomacromolecules. 14 (2013) 248-253.

[88] S. Paavilainen, J.L. McWhirter, T. Róg, J. Järvinen, I. Vattulainen, J.A. Ketoja, Mechanical properties of cellulose nanofibrils determined through atomistic molecular dynamics simulations, Nordic Pulp and Paper Research Journal. 27 (2012) 282-286.

[89] M. Matsuo, C. Sawatari, Y. Iwai, F. Ozaki, Effect of orientation distribution and crystallinity on the measurement by X-ray diffraction of the crystal lattice moduli of cellulose I and II, Macromolecules. 23 (1990) 3266-3275.

[90] I. Diddens, B. Murphy, M. Krisch, M. Müller, Anisotropic elastic properties of cellulose measured using inelastic X-ray scattering, Macromolecules. 41 (2008) 9755-9759.

[91] T. Miyamoto, S. Takahashi, H. Ito, H. Inagaki, Y. Noishiki, Tissue biocompatibility of cellulose and its derivatives, J. Biomed. Mater. Res. 23 (1989) 125-133.

[92] M. Märtson, J. Viljanto, T. Hurme, P. Laippala, P. Saukko, Is cellulose sponge degradable or stable as implantation material? An in vivo subcutaneous study in the rat, Biomaterials. 20 (1999) 1989-1995.

[93] K. Hannukainen, S. Suhonen, K. Savolainen, H. Norppa, Genotoxicity of nanofibrillated cellulose in vitro as measured by enzyme comet assay, Toxicol. Lett. 211 (2012) S71-S71.

[94] K. Hua, D.O. Carlsson, E. Ålander, T. Lindström, M. Strømme, A. Mihranyan, N. Ferraz, Translational study between structure and biological response of nanocellulose from wood and green algae, RSC Advances. 4 (2013) 2892-2903.

[95] J. Vartiainen, T. Pöhler, K. Sirola, L. Pylkkänen, H. Alenius, J. Hokkinen, U. Tapper, P. Lahtinen, A. Kapanen, K. Putkisto, P. Hiekkataipale, P. Eronen, J. Ruokolainen, A. Laukkanen, Health and environmental safety aspects of friction grinding and spray drying of microfibrillated cellulose, Cellulose. 18 (2011) 775-786.

[96] L. Alexandrescu, K. Syverud, A. Gatti, G. Chinga-Carrasco, Cytotoxicity tests of cellulose nanofibril-based structures, Cellulose. 20 (2013) 1765-1775.

[97] N. Halib, F. Perrone, M. Cemazar, B. Dapas, R. Farra, M. Abrami, G. Chiarappa, G. Forte, F. Zanconati, G. Pozzato, Potential Applications of Nanocellulose-Containing Materials in the Biomedical Field, Materials. 10 (2017) 977.

[98] P. Laurén, Y. Lou, M. Raki, A. Urtti, K. Bergström, M. Yliperttula, Technetium-99m-labeled nanofibrillar cellulose hydrogel for in vivo drug release, European Journal of Pharmaceutical Sciences. 65 (2014) 79-88.

[99] P. Laurén, P. Somersalo, I. Pitkänen, Y. Lou, A. Urtti, J. Partanen, J. Seppälä, M. Madetoja, T. Laaksonen, A. Mäkitie, Nanofibrillar cellulose-alginate hydrogel coated surgical sutures as cell-carrier systems, PLoS One. 12 (2017) e0183487.

[100] H. Thérien-Aubin, Y. Wang, K. Nothdurft, E. Prince, S. Cho, E. Kumacheva, Temperature-Responsive Nanofibrillar Hydrogels for Cell Encapsulation, Biomacromolecules. 17 (2016) 3244-3251.

[101] A.C. Borges, C. Eyholzer, F. Duc, P. Bourban, P. Tingaut, T. Zimmermann, D.P. Pioletti, J.E. Månson, Nanofibrillated cellulose composite hydrogel for the replacement of the nucleus pulposus, Acta Biomaterialia. 7 (2011) 3412-3421.

[102] Y. Lou, L. Kanninen, T. Kuisma, J. Niklander, L.A. Noon, D. Burks, A. Urtti, M. Yliperttula, The use of nanofibrillar cellulose hydrogel as a flexible three-dimensional model to culture human pluripotent stem cells, Stem cells and development. 23 (2014) 380-392.

[103] Y.R. Lou, L. Kanninen, B. Kaehr, J.L. Townson, J. Niklander, R. Harjumaki, C. Jeffrey Brinker, M. Yliperttula, Silica bioreplication preserves three-dimensional spheroid structures of human pluripotent stem cells and HepG2 cells, Sci. Rep. 5 (2015) 13635.

[104] M.M. Malinen, L.K. Kanninen, A. Corlu, H.M. Isoniemi, Y. Lou, M.L. Yliperttula, A.O. Urtti, Differentiation of liver progenitor cell line to functional organotypic cultures in 3D nanofibrillar cellulose and hyaluronan-gelatin hydrogels, Biomaterials. 35 (2014) 5110-5121.

[105] T. Hakkarainen, R. Koivuniemi, M. Kosonen, C. Escobedo-Lucea, A. Sanz-Garcia, J. Vuola, J. Valtonen, P. Tammela, A. Mäkitie, K. Luukko, M. Yliperttula, H. Kavola, Nanofibrillar cellulose wound dressing in skin graft donor site treatment, Journal of Controlled Release. 244 (2016) 292-301.

[106] H. Valo, S. Arola, P. Laaksonen, M. Torkkeli, L. Peltonen, M.B. Linder, R. Serimaa, S. Kuga, J. Hirvonen, T. Laaksonen, Drug release from nanoparticles embedded in four different nanofibrillar cellulose aerogels, European Journal of Pharmaceutical Sciences. 50 (2013) 69-77.

[107] R. Kolakovic, L. Peltonen, T. Laaksonen, K. Putkisto, A. Laukkanen, J. Hirvonen, Spray-dried cellulose nanofibers as novel tablet excipient, Aaps Pharmscitech. 12 (2011) 1366-1373.

[108] R. Kolakovic, T. Laaksonen, L. Peltonen, A. Laukkanen, J. Hirvonen, Spray-dried nanofibrillar cellulose microparticles for sustained drug release, Int. J. Pharm. 430 (2012) 47-55.

[109] R. Kolakovic, L. Peltonen, A. Laukkanen, J. Hirvonen, T. Laaksonen, Nanofibrillar cellulose films for controlled drug delivery, European Journal of Pharmaceutics and Biopharmaceutics. 82 (2012) 308-315.

[110] R. Kolakovic, L. Peltonen, A. Laukkanen, M. Hellman, P. Laaksonen, M.B. Linder, J. Hirvonen, T. Laaksonen, Evaluation of drug interactions with nanofibrillar cellulose, European Journal of Pharmaceutics and Biopharmaceutics. 85 (2013) 1238-1244.

[111] R. Weishaupt, G. Siqueira, M. Schubert, P. Tingaut, K. Maniura-Weber, T. Zimmermann, L. Thöny-Meyer, G. Faccio, J. Ihssen, TEMPO-oxidized nanofibrillated cellulose as a high density carrier for bioactive molecules, Biomacromolecules. 16 (2015) 3640-3650.

[112] D. Trache, M.H. Hussin, C.T. Hui Chuin, S. Sabar, M.R.N. Fazita, O.F.A. Taiwo, T.M. Hassan, M.K.M. Haafiz, Microcrystalline cellulose: Isolation, characterization and bio-composites application—A review, International Journal of Biological Macromolecules. 93 (2016) 789-804.

[113] J. Nsor-Atindana, M. Chen, H.D. Goff, F. Zhong, H.R. Sharif, Y. Li, Functionality and nutritional aspects of microcrystalline cellulose in food, Carbohydrate Polymers. 172 (2017) 159-174.

[114] B.G. Rånby, A. Banderet, L.G. Sillén, Aqueous colloidal solutions of cellulose micelles, Acta Chem. Scand. 3 (1949) 649-650.

[115] K. Leppänen, S. Andersson, M. Torkkeli, M. Knaapila, N. Kotelnikova, R. Serimaa, Structure of cellulose and microcrystalline cellulose from various wood species, cotton and flax studied by X-ray scattering, Cellulose. 16 (2009) 999-1015.

[116] M. Hanna, G. Biby, V. Miladinov, Production of microcrystalline cellulose by reactive extrusion, US Patent 6228213 (2001).

[117] H. Stupińska, E. Iller, Z. Zimek, D. Wawro, D. Ciechańska, E. Kopania, J. Palenik, S. Milczarek, W. Stęplewski, G. Krzyżanowska, An environment-friendly method to prepare microcrystalline cellulose, Fibres & Textiles in Eastern Europe. 15 (2007) 167-172.

[118] E.A. DeLong, Method of producing level off DP microcrystallinecellulose and glucose from lignocellulosic material, US Patent 4645541 (1987).

[119] E.Y. Ha, C.D. Landi, Method for producing microcrystalline cellulose, US Patent 5769934 (1998).

[120] M.K. Mohamad Haafiz, S.J. Eichhorn, A. Hassan, M. Jawaid, Isolation and characterization of microcrystalline cellulose from oil palm biomass residue, Carbohydrate Polymers. 93 (2013) 628-634.

[121] J. Araki, M. Wada, S. Kuga, T. Okano, Flow properties of microcrystalline cellulose suspension prepared by acid treatment of native cellulose, Colloids and Surfaces A: Physicochemical and Engineering Aspects. 142 (1998) 75-82.

[122] O.A. Battista, P.A. Smith, Microcrystalline cellulose, Ind. Eng. Chem. 54 (1962) 20-29.

[123] K.M. Vanhatalo, O.P. Dahl, Effect of mild acid hydrolysis parameters on properties of microcrystalline cellulose, BioResources. 9 (2014) 4729-4740.

[124] R. Salminen, M. Reza, K. Vanhatalo, E. Kontturi, Influence of the quality of microcrystalline cellulose on the outcome of TEMPO-mediated oxidation, Cellulose. 24 (2017) 5697-5704.

[125] G.K. Bolhuis, N. Anthony Armstrong, Excipients for direct compaction—An update, Pharm. Dev. Technol. 11 (2006) 111-124.

[126] H.F. Mostafa, M.A. Ibrahim, A. Sakr, Development and optimization of dextromethorphan hydrobromide oral disintegrating tablets: effect of formulation and process variables, Pharm. Dev. Technol. 18 (2013) 454-463.

[127] P. Kleinebudde, The crystallite-gel-model for microcrystalline cellulose in wet-granulation, extrusion, and spheronization, Pharm. Res. 14 (1997) 804-809.

[128] I. Kalashnikova, H. Bizot, B. Cathala, I. Capron, New Pickering emulsions stabilized by bacterial cellulose nanocrystals, Langmuir. 27 (2011) 7471-7479.

[129] K.P. Oza, S.G. Frank, Drug release from emulsions stabilized by colloidal macrocrystalline cellulose, Journal of Dispersion Science and Technology. 10 (1989) 187-210.

[130] J. Dan, Y. Ma, P. Yue, Y. Xie, Q. Zheng, P. Hu, W. Zhu, M. Yang, Microcrystalline cellulose-carboxymethyl cellulose sodium as an effective dispersant for drug nanocrystals: A case study, Carbohydrate Polymers. 136 (2016) 499-506.

[131] L. Shargel, S. Wu-Pong, A.B. Yu., Modified-Release Drug Products, in: Applied Biopharmaceutics & Pharmacokinetics, 6th ed., McGraw-Hill Companies, New York, 2012, pp. 469-503.

[132] D.L. Wise, Handbook of Pharmaceutical Controlled Release Technology, CRC Press, 2000.

[133] K. Park, Controlled drug delivery systems: Past forward and future back, Journal of Controlled Release. 190 (2014) 3-8.

[134] A.K. Bajpai, S.K. Shukla, S. Bhanu, S. Kankane, Responsive polymers in controlled drug delivery, Progress in Polymer Science. 33 (2008) 1088-1118.

[135] K.E. Uhrich, S.M. Cannizzaro, R.S. Langer, K.M. Shakesheff, Polymeric systems for controlled drug release, Chem. Rev. 99 (1999) 3181-3198.

[136] Y.W. Chien, S. Lin, Drug delivery: Controlled release, in: Encyclopedia of pharmaceutical technology, 3rd ed., Informa Healthcare, 2006.

[137] J. Siepmann, R.A. Siegel, F. Siepmann, Diffusion controlled drug delivery systems, in: J. Siepmann, R. Siegel, M. Rathbone (Eds) Fundamentals and Applications of Controlled Release Drug Delivery, Springer, Boston, 2012, pp. 127-152.

[138] J. Heller, Controlled release of biologically active compounds from bioerodible polymers, Biomaterials. 1 (1980) 51-57.

[139] W. Chen, F. Meng, F. Li, S. Ji, Z. Zhong, pH-responsive biodegradable micelles based on acid-labile polycarbonate hydrophobe: synthesis and triggered drug release, Biomacromolecules. 10 (2009) 1727-1735.

[140] T. Lajunen, R. Nurmi, L. Kontturi, L. Viitala, M. Yliperttula, L. Murtomäki, A. Urtti, Light activated liposomes: functionality and prospects in ocular drug delivery, J. Controlled Release. 244 (2016) 157-166.

[141] K. Ulbrich, K. Holá, V. Šubr, A. Bakandritsos, J. Tucek, R. Zboril, Targeted drug delivery with polymers and magnetic nanoparticles: covalent and noncovalent approaches, release control, and clinical studies, Chem. Rev. 116 (2016) 5338-5431.

[142] V. Brunella, S.A. Jadhav, I. Miletto, G. Berlier, E. Ugazio, S. Sapino, D. Scalarone, Hybrid drug carriers with temperature-controlled on–off release: A simple and reliable synthesis of PNIPAM-functionalized mesoporous silica nanoparticles, React Funct Polym. 98 (2016) 31-37.

[143] J.K. Awino, S. Gudipati, A.K. Hartmann, J.J. Santiana, D.F. Cairns-Gibson, N. Gomez, J.L. Rouge, Nucleic Acid Nanocapsules for Enzyme-Triggered Drug Release, J. Am. Chem. Soc. 139 (2017) 6278-6281.

[144] S.S. Satav, S. Bhat, S. Thayumanavan, Feedback regulated drug delivery vehicles: carbon dioxide responsive cationic hydrogels for antidote release, Biomacromolecules. 11 (2010) 1735-1740.

[145] L. Zhao, C. Xiao, G. Gai, J. Ding, Glucose-sensitive polymer nanoparticles for self-regulated drug delivery, Chemical Communications. 52 (2016) 7633-7652.

[146] R.A. Siegel, Stimuli sensitive polymers and self regulated drug delivery systems: a very partial review, J. Controlled Release. 190 (2014) 337-351.

[147] Y. Bae, W. Jang, N. Nishiyama, S. Fukushima, K. Kataoka, Multifunctional polymeric micelles with folate-mediated cancer cell targeting and pH-triggered drug releasing properties for active intracellular drug delivery, Molecular BioSystems. 1 (2005) 242-250.

[148] Q. Liu, L. Song, S. Chen, J. Gao, P. Zhao, J. Du, A superparamagnetic polymersome with extremely high T 2 relaxivity for MRI and cancer-targeted drug delivery, Biomaterials. 114 (2017) 23-33.

[149] J. Siepmann, A. Ainaoui, J. Vergnaud, R. Bodmeier, Calculation of the dimensions of drug–polymer devices based on diffusion parameters, J. Pharm. Sci. 87 (1998) 827-832.

[150] J. Siepmann, F. Lecomte, R. Bodmeier, Diffusion-controlled drug delivery systems: calculation of the required composition to achieve desired release profiles, J. Controlled Release. 60 (1999) 379-389.

[151] J. Siepmann, F. Siepmann, Modeling of diffusion controlled drug delivery, J. Controlled Release. 161 (2012) 351-362.

[152] Y.W. Chien, H.J. Lambert, Controlled drug release from polymeric delivery devices II: Differentiation between partition-controlled and matrix-controlled drug release mechanisms, J. Pharm. Sci. 63 (1974) 515-519.

[153] A. Fick, Ueber diffusion, Annalen der Physik. 170 (1855) 59-86.

[154] T. Higuchi, Rate of release of medicaments from ointment bases containing drugs in suspension, J. Pharm. Sci. 50 (1961) 874-875.

[155] T. Higuchi, Mechanism of sustained-action medication. Theoretical analysis of rate of release of solid drugs dispersed in solid matrices, J. Pharm. Sci. 52 (1963) 1145-1149.

[156] J. Siepmann, N.A. Peppas, Higuchi equation: derivation, applications, use and misuse, Int. J. Pharm. 418 (2011) 6-12.

[157] M. Jug, A. Hafner, J. Lovrić, M.L. Kregar, I. Pepić, Ž Vanić, B. Cetina-Čižmek, J. Filipović-Grčić, An overview of in vitro dissolution/release methods for novel mucosal drug delivery systems, Journal of Pharmaceutical and Biomedical Analysis. 147 (2018) 350-366.

[158] S.V. Deshmane, M.A. Channawar, A.V. Chandewar, U.M. Joshi, K.R. Biyani, Chitosan based sustained release mucoadhesive buccal patches containing verapamil HCl, Int. J. Pharm. 1 (2009) 216-229.

[159] L. Perioli, V. Ambrogi, D. Rubini, S. Giovagnoli, M. Ricci, P. Blasi, C. Rossi, Novel mucoadhesive buccal formulation containing metronidazole for the treatment of periodontal disease, J. Controlled Release. 95 (2004) 521-533.

[160] V. Hearnden, V. Sankar, K. Hull, D.V. Juras, M. Greenberg, A.R. Kerr, P.B. Lockhart, L.L. Patton, S. Porter, M.H. Thornhill, New developments and opportunities in oral mucosal drug delivery for local and systemic disease, Adv. Drug Deliv. Rev. 64 (2012) 16-28.

[161] V.F. Patel, F. Liu, M.B. Brown, Modeling the oral cavity: In vitro and in vivo evaluations of buccal drug delivery systems, Journal of Controlled Release. 161 (2012) 746-756.

[162] N. Salamat-Miller, M. Chittchang, T.P. Johnston, The use of mucoadhesive polymers in buccal drug delivery, Adv. Drug Deliv. Rev. 57 (2005) 1666-1691.

[163] O. Svensson, T. Arnebrant, Mucin layers and multilayers-Physicochemical properties and applications, Current Opinion in Colloid & Interface Science. 15 (2010) 395-405.

[164] R. Bansil, B.S. Turner, Mucin structure, aggregation, physiological functions and biomedical applications, Current Opinion in Colloid & Interface Science. 11 (2006) 164-170.

[165] S. Linden, P. Sutton, N. Karlsson, V. Korolik, M. McGuckin, Mucins in the mucosal barrier to infection, Mucosal immunology. 1 (2008) 183-197.

[166] O. Lieleg, K. Ribbeck, Biological hydrogels as selective diffusion barriers, Trends Cell Biol. 21 (2011) 543-551.

[167] S. Mansuri, P. Kesharwani, K. Jain, R.K. Tekade, N.K. Jain, Mucoadhesion: A promising approach in drug delivery system, Reactive and Functional Polymers. 100 (2016) 151-172.

[168] D. Dodou, P. Breedveld, P.A. Wieringa, Mucoadhesives in the gastrointestinal tract: revisiting the literature for novel applications, European journal of Pharmaceutics and Biopharmaceutics. 60 (2005) 1-16.

[169] J.M. Gu, J.R. Robinson, S.H. Leung, Binding of acrylic polymers to mucin/epithelial surfaces: structure-property relationships, Crit. Rev. Ther. Drug Carrier Syst. 5 (1988) 21-67.

[170] A. Ahuja, R.K. Khar, J. Ali, Mucoadhesive drug delivery systems, Drug Dev. Ind. Pharm. 23 (1997) 489-515.

[171] N.A. Peppas, Y. Huang, Nanoscale technology of mucoadhesive interactions, Advanced Drug Delivery Reviews. 56 (2004) 1675-1687.

[172] V. Zargar, M. Asghari, A. Dashti, A review on chitin and chitosan polymers: structure, chemistry, solubility, derivatives, and applications, ChemBioEng Reviews. 2 (2015) 204-226.

[173] G.M. El-Mahrouk, O.N. El-Gazayerly, A.A. Aboelwafa, M.S. Taha, Chitosan lactate wafer as a platform for the buccal delivery of tizanidine HCl: in vitro and in vivo performance, Int. J. Pharm. 467 (2014) 100-112.

[174] N. Thirawong, J. Nunthanid, S. Puttipipatkhachorn, P. Sriamornsak, Mucoadhesive properties of various pectins on gastrointestinal mucosa: an in vitro evaluation using texture analyzer, European Journal of Pharmaceutics and Biopharmaceutics. 67 (2007) 132-140.

[175] L. Ashton, P.D.A. Pudney, E.W. Blanch, G.E. Yakubov, Understanding glycoprotein behaviours using Raman and Raman optical activity spectroscopies: Characterising the entanglement induced conformational changes in oligosaccharide chains of mucin, Advances in Colloid and Interface Science. 199-200 (2013) 66-77.

[176] J. Jacobsen, B. van Deurs, M. Pedersen, M.R. Rassing, TR146 cells grown on filters as a model for human buccal epithelium: I. Morphology, growth, barrier properties, and permeability, International Journal of Pharmaceutics. 125 (1995) 165-184.

[177] H.M. Nielsen, M.R. Rassing, TR146 cells grown on filters as a model of human buccal epithelium: IV. Permeability of water, mannitol, testosterone and β-adrenoceptor antagonists. Comparison to human, monkey and porcine buccal mucosa, International Journal of Pharmaceutics. 194 (2000) 155-167.

[178] M.L. Bruschi, D.S. Jones, H. Panzeri, M.P. Gremião, O. De Freitas, E.H. Lara, Semisolid systems containing propolis for the treatment of periodontal disease: in vitro release kinetics, syringeability, rheological, textural, and mucoadhesive properties, J. Pharm. Sci. 96 (2007) 2074-2089.

[179] A.H. El-Kamel, L.Y. Ashri, I.A. Alsarra, Micromatricial metronidazole benzoate film as a local mucoadhesive delivery system for treatment of periodontal diseases, AAPS PharmSciTech. 8 (2007) E184-E194.

[180] X.C. Tang, M.J. Pikal, Design of freeze-drying processes for pharmaceuticals: practical advice, Pharm. Res. 21 (2004) 191-200.

[181] J.C. Kasper, G. Winter, W. Friess, Recent advances and further challenges in lyophilization, European Journal of Pharmaceutics and Biopharmaceutics. 85 (2013) 162-169.

[182] S.C. Tsinontides, P. Rajniak, D. Pham, W.A. Hunke, J. Placek, S.D. Reynolds, Freeze drying-principles and practice for successful scale-up to manufacturing, International Journal of Pharmaceutics. 280 (2004) 1-16.

[183] A. Ganguly, A.A. Alexeenko, S.G. Schultz, S.G. Kim, Freeze-drying simulation framework coupling product attributes and equipment capability: Toward accelerating process by equipment modifications, European Journal of Pharmaceutics and Biopharmaceutics. 85 (2013) 223-235.

[184] F. Franks, Freeze-drying of bioproducts: putting principles into practice, European Journal of Pharmaceutics and Biopharmaceutics. 45 (1998) 221-229.

[185] J.F. Carpenter, M.J. Pikal, B.S. Chang, T.W. Randolph, Rational design of stable lyophilized protein formulations: some practical advice, Pharm. Res. 14 (1997) 969-975.

[186] C. Lerici, M. Piva, M. Dalla Rosa, Water activity and freezing point depression of aqueous solutions and liquid foods, J. Food Sci. 48 (1983) 1667-1669.

[187] J.C. Kasper, W. Friess, The freezing step in lyophilization: Physico-chemical fundamentals, freezing methods and consequences on process performance and quality attributes of biopharmaceuticals, European Journal of Pharmaceutics and Biopharmaceutics. 78 (2011) 248-263.

[188] R. Geidobler, G. Winter, Controlled ice nucleation in the field of freeze-drying: Fundamentals and technology review, European Journal of Pharmaceutics and Biopharmaceutics. 85 (2013) 214-222.

[189] F. Franks, T. Auffret, Freeze-Drying of Pharmaceuticals and Biopharmaceuticals: Principles and Practice, The Royal Society of Chemistry, Cambridge, 2007, pp. 105-120.

[190] J.A. Searles, J.F. Carpenter, T.W. Randolph, The ice nucleation temperature determines the primary drying rate of lyophilization for samples frozen on a temperature-controlled shelf, Journal of Pharmaceutical Sciences. 90 (2001) 860-871.

[191] L. Qian, H. Zhang, Controlled freezing and freeze drying: a versatile route for porous and micro-/nano-structured materials, Journal of Chemical Technology and Biotechnology. 86 (2011) 172-184.

[192] W. Abdelwahed, G. Degobert, S. Stainmesse, H. Fessi, Freeze-drying of nanoparticles: Formulation, process and storage considerations, Adv. Drug Deliv. Rev. 58 (2006) 1688-1713.

[193] Y. Roos, Frozen state transitions in relation to freeze drying, Journal of Thermal Analysis and Calorimetry. 48 (1997) 535-544.

[194] W. Wagner, A. Saul, A. Pruss, International equations for the pressure along the melting and along the sublimation curve of ordinary water substance, Journal of Physical and Chemical Reference Data. 23 (1994) 515-527.

[195] A.A. Barresi, R. Pisano, D. Fissore, V. Rasetto, S.A. Velardi, A. Vallan, M. Parvis, M. Galan, Monitoring of the primary drying of a lyophilization process in vials, Chemical Engineering and Processing: Process Intensification. 48 (2009) 408-423.

[196] M. Pikal, M. Roy, S. Shah, Mass and heat transfer in vial freeze-drying of pharmaceuticals: Role of the vial, J. Pharm. Sci. 73 (1984) 1224-1237.

[197] M.J. Pikal, S. Shah, Intravial distribution of moisture during the secondary drying stage of freeze drying, PDA J. Pharm. Sci. Technol. 51 (1997) 17-24.

[198] I. Oddone, A.A. Barresi, R. Pisano, Influence of controlled ice nucleation on the freeze-drying of pharmaceutical products: the secondary drying step, International Journal of Pharmaceutics. 524 (2017) 134-140.

[199] J. Liu, Physical characterization of pharmaceutical formulations in frozen and freeze-dried solid states: techniques and applications in freeze-drying development, Pharm. Dev. Technol. 11 (2006) 3-28.

[200] R. Ohori, C. Yamashita, Effects of temperature ramp rate during the primary drying process on the properties of amorphous-based lyophilized cake, Part 1: Cake characterization, collapse temperature and drying behavior, Journal of Drug Delivery Science and Technology. 39 (2017) 131-139.

[201] M.J. Pikal, S. Shah, The collapse temperature in freeze drying: Dependence on measurement methodology and rate of water removal from the glassy phase, International Journal of Pharmaceutics. 62 (1990) 165-186.

[202] K. Kasraian, T.M. Spitznagel, J.A. Juneau, K. Yim, Characterization of the sucrose/glycine/water system by differential scanning calorimetry and freeze-drying microscopy, Pharm. Dev. Technol. 3 (1998) 233-239.

[203] E. Meister, H. Gieseler, Freeze-dry microscopy of protein/sugar mixtures: Drying behavior, interpretation of collapse temperatures and a comparison to corresponding glass transition data, J. Pharm. Sci. 98 (2009) 3072-3087.

[204] W. Wang, Lyophilization and development of solid protein pharmaceuticals, Int. J. Pharm. 203 (2000) 1-60.

[205] E.Y. Chi, S. Krishnan, T.W. Randolph, J.F. Carpenter, Physical stability of proteins in aqueous solution: mechanism and driving forces in nonnative protein aggregation, Pharm. Res. 20 (2003) 1325-1336.

[206] T.E. Creighton, Disulphide bonds and protein stability, BioEssays. 8 (1988) 57-63.

[207] H.R. Costantino, R. Langer, A.M. Klibanov, Solid-phase aggregation of proteins under pharmaceutically relevant conditions, J. Pharm. Sci. 83 (1994) 1662-1669.

[208] L.L. Chang, D. Shepherd, J. Sun, D. Ouellette, K.L. Grant, X.C. Tang, M.J. Pikal, Mechanism of protein stabilization by sugars during freeze-drying and storage: Native structure preservation, specific interaction, and/or immobilization in a glassy matrix?, J. Pharm. Sci. 94 (2005) 1427-1444.

[209] S. Luthra, J. Obert, D.S. Kalonia, M.J. Pikal, Investigation of drying stresses on proteins during lyophilization: Differentiation between primary and secondary-drying stresses on lactate dehydrogenase using a humidity controlled mini freeze-dryer, J. Pharm. Sci. 96 (2007) 61-70.

[210] J.L. Cleland, X. Lam, B. Kendrick, J. Yang, T. Yang, D. Overcashier, D. Brooks, C. Hsu, J.F. Carpenter, A specific molar ratio of stabilizer to protein is required for storage stability of a lyophilized monoclonal antibody, J. Pharm. Sci. 90 (2001) 310-321.

[211] M.J. Pikal, Freeze-Drying of Proteins: Process, Formulation, and Stability, in: J.L. Cleland, R. Langer (Eds) Formulation and Delivery of Proteins and Peptides, American Chemical Society, 1994, pp. 120-133.

[212] Z. Hubálek, Protectants used in the cryopreservation of microorganisms, Cryobiology. 46 (2003) 205-229.

[213] I. Roy, M.N. Gupta, Freeze-drying of proteins: Some emerging concerns, Biotechnol. Appl. Biochem. 39 (2004) 165-177.

[214] K. Izutsu, S. Kojima, Excipient crystallinity and its protein-structure-stabilizing effect during freeze-drying, J. Pharm. Pharmacol. 54 (2002) 1033-1039.

[215] A.I. Kim, M.J. Akers, S.L. Nail, The physical state of mannitol after freeze-drying: Effects of mannitol concentration, freezing rate, and a noncrystallizing cosolute, J. Pharm. Sci. 87 (1998) 931-935.

[216] N. Jovanović, A. Bouchard, G.W. Hofland, G. Witkamp, D.J.A. Crommelin, W. Jiskoot, Distinct effects of sucrose and trehalose on protein stability during supercritical fluid drying and freeze-drying, European Journal of Pharmaceutical Sciences. 27 (2006) 336-345.

[217] L. Kreilgaard, S. Frokjaer, J.M. Flink, T.W. Randolph, J.F. Carpenter, Effects of Additives on the Stability of Humicola Lanuginosa Lipase During Freeze-Drying and Storage in the Dried Solid, Journal of Pharmaceutical Sciences. 88 (1999) 281-290.

[218] W. Garzon-Rodriguez, R.L. Koval, S. Chongprasert, S. Krishnan, T.W. Randolph, N.W. Warne, J.F. Carpenter, Optimizing storage stability of lyophilized recombinant human interleukin-11 with disaccharide/hydroxyethyl starch mixtures, J. Pharm. Sci. 93 (2004) 684-696.

[219] S.D. Allison, M.C. Manning, T.W. Randolph, K. Middleton, A. Davis, J.F. Carpenter, Optimization of storage stability of lyophilized actin using combinations of disaccharides and dextran, J. Pharm. Sci. 89 (2000) 199-214.

[220] B.S. Chang, R.M. Beauvais, A. Dong, J.F. Carpenter, Physical factors affecting the storage stability of freeze-dried interleukin-1 receptor antagonist: glass transition and protein conformation, Arch. Biochem. Biophys. 331 (1996) 249-258.

[221] J.F. Carpenter, T. Arakawa, J.H. Crowe, Interactions of stabilizing additives with proteins during freeze-thawing and freeze-drying, Dev. Biol. Stand. 74 (1992) 225-238; discussion 238.

[222] J.F. Carpenter, J.H. Crowe, T. Arakawa, Comparison of Solute-Induced Protein Stabilization in Aqueous Solution and in the Frozen and Dried States, Journal of Dairy Science. 73 (1990) 3627-3636.

[223] R. Liebner, S. Bergmann, T. Hey, G. Winter, A. Besheer, Freeze-drying of HESylated IFNα-2b: Effect of HESylation on storage stability in comparison to PEGylation, International Journal of Pharmaceutics. 495 (2015) 608-611.

[224] K. Schersch, O. Betz, P. Garidel, S. Muehlau, S. Bassarab, G. Winter, Systematic investigation of the effect of lyophilizate collapse on pharmaceutically relevant proteins I: Stability after freeze-drying, J. Pharm. Sci. 99 (2010) 2256-2278.

[225] S. Kadoya, K. Fujii, K. Izutsu, E. Yonemochi, K. Terada, C. Yomota, T. Kawanishi, Freeze-drying of proteins with glass-forming oligosaccharide-derived sugar alcohols, International Journal of Pharmaceutics. 389 (2010) 107-113.

[226] S.J. Prestrelski, N. Tedeschi, T. Arakawa, J.F. Carpenter, Dehydration-induced conformational transitions in proteins and their inhibition by stabilizers, Biophys. J. 65 (1993) 661-671.

[227] V.P. Heljo, V. Filipe, S. Romeijn, W. Jiskoot, A.M. Juppo, Stability of Rituximab in Freeze-Dried Formulations Containing Trehalose or Melibiose Under Different Relative Humidity Atmospheres, Journal of Pharmaceutical Sciences. 102 (2013) 401-414.

[228] S.D. Allison, T.W. Randolph, M.C. Manning, K. Middleton, A. Davis, J.F. Carpenter, Effects of Drying Methods and Additives on Structure and Function of Actin: Mechanisms of Dehydration-Induced Damage and Its Inhibition, Archives of Biochemistry and Biophysics. 358 (1998) 171-181.

[229] T.J. Anchordoquy, J.F. Carpenter, Polymers protect lactate dehydrogenase during freeze-drying by inhibiting dissociation in the frozen state, Arch. Biochem. Biophys. 332 (1996) 231-238.

[230] K. Nakagawa, Y. Goto, Preparation of α-amylase-immobilized freeze-dried poly(vinyl alcohol) foam and its application to microfluidic enzymatic reactor, Chemical Engineering and Processing: Process Intensification. 91 (2015) 35-42.

[231] S. Nema, K.E. Avis, Freeze-thaw studies of a model protein, lactate dehydrogenase, in the presence of cryoprotectants, J. Parenter. Sci. Technol. 47 (1993) 76-83.

[232] J. Carpenter, S. Prestrelski, T. Arakawa, Separation of freezing-and drying-induced denaturation of lyophilized proteins using stress-specific stabilization: I. Enzyme activity and calorimetric studies, Arch. Biochem. Biophys. 303 (1993) 456-464.

[233] T. Koseki, N. Kitabatake, E. Doi, Freezing denaturation of ovalbumin at acid pH, The Journal of Biochemistry. 107 (1990) 389-394.

[234] B.S. Chang, B.S. Kendrick, J.F. Carpenter, Surface-induced denaturation of proteins during freezing and its inhibition by surfactants, J. Pharm. Sci. 85 (1996) 1325-1330.

[235] M.L. Roy, M.J. Pikal, E.C. Rickard, A.M. Maloney, The effects of formulation and moisture on the stability of a freeze-dried monoclonal antibody-vinca conjugate: a test of the WLF glass transition theory, Dev. Biol. Stand. 74 (1992) 323-239; discussion 340.

[236] W.F. Wolkers, F. Tablin, J.H. Crowe, From anhydrobiosis to freeze-drying of eukaryotic cells, Comparative Biochemistry and Physiology, Part A. 131 (2002) 535-543.

[237] R.D. Lins, C.S. Pereira, P.H. Hünenberger, Trehalose–protein interaction in aqueous solution, Proteins: Structure, Function, and Bioinformatics. 55 (2004) 177-186.

[238] K. Missoum, J. Bras, M.N. Belgacem, Water redispersible dried nanofibrillated cellulose by adding sodium chloride, Biomacromolecules. 13 (2012) 4118-4125.

[239] C.P. Mora, F. Martínez, Thermodynamic quantities relative to solution processes of naproxen in aqueous media at pH 1.2 and 7.4, Phys Chem Liq. 44 (2006) 585-596.

[240] S.H. Yalkowsky, Y. He, Handbook of Aqueous Solubility Data, 1st ed., CRC press, Boca Raton, 2003, p 962.

[241] S.H. Yalkowsky, R.M. Dannenfelser, Aquasol database of aqueous solubility, College of Pharmacy, University of Arizona, Tucson, 1992.

[242] S. Lerdkanchanaporn, D. Dollimore, S.J. Evans, Phase diagram for the mixtures of ibuprofen and stearic acid, Thermochimica Acta. 367 (2001) 1-8.

[243] K.A. Levis, M.E. Lane, O.I. Corrigan, Effect of buffer media composition on the solubility and effective permeability coefficient of ibuprofen, Int. J. Pharm. 253 (2003) 49-59.

[244] A.K. Singhai, S. Jain, N.K. Jain, Cosolvent solubilization and formulation of an aqueous injection of ketoprofen, Die Pharmazie. 51 (1996) 737-740.

[245] A. Avdeef, C.M. Berger, C. Brownell, pH-metric solubility. 2: correlation between the acid-base titration and the saturation shake-flask solubility-pH methods, Pharm. Res. 17 (2000) 85-89.

[246] C. Zhou, Y. Jin, J.R. Kenseth, M. Stella, K.R. Wehmeyer, W.R. Heineman, Rapid pKa estimation using vacuum-assisted multiplexed capillary electrophoresis (VAMCE) with ultraviolet detection, J. Pharm. Sci. 94 (2005) 576-589.

[247] J.J. Sheng, N.A. Kasim, R. Chandrasekharan, G.L. Amidon, Solubilization and dissolution of insoluble weak acid, ketoprofen: Effects of pH combined with surfactant, European Journal of Pharmaceutical Sciences. 29 (2006) 306-314.

[248] A. Avdeef, C.M. Berger, pH-metric solubility.: 3. Dissolution titration template method for solubility determination, European Journal of Pharmaceutical Sciences. 14 (2001) 281-291.

[249] H. Kim, Y. Lee, H. Yoo, J. Kim, H. Kong, J. Yoon, Y. Jung, Y.M. Kim, Synthesis and evaluation of sulfate conjugated metronidazole as a colon-specific prodrug of metronidazole, J. Drug Target. 20 (2012) 255-263.

[250] Y. Wu, R. Fassihi, Stability of metronidazole, tetracycline HCl and famotidine alone and in combination, Int. J. Pharm. 290 (2005) 1-13.

[251] G. Yohannes, S.K. Wiedmer, M. Elomaa, M. Jussila, V. Aseyev, M. Riekkola, Thermal aggregation of bovine serum albumin studied by asymmetrical flow field-flow fractionation, Anal. Chim. Acta. 675 (2010) 191-198.

[252] Sigma-Aldrich, Supplier's data.

[253] M. Fritz, M. Radmacher, J.P. Cleveland, M.W. Allersma, R.J. Stewart, R. Gieselmann, P. Janmey, C.F. Schmidt, P.K. Hansma, Imaging globular and filamentous proteins in physiological buffer solutions with tapping mode atomic force microscopy, Langmuir. 11 (1995) 3529-3535.

[254] A. Szymańska, G. Ślósarek, Light Scattering Studies of Hydration and Structural Transformations of Lysozyme. Acta Physica Polonica A. 121 (2012) 694-698.

[255] V. Thakkar, P. Shah, T. Soni, M. Parmar, M. Gohel, T. Gandhi, Goodness-of-fit model-dependent approach for release kinetics of levofloxacin hemihydrates floating tablet, Dissolution Technologies. 16 (2009) 35-39.

[256] M.M. Bradford, A rapid and sensitive method for the quantitation of microgram quantities of protein utilizing the principle of protein-dye binding, Anal. Biochem. 72 (1976) 248-254.

[257] O. Ernst, T. Zor, Linearization of the bradford protein assay, J. Vis. Exp. 38 (2010) 1918.

[258] S.O. Lumsdon, J. Green, B. Stieglitz, Adsorption of hydrophobin proteins at hydrophobic and hydrophilic interfaces, Colloids and Surfaces B: Biointerfaces. 44 (2005) 172-178.

[259] K. Kisko, G.R. Szilvay, U. Vainio, M.B. Linder, R. Serimaa, Interactions of hydrophobin proteins in solution studied by small-angle X-ray scattering, Biophys. J. 94 (2008) 198-206.

[260] Y. Maa, C.C. Hsu, Performance of sonication and microfluidization for liquid–liquid emulsification, Pharm. Dev. Technol. 4 (1999) 233-240.

[261] N. Garti, Hydrocolloids as emulsifying agents for oil-in-water emulsions, J. Dispersion Sci. Technol. 20 (1999) 327-355.

[262] K. Xhanari, K. Syverud, G. Chinga-Carrasco, K. Paso, P. Stenius, Structure of nanofibrillated cellulose layers at the o/w interface, J. Colloid Interface Sci. 356 (2011) 58-62.

[263] A.A. Date, M.S. Nagarsenker, Parenteral microemulsions: An overview, Int. J. Pharm. 355 (2008) 19-30.

[264] H. Chen, X. Chang, D. Du, J. Li, H. Xu, X. Yang, Microemulsion-based hydrogel formulation of ibuprofen for topical delivery, Int. J. Pharm. 315 (2006) 52-58.

[265] B. Sharif Makhmalzadeh, S. Torabi, A. Azarpanah, Optimization of ibuprofen delivery through rat skin from traditional and novel nanoemulsion formulations, Iran. J. Pharm. Res. 11 (2012) 47-58.

[266] M. Llinàs, G. Calderó, M.J. García-Celma, A. Patti, C. Solans, New insights on the mechanisms of drug release from highly concentrated emulsions, J. Colloid Interface Sci. 394 (2013) 337-345.

[267] H.K. Valo, P.H. Laaksonen, L.J. Peltonen, M.B. Linder, J.T. Hirvonen, T.J. Laaksonen, Multifunctional hydrophobin: toward functional coatings for drug nanoparticles, ACS Nano. 4 (2010) 1750-1758.

[268] F. Jiang, Y. Hsieh, Self-assembling of TEMPO Oxidized Cellulose Nanofibrils As Affected by Protonation of Surface Carboxyls and Drying Methods, ACS Sustainable Chemistry & Engineering. 4 (2016) 1041-1049.

[269] S. Jeon, J. Lee, J. Andrade, P. De Gennes, Protein-surface interactions in the presence of polyethylene oxide: I. Simplified theory, J. Colloid Interface Sci. 142 (1991) 149-158.

[270] K. Dimić-Mišić, Y. Sanavane, J. Paltakari, T. Maloney, Small scale rheological observation of high consistency nanofibrillar material based furnishes, Journal of Applied Engineering Science. 11 (2013) 145-151.

[271] J.R. Hazel, B.D. Sidell, A method for the determination of diffusion coefficients for small molecules in aqueous solution, Anal. Biochem. 166 (1987) 335-341.

[272] R.R. Walters, J.F. Graham, R.M. Moore, D.J. Anderson, Protein diffusion coefficient measurements by laminar flow analysis: method and applications, Anal. Biochem. 140 (1984) 190-195.

[273] S. Koutsopoulos, L.D. Unsworth, Y. Nagai, S. Zhang, Controlled release of functional proteins through designer self-assembling peptide nanofiber hydrogel scaffold, Proc. Natl. Acad. Sci. U. S. A. 106 (2009) 4623-4628.

[274] M.A. Chowdhury, The controlled release of bioactive compounds from lignin and lignin-based biopolymer matrices, International Journal of Biological Macromolecules. 65 (2014) 136-147.

[275] H. Orelma, I. Filpponen, L. Johansson, M. Österberg, O.J. Rojas, J. Laine, Surface functionalized nanofibrillar cellulose (NFC) film as a platform for immunoassays and diagnostics, Biointerphases. 7 (2012) 61.

[276] J. Gum, Mucin genes and the proteins they encode: structure, diversity, and regulation, Am. J. Respir. Cell Mol. Biol. 7 (1992) 557-564.

[277] A.W. Zykwinska, M.C. Ralet, C.D. Garnier, J.F. Thibault, Evidence for in vitro binding of pectin side chains to cellulose, Plant Physiol. 139 (2005) 397-407.

[278] M. Dick-Pérez, Y. Zhang, J. Hayes, A. Salazar, O.A. Zabotina, M. Hong, Structure and interactions of plant cell-wall polysaccharides by two-and three-dimensional magic-angle-spinning solid-state NMR, Biochemistry. 50 (2011) 989-1000.

[279] C. Han, J. Chen, X. Wu, Y. Huang, Y. Zhao, Detection of metronidazole and ronidazole from environmental samples by surface enhanced Raman spectroscopy, Talanta. 128 (2014) 293-298.

[280] R. Gnanasambandam, A. Proctor, Determination of pectin degree of esterification by diffuse reflectance Fourier transform infrared spectroscopy, Food Chemistry. 68 (2000) 327-332.

[281] I.A. Sacui, R.C. Nieuwendaal, D.J. Burnett, S.J. Stranick, M. Jorfi, C. Weder, E.J. Foster, R.T. Olsson, J.W. Gilman, Comparison of the properties of cellulose nanocrystals and cellulose nanofibrils isolated from bacteria, tunicate, and wood processed using acid, enzymatic, mechanical, and oxidative methods, ACS Applied Materials and Interfaces. 6 (2014) 6127-6138.

[282] J. De Gelder, K. De Gussem, P. Vandenabeele, L. Moens, Reference database of Raman spectra of biological molecules, J. Raman Spectrosc. 38 (2007) 1133-1147.

[283] C.M. Oh, P.W.S. Heng, L.W. Chan, Influence of hydroxypropyl methylcellulose on metronidazole crystallinity in spray-congealed polyethylene glycol microparticles and its impact with various additives on Metronidazole release, AAPS PharmSciTech. 16 (2015) 1357-1367.

[284] A. Zykwinska, J. Thibault, M. Ralet, Competitive binding of pectin and xyloglucan with primary cell wall cellulose, Carbohydr. Polym. 74 (2008) 957-961.

[285] D.J. Cosgrove, Re-constructing our models of cellulose and primary cell wall assembly, Curr. Opin. Plant Biol. 22 (2014) 122-131.

[286] J. Mahood, R. Willson, Cytotoxicity of metronidazole (Flagyl) and misonidazole (Ro-07-0582): enhancement by lactate, Br. J. Cancer. 43 (1981) 350-354.